

HONG KONG

The official publication of the
Hong Kong Academy of Medicine and
the Hong Kong Medical Association

MEDICAL JOURNAL

香港醫學雜誌

Health and Medical Research Fund

Research Dissemination Reports

醫療衛生研究基金

研究成果報告

Traditional Chinese medicine
中藥

Respiratory infection
呼吸道感染

Infectious diseases
傳染病



ISSN 1024-2708

香港醫學專科學院出版社
HONG KONG ACADEMY OF MEDICINE PRESS

EDITOR-IN-CHIEF

Martin CS Wong 黃至生

SENIOR EDITORS

LW Chu 朱亮榮

Albert KK Chui 徐家強

Michael G Irwin

Bonnie CH Kwan 關清霞

Eric CH Lai 賴俊雄

KY Leung 梁國賢

Anthony CF Ng 吳志輝

EDITORS

KS Chan 陳健生

Sherry KW Chan 陳喆輝

Jason PY Cheung 鍾培言

Kelvin KL Chong 莊金隆

Velda LY Chow 周令宇

Jacqueline PW Chung 鍾佩樺

Brian SH Ho 何思灝

Ellis KL Hon 韓錦倫

Junjie Huang 黃俊杰

KW Huang 黃凱文

WK Hung 熊維嘉

Bonnie CH Kwan 關清霞

Ho Lam 林賀

Arthur CW Lau 劉俊穎

PY Lau 蕤培友

Danny WH Lee 李偉雄

WK Leung 梁蕙強

Kenneth KW Li 李啟煌

Janice YC Lo 羅懿之

Herbert HF Loong 龍浩鋒

Rashid Lui 雷諾信

James KH Luk 陸嘉熙

Arthur DP Mak 麥敦平

Henry FK Mak 麥嘉豐

Martin W Pak 白威

Walter WK Seto 司徒偉基

Regina WS Sit 薛詠珊

Jeremy YC Teoh 張源津

KY Tse 謝嘉瑜

Harry HX Wang 王皓翔

HL Wong 黃學良

Kenneth KY Wong 黃格元

Hao Xue 薛浩

Jason CS Yam 任卓昇

Bryan PY Yan 甄秉言

TK Yau 游子覺

Kelvin KH Yiu 姚啟恒

Vivian MY Yuen 袁文英

EPIDEMIOLOGY ADVISERS

Daniel SY Ho 何世賢

Eman Leung 梁以文

Edmond SK Ma 馬紹強

Gary Tse 謝家偉

Shelly LA Tse 謝立亞

Ian YH Wong 王逸軒

Esther YT Yu 余懿德

Hunter KL Yuen 袁國禮

STATISTICAL ADVISERS

Marc KC Chong 莊家俊

William B Goggins

Eddy KF Lam 林國輝

Carlos KH Wong 黃競浩

HONORARY ADVISERS

David VK Chao 周偉強

Paul BS Lai 賴寶山

Health and Medical Research Fund**Research Dissemination Reports****Editorial**

3

TRADITIONAL CHINESE MEDICINE**Electroacupuncture to reduce sedative and analgesic demands during endoscopic ultrasonography: a prospective, randomised, double-blind, sham-controlled study (abridged secondary publication)**

4

AYB Teoh, CCN Chong, WW Leung, SKC Chan, YK Tse, EKW Ng, PBS Lai, JCY Wu, JYW Lau

Tumour-shrinking decoction for symptomatic uterine fibroids: a double-blind, randomised, two-dose trial (abridged secondary publication)

8

W Meng, L Lao, ZJ Zhang, WL Lin, YB Zhang, WF Yeung, YMB Yu, HYE Ng, JP Chen, J Su, JH Rong, PYF Lam, E Lee

Danshen Gegen capsule for intermittent claudication in patients with peripheral arterial disease: abridged secondary publication

11

BPY Yan, KP Fung, P Chook, JCM Koon, JYW Chan

Inflammatory properties of ribosome-inactivating protein momorcharin derived from bitter melon: abridged secondary publication

14

YJ Chen, ZL Yu, AKW Tse

Combination of atorvastatin or hydrochlorothiazide/amlodipine with *Salvia miltiorrhiza* (Danshen) and *Pueraria lobata* (Gegen) for atherosclerosis, hyperlipidaemia, and hypertension: a preclinical in vivo study (abridged secondary publication)

18

DWS Cheung, JCM Koon, PH Wong, KC Yau, ECL Wat, JYW Chan, VKM Lau, ECH Ko, MMY Waye, KP Fung

**INTERNATIONAL EDITORIAL
ADVISORY BOARD**

Sabaratnam Arulkumaran
United Kingdom

Peter Cameron
Australia

Daniel KY Chan
Australia

David Christiani
United States

Andrew Coats
Australia

James Dickinson
Canada

Willard Fee, Jr
United States

Robert Hoffman
United States

Michael Kidd
Australia

Arthur Kleinman
United States

Stephen Leeder
Australia

Xiaoping Luo
PR China

William Rawlinson
Australia

Jonathan Samet
United States

Yaojiang Shi
PR China

David Weller
United Kingdom

Max Wintermark
United States

Wanghong Xu
PR China

Atsuyuki Yamataka
Japan

Homer Yang
Canada

KG Yeoh
Singapore

Zhijie Zheng
PR China

Full details of the Editorial Board
are available online at
<https://www.hkmj.org/about/eo.html>

RESPIRATORY INFECTION

Molecular diversity and evolution of bat group C betacoronaviruses: origin of the novel human group C betacoronavirus (abridged secondary publication) 23

SKP Lau, PCY Woo, BJ Zheng

Tropism of the novel human betacoronavirus lineage C virus in human ex vivo and in vitro cultures: potential transmissibility and pathogenesis in humans (abridged secondary publication) 28

MCW Chan, RWY Chan, JM Nicholls, JSM Peiris

Mechanism of inflammasome activation by SARS coronavirus 3a protein: abridged secondary publication 33

DY Jin, BJ Zheng, HMV Tang

Respiratory infectious diseases transmission in high-rise residential environment: abridged secondary publication 36

JL Niu, TCW Tung, Y Wu

INFECTIOUS DISEASES

Prevalence and contextual risk factors of sexually transmitted infections in Hong Kong: abridged secondary publication 40

WCW Wong, JD Tucker, HK Man, M Emch, LG Yang, Y Zhao

Symptom-specific health-seeking behaviour for common infectious diseases and implications in disease control and surveillance: abridged secondary publication 44

EHY Lau, IOL Wong, DKM Ip, KO Kwok, BJ Cowling

Author index & Disclaimer 48

MANAGING EDITOR
Alan Purvis

DEPUTY MANAGING EDITOR
Betty Lau 劉薇薇

ASSISTANT MANAGING EDITOR
Warren Chan 陳俊華

Editorial

Dissemination reports are concise informative reports of health-related research supported by the Health and Medical Research Fund administered by the Food and Health Bureau. In this edition, we present 11 dissemination reports of projects related to traditional Chinese medicine, respiratory infection, and infectious diseases. In particular, three projects are highlighted due to their potentially significant findings, impact on healthcare delivery and practice, and/or contribution to health policy formulation in Hong Kong.

Accumulating evidence suggests electroacupuncture may have an analgesic effect in specific clinical settings. Teoh et al¹ conducted a double-blind randomised controlled study in 128 consecutive patients undergoing diagnostic endoscopic ultrasonography (EUS) for the first time to investigate the efficacy of electroacupuncture in reducing endoscopy-related pain and discomfort and the consumption of sedatives and analgesics during EUS. The primary outcome was the dosage of patient-controlled analgesia consumed. The secondary outcomes included pain, patient satisfaction, endoscopist satisfaction, patient willingness to repeat the procedure, total procedure time, episodes of hypotension (defined as systolic blood pressure of <90 mmHg), and desaturation (defined as SaO₂ of <90%). The results showed that electroacupuncture reduced sedative and analgesic demands with low risk of adverse events and improved patient experience during EUS. Electroacupuncture could reduce the use of propofol and the need of the presence of an anaesthesiologist during endoscopic ultrasonography. It could avoid the potential adverse effects related to propofol usage and improve the safety of sedation and analgesia. The recovery time from anaesthesia could be significantly reduced.

In 2012, a novel human coronavirus (CoV) in the Middle East region was found to be associated with severe respiratory illness with high mortality rate. This novel lineage C betaCoV was named Middle East respiratory syndrome-related coronavirus (MERS-CoV). Lau et al² conducted extensive surveillance of betaCoVs in bats of different species to better understand the origin of

the ancestor of MERS-CoV. The project team found betaCoVs in 267 of 9866 bats sampled and noted that at least five different betaCoV species were circulating in specific bat species. This indicates that bats are a very important reservoir for betaCoVs. The results are important for future research on the emergence of CoVs in humans and provide clues on the animal origins and evolutionary pathways of MERS-CoV and SARS-CoV.

Sexually transmitted infections (STIs) are preventable through early identification and effective intervention. Population-based prevalence data can be used to understand the disease burden and distribution as well as effective prevention and control measures. To provide guidance information for future STI control and prevention, Wong et al³ conducted a territory-wide STI and sexual health survey to determine the prevalence and associated individual and contextual risk factors of genital chlamydia, gonorrhoea, and syphilis in a representative sample of nearly 900 adults aged 18 to 49 years in Hong Kong. They found that the prevalence of composite STIs was 1.9%, with 1.2% among men and 2.5% among women, and similarly for chlamydia at 1.4% overall, with 1.2% for men and 1.7% for women. However, the prevalence of chlamydial infection was 5.8% in young sexually active women, 4.8% in sexually active men, and 4.1% in sexually active women aged 40 to 49 years. Younger age, living alone, and males (or females with male partners) travelling outside Hong Kong in the past 12 months were identified as independent risk factors for both composite STIs and chlamydia. The authors suggest that mandatory surveillance and reporting of STIs and large population-based screening of chlamydia should be considered.

We hope you will enjoy this selection of research dissemination reports. Electronic copies of these dissemination reports and the corresponding full reports can be downloaded individually from the Research Fund Secretariat website (<https://rfs2.fhb.gov.hk/>). Researchers interested in the funds administered by the Food and Health Bureau also may visit the website for detailed information about application procedures.

Supplement co-editors

Dr Richard A Collins
Chief Scientific Reviewer
(Research Office)
Food and Health Bureau

Dr Martin Chan Chi-wai
Senior Scientific Reviewer
(Research Office)
Food and Health Bureau

References

- Teoh AYB, Chong CCN, Leung WW, et al. Electroacupuncture to reduce sedative and analgesic demands during endoscopic ultrasonography: a prospective, randomised, double-blind, sham-controlled study (abridged secondary publication). *Hong Kong Med J* 2021;27(Suppl 2):S23-7.
- Lau SKP, Woo PCY, Zheng BJ. Molecular diversity and

evolution of bat group C betacoronaviruses: origin of the novel human group C betacoronavirus (abridged secondary publication). *Hong Kong Med J* 2021;27(Suppl 2):S23-7.

- Wong WCW, Tucker JD, Man HK, Emch M, Yang LG, Zhao Y. Prevalence and contextual risk factors of sexually transmitted infections in Hong Kong: abridged secondary publication. *Hong Kong Med J* 2021;27(Suppl 2):S40-3.

Electroacupuncture to reduce sedative and analgesic demands during endoscopic ultrasonography: a prospective, randomised, double-blind, sham-controlled study (abridged secondary publication)

AYB Teoh *, CCN Chong, WW Leung, SKC Chan, YK Tse, EKW Ng, PBS Lai, JCY Wu, JYW Lau

KEY MESSAGES

1. Electroacupuncture reduced sedative and analgesic demands, improved patient experience, and was associated with low risk of adverse events during endoscopic ultrasonography.
2. Electroacupuncture could reduce the use of propofol and the need of the presence of an anaesthesiologist during endoscopic ultrasonography. It could avoid the potential adverse effects related to propofol usage and improve the safety of sedation and analgesia.
3. The recovery time from anaesthesia could be significantly reduced.

Hong Kong Med J 2021;27(Suppl 2):S4-7

HMRF project number: 11122771

¹ AYB Teoh, ¹ CCN Chong, ¹ WW Leung, ² SKC Chan, ³ YK Tse, ^{1,3} EKW Ng, ^{1,3} PBS Lai, ^{3,4} JCY Wu, ^{1,2} JYW Lau

Prince of Wales Hospital, The Chinese University of Hong Kong:

¹ Department of Surgery

² Department of Anaesthesia and Intensive Care

³ Institute of Digestive Disease

⁴ Institute of Integrative Medicine

* Principal applicant and corresponding author:
anthonyteoh@surgery.cuhk.edu.hk

Introduction

The role of electroacupuncture in reducing sedative and analgesic requirements during endoscopy is uncertain. The aim of the current study is to investigate the efficacy of electroacupuncture in reducing procedure-related pain and discomfort, and the consumption of sedatives and analgesics during endoscopic ultrasonography (EUS). We hypothesised that electroacupuncture could reduce procedure-related pain and discomfort as well as consumption of sedatives and analgesics during EUS.

Methods

This double-blind randomised controlled study was conducted between March 2014 and July 2016, in accordance with the Declaration of Helsinki and the International Conference on Harmonization good clinical practice guidelines. Informed consent was obtained from all patients. Consecutive patients scheduled for diagnostic EUS for the first instance were recruited and assigned at random to the electroacupuncture group or sham-electroacupuncture group. The randomisation was stratified according to whether the patients received radial and linear EUS. Recruited patients, endoscopists, anaesthetists, endoscopy nurses, and the assessor were blinded to the type of intervention.

Patients were instructed by an anaesthetist on

the use of the patient-controlled analgesia (PCA) when they experienced any discomfort during EUS. PCA was a mixture of propofol (200 mg in 20 mL) and alfentanil (0.5 mg in 1 mL) delivered via a 25-mL syringe pump to the patient's right arm. Each push of the button delivered 0.5 mL bolus of 4.8 mg propofol and 12 µg alfentanil. No loading dose was used, and the lockout time was set to 1 minute. 2 L/min of nasal oxygen was given to all patients. Their pulse rate and oxygen saturation were monitored continuously, and blood pressure was recorded every 5 minutes throughout the procedure and during the recovery period. An anaesthetist was present to monitor for any adverse events. After EUS, the syringe pumps were removed, and an endoscopy nurse monitored the patients closely until full recovery.

Patients were kept nil per oral for 6 hours prior to EUS. EUS was performed by two physicians who have performed >500 EUS procedures before. Conventional radial or linear echoendoscopes (GF-UE260-AL5, UM 2R/3R, GF-UCT260; Olympus Medical, Tokyo, Japan) were used. Patients were then subjected to 45 minutes of electroacupuncture or sham procedure before EUS and throughout the whole procedure. After EUS, the acupuncture needles were removed and discarded.

Electroacupuncture was at acupoints relevant to the treatment of abdominal pain and anxiety, including *Hegu* (large intestine meridian, LI-4),

Neiguan (pericardium meridian, PC-6), and *Zusanli* (stomach meridian, ST-36) [Fig]. These acupoints are most relevant to the organs in concern.¹ Sterile acupuncture needles (Hwato needles 0.22 × 25 mm, Suzhou Medical Appliance Factory, China) were inserted into the acupoints to a depth of 15 mm, via a sterile plastic tube stabilised by a foam block (Fig).^{2,3} Regular electric stimulation was applied to the needles with the ES-160 6-channel programmable electroacupuncture device (Ito Company Limited, Tokyo, Japan). A stimulation protocol of frequency 2 Hz, pulse width 200 µs, and stimulation intensity “short of discomfort” was used. This setting was shown to be effective in relieving pain to the organs in concern.²

For sham procedure, sterile blunt-tip needles (self-prepared from Hwato needles 0.22 × 13 mm, Suzhou Medical Appliance Factory, China) were placed 15 mm from the acupoints. The needles were first inserted through a sterile plastic tube mounted on a foam block, and then pressed on the skin. The compression provided by the foam block gave a false impression that the needles were penetrating the skin, thus providing a sham acupuncture effect.^{2,3} Electrical stimulation was simulated by connecting the needle to the incorrect output socket of the electroacupuncture device, resulting in absence of electrical current flow. Patients were also informed that the stimulation frequency was not perceivable by human and they would not be able to sense the stimulation.

The primary outcome was the dosage of PCA consumed. The secondary outcomes included pain, patient satisfaction, endoscopist satisfaction, patient willingness to repeat the procedure, total procedure time, episodes of hypotension (defined as systolic blood pressure of <90 mmHg), and desaturation (defined as SaO₂ of <90%).

In a study comparing the efficacy of electroacupuncture and sham procedure in reducing discomfort associated with colonoscopy, the mean maximal tolerable pressure/pain threshold was significantly higher in the electroacupuncture group (>20% difference).² Assuming that electroacupuncture during EUS reduced the consumption of propofol by 30% from 1 mg/kg to 0.7 mg/kg (standard deviation, 0.6 mg/kg), a sample size of 64 patients in each group is required to yield a power of 80% with a significance level of 0.05. The two groups were compared using Student's *t* test for parametric data and Mann-Whitney *U* test for non-parametric data. Categorical data were compared with Pearson Chi-squared test or Fisher's exact test. The pre- and intra-procedural scores were compared using Wilcoxon signed-rank test. The predictors to PCA consumption were analysed by multiple linear regression. A two-sided *P* value of <0.05 was considered statistically significant.

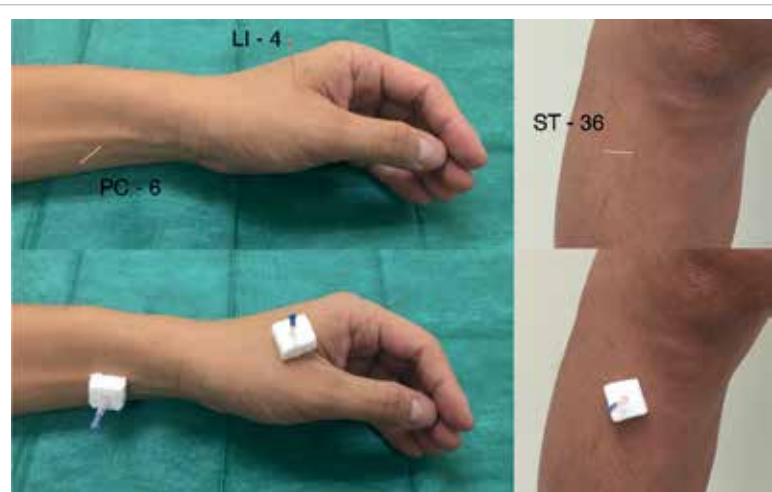


FIG. Acupoints of Hegu (LI-4) for large intestine meridian, Neiguan (PC-6) for pericardium meridian, and Zusanli (ST-36) for stomach meridian. Acupuncture needles inserted into the acupoints and stabilised by foam boxes. Hegu (LI-4) is located on the dorsum of the hand, between the 1st and 2nd metacarpal bones. Neiguan (PC-6) is located on the palmar aspect of the forearm, two cun above the transverse crease of the wrist between the flexor carpi radialis and palmaris longus tendons. Zusanli (ST-36) is located on the anterior aspect of the leg, three cun below the kneecap and one finger-breath from the anterior crest of the tibia. One cun is the distance between the interphalangeal creases of the subject's middle finger.

Results

A total of 128 patients were recruited. The two groups were comparable in terms of demographics, indications of procedure, and types of endoscopes used. Patients in the electroacupuncture group had significantly fewer demands for PCA (4.06 ± 4.81 vs 28.27 ± 30.43 , *P*<0.001), fewer successful demands (2.73 ± 2.30 vs 10.39 ± 7.70 , *P*<0.001), lower total dose of propofol (0.23 ± 0.21 mg/kg vs 0.83 ± 0.62 mg/kg, *P*<0.001), and lower total dose of alfentanil (0.58 ± 0.53 mg/kg vs 2.07 ± 1.54 mg/kg, *P*<0.001), compared with the sham procedure group (Table 1). Patients in the electroacupuncture group also had significantly lower procedural pain score (2.5 ± 2.0 vs 6.1 ± 2.9 , *P*<0.001), lower anxiety score (2.4 ± 2.5 vs 4.8 ± 3.2 , *P*<0.001), higher satisfaction score (8.7 ± 1.4 vs 6.9 ± 2.4 , *P*<0.001), and they were more willing to repeat the procedure if required (*P*<0.001), compared with the sham procedure group. The endoscopist satisfaction score was also higher for patients in the electroacupuncture group (8.1 ± 1.9 vs 7.1 ± 2.7 , *P*=0.003). The procedural time was shorter in the electroacupuncture group than in the sham procedure group (895.6 ± 559.5 s vs 1265 ± 841.3 s, *P*=0.007). No adverse events were observed in either group.

When comparing the pre-procedural and intra-procedural abdominal pain scores, both groups

TABLE 1. Comparison of outcomes between electroacupuncture and sham procedure groups.

	Electro-acupuncture (n=64)*	Sham procedure (n=64)*	P value
Highest systolic blood pressure, mmHg	156.52±26.57	157.14±30.56	0.819
Highest diastolic blood pressure, mmHg	83.98±17.10	90.20±21.81	0.083
Highest pulse rate, bpm	89.64±17.30	92.14±17.79	0.590
Total No. of demands for patient-controlled analgesia	4.06±4.81	28.27±30.43	<0.001
No. of successful patient-controlled analgesia demands	2.73±2.30	10.39±7.70	<0.001
Total dose of propofol consumed, mg/kg	0.23±0.21	0.83±0.62	<0.001
Total dose of alfentanil consumed, mg/kg	0.58±0.53	2.07±1.54	<0.001
Procedural pain score	2.5±2.0	6.1±2.9	<0.001
Procedural anxiety score	2.4±2.5	4.8±3.2	<0.001
Satisfaction score	8.7±1.4	6.9±2.4	<0.001
Patient willingness to repeat the procedure (yes/no)	32/32	12/52	<0.001
Endoscopists' satisfaction score	8.4±1.9	7.1±2.7	0.003
Procedural time, s	895.6±559.5	1265.4±941.3	0.007

* Data are presented as mean ± standard deviation unless otherwise specified

TABLE 2. Predictors for increased patient-controlled analgesia demands in multivariate linear regression analysis.

Parameter	Relative risk (95% confidence interval)	P value
Age	-0.65 (-0.14-0.11)	0.095
Male sex	1.17 (-1.03-0.67)	0.159
Body mass index	-0.50 (-0.27-0.17)	0.658
Type of echoendoscope	-0.05 (-1.08-0.98)	0.927
The need of fine needle aspiration cytology	-0.18 (-1.03-0.67)	0.679
Sham procedure group	5.83 (4.18-7.49)	<0.001
Procedural time	0.005 (0.004-0.006)	<0.001

had significantly more pain during the procedure but more so in the sham procedure group. The anxiety scores reduced significantly during the procedure in the electroacupuncture group ($P<0.001$), whereas the pre- and intra-procedural anxiety scores remained similar in the sham procedure group ($P=0.257$).

The predictors to PCA demands were analysed by linear regression analysis. Being in the sham procedure group and the procedural time were significant predictors to increased PCA demands (all $P<0.001$, Table 2).

Discussion

EUS is technically demanding and time-consuming. Electroacupuncture as a means to reduce analgesia and sedation during EUS was shown to be associated with fewer PCA demands, lower pain and anxiety scores, shorter procedural time, higher patient and endoscopist satisfaction scores, and more willingness to repeat the procedure. Electroacupuncture and the procedural time were significant predictors to increased PCA demands.

Sedation and analgesia for advanced endoscopic procedures is commonly achieved by the use of benzodiazepines and opioids.⁴ In patients that require deep sedation, propofol is frequently used. However, the use of propofol can cause negative cardiac inotropy and respiratory depression. Furthermore, the drug has no reversal agent. Thus, trained personnel in the administration of propofol with the expertise in emergency airway management must be present. Patient physiologic parameters must be continuously monitored. Age-appropriate equipment for airway management and resuscitation must be available immediately if required. Post-procedurally, patients are required to be monitored in the recovery and are advised not to engage in activities that require a certain amount of concentration for the remaining of the day (eg, driving). These requirements add to the cost and inconvenience to the procedures.

Acupuncture has been used for curing diseases or promoting health. It involves insertion of needles into specific points in the body and manipulation of the needles (lifting, thrusting, twisting, twirling or other complex combination) to elicit a characteristic sensation called De-Qi,⁵ which is believed to be responsible for causing the release of endorphins in the brain. Manipulation of the needles is an important aspect to promote further release of endorphins. However, the manipulation of acupuncture needles is operator-dependent and thus electroacupuncture has been introduced to provide a constant and reproducible stimulation with fixed frequency, pulse width, and current to the needles. Low-frequency electroacupuncture leads to supraspinal release of the μ opioid receptor ligand β -endorphin. This could positively influence a range of symptoms experienced during endoscopy including gagging, pain, and anxiety.

Acupuncture may have an effect on gastrointestinal motility and sensation, gastric acid secretion, anti-emesis, cancer pain management, postoperative ileus, and functional bowel disease.^{2,3} Three randomised trials have investigated analgesia in gastroscopy or colonoscopy, and the results of these studies suggest that acupuncture may have a role in reducing discomfort or pain during endoscopy. However, these studies have methodological flaws,

including inappropriate and small sample size, unclear randomisation method, poorly defined outcomes, and unvalidated outcome measures.

In the current study, electroacupuncture was standardised by a programmable electroacupuncture device that delivered a fixed electric stimulation. In addition, pain experienced by patients during EUS was assessed objectively through the demand for PCA, which was compared among patients, and the results were highly reproducible. Furthermore, PCA demands were supplemented by subjective outcomes. However, there are drawbacks to the current study. The application of the acupuncture needles requires specific training, and trained acupuncturist may not be readily available. The need for an acupuncturist may also add to the cost of the procedure. There is no consensus or standardisation of electroacupuncture application and hence the acupoints and optimal duration of electroacupuncture prior to the procedure for maximal efficacy is uncertain. The anxiety, satisfaction, and willingness to repeat the procedure were not measured using a validated questionnaire and thus the results may not be reproducible.

Conclusions

Electroacupuncture reduced sedative and analgesic demands with low risk of adverse events and improved patient experience during EUS. Further studies are required to determine the optimal duration of electroacupuncture for the optimal efficacy.

Funding

This study was supported by the Health and Medical Research Fund, Food and Health Bureau, Hong Kong SAR Government (#11122771). The full report is available from the Health and Medical Research Fund website (<https://rfs1.fhb.gov.hk/index.html>).

Disclosure

The results of this research have been previously published in:

1. Teoh AYB, Chong CCN, Leung WW, et al. Electroacupuncture-reduced sedative and analgesic requirements for diagnostic EUS: a prospective, randomized, double-blinded, sham-controlled study. *Gastrointest Endosc* 2018;87:476-85.

References

1. Dill SG. Acupuncture for gastrointestinal disorders. *Probl Vet Med* 1992;4:144-54.
2. Leung WW, Jones AY, Ng SS, Wong CY, Lee JF. Electroacupuncture in reduction of discomfort associated with barostat-induced rectal distension--a randomized controlled study. *J Gastrointest Surg* 2011;15:660-6.
3. Ng SS, Leung WW, Mak TW, et al. Electroacupuncture reduces duration of postoperative ileus after laparoscopic surgery for colorectal cancer. *Gastroenterology* 2013;144:307-13.e1.
4. Standards of Practice Committee of the American Society for Gastrointestinal Endoscopy, Lichtenstein DR, Jagannath S, et al. Sedation and anesthesia in GI endoscopy. *Gastrointest Endosc* 2008;68:815-26.
5. Lee H, Ernst E. Acupuncture for GI endoscopy: a systematic review. *Gastrointest Endosc* 2004;60:784-9.

Tumour-shrinking decoction for symptomatic uterine fibroids: a double-blind, randomised, two-dose trial (abridged secondary publication)

W Meng ^{*}, L Lao, ZJ Zhang, WL Lin, YB Zhang, WF Yeung, YMB Yu, HYE Ng, JP Chen, J Su, JH Rong, PYF Lam, E Lee

KEY MESSAGE

Both low-dose and high-dose tumour-shrinking decoction could improve the uterine fibroid-related symptoms and reduce the fibroid size after 16 weeks of treatment.

Hong Kong Med J 2021;27(Suppl 2):S8-10

HMRF project number: 11121841

¹ W Meng, ¹ L Lao, ¹ ZJ Zhang, ² WL Lin, ¹ YB Zhang, ³ WF Yeung,

³ YMB Yu, ¹ HYE Ng, ¹ JP Chen, ¹ J Su, ¹ JH Rong, ¹ PYF Lam, ¹ E Lee

¹ LKS Faculty of Medicine, The University of Hong Kong

² Hong Kong Institute of Integrative Medicine, Faculty of Medicine, The Chinese University of Hong Kong

³ School of Nursing, The Hong Kong Polytechnic University

* Principal applicant and corresponding author: bmeng@hku.hk

Background

Uterine fibroids (UFs) are the most common benign tumours in women in the middle and later reproductive ages.¹ These women may experience irregular vaginal bleeding, heavy or painful periods, abdominal discomfort or bloating, painful defecation, back ache, urinary frequency or retention, miscarriage, premature labour, and even infertility, depending upon the location, size, and number of UFs. A formula called tumour-shrinking decoction (TSD) was developed for the treatment of UFs. The preliminary results from experimental and clinical studies^{2,3} and the empirical evidence from clinical practice have warranted a controlled trial to examine the effectiveness of TSD for treating UFs.

We hypothesised that TSD could effectively reduce the fibroid size and improve the symptoms associated with UFs, and its greater anti-tumour potency was associated with higher therapeutic doses. We aimed (1) to evaluate the efficacy and safety of TSD in the treatment of UFs, including alleviating the UF-related symptoms and reducing the fibroid size, (2) to verify if high dose is more effective than low dose, and (3) to explore the effect of the quality control of TSD on the clinical research.

Methods

This was a double-blind randomised controlled trial. A total of 78 women with symptomatic UFs were recruited and randomised to receive either low (69 g/day) or high (217 g/day) dose daily TSD for 16 weeks. The severity of UF-related symptoms and the quality of life were evaluated using the 37-item Uterine Fibroid Symptom Health-Related

Quality of Life Questionnaire (UFS-QOL). Blood loss, pelvic pain, traditional Chinese medicine (TCM) syndrome, magnetic resonance imaging (MRI) findings, serum concentrations of follicle-stimulating hormone, oestradiol, and haemoglobin were also assessed. Adverse events were closely monitored and recorded. The quality of the herbs in TSD was established using the ultra-performance liquid chromatography and high-performance liquid chromatography.

Results

Between May 2014 and May 2016, five (6.4%) of the 78 women dropped out. All the tested samples fulfilled the Hong Kong Chinese Materia Medica Standards. The linear mixed effects model showed no significant difference between the low-dose and high-dose groups in terms of symptom severity, health-related quality of life, pictorial blood assessment chart, and pelvic pain. Similar results were obtained after controlling for age, duration of illness, and co-medication. Therefore, high-dose group was not more efficacious than low-dose group in reducing UF symptoms, blood loss, pelvic pain, or improving quality of life across study time points.

There was significant within-group improvement from baseline to end-point in terms of UF-related symptoms, with the strongest effect on pelvic pain, followed by symptom severity, pictorial blood assessment chart, and quality of life. There was no significant between-group difference in follicle-stimulating hormone, oestradiol, haemoglobin, or pelvic MRI data (Table 1).

Both low-dose and high-dose groups had

reduction in the fibroids size. The low-dose group had significantly higher reduction of TCM syndrome score than the high-dose group ($P<0.01$), even after adjusting for age, duration of illness, and co-medication (Tables 2 and 3).

Discussion

Both low-dose and high-dose groups could effectively improve UF symptom severity, pelvic pain, TCM syndrome, and fibroids size after 16 weeks of treatment. Surprisingly, there was no significant difference in efficacy between the two groups; the low-dose TSD had similar efficacy as the high-dose one. There was significant improvement in quality of life and blood loss in the low-dose group. The dose-effect relationship of TSD was not proportional because the efficacy of the formula depends on the proper usage and combination of herbs according to the TCM theory of 'Jun-chen-zuo-shi' (ie, monarch, minister, assistant, and emissary) and syndrome differentiation. Reduction on routine drug dosage may be cost-effective by saving medicinal resource and decreasing the potential adverse reactions.

The amount of blood loss was counted using the pictorial blood assessment chart. After the treatment, the irregular bleeding condition was significantly improved. Most women had built up the menstrual cycle, with the menstrual period for about 7 days. Moreover, most women reduced the in-take amount of haemostatic Western medicine or even stop taking it. Therefore, with the function of tonifying Qi, resolving blood stasis, and reducing blood loss, TSD was effective in treating the symptomatic UFs.

About one-third of the women had menstrual pain and chronic pelvic pain. The causes of pain included oppression from UFs and complicating adenomyosis. Both low-dose and high-dose TSD could reduce the pelvic pain effectively. This indicated that the function of resolving blood stasis and dissipating binds of TSD played an important role in improving the pelvic microenvironment.

After the treatment, the UFs shrank or the rate of growth reduced, which was closely related to resolving blood stasis, softening the hardness, and dissipating binds of TSD. We speculate that the TSD has a regulatory role in cell signalling, cell cycle, gene transcription, and gene encoding of protein kinase activity in UFs, such as up-regulation of genes CYCS (which might be associated with apoptosis of leiomyoma), up-regulation of genes KLF6 (which inhibits the proliferation of leiomyoma cells), and regulation of cells proliferation and apoptosis of UFs through the pathways mediated by OP18.⁴

The treatment continued during the menstruation period as the efficacy of TSD was not achieved by suppressing the hormonal activity. This mechanism in treating UFs differs from that of

TABLE I. Results of Uterine Fibroid Symptom Health-Related Quality of Life Questionnaire, pictorial blood assessment chart, and pelvic pain across study time points

Variables	Low-dose group (n=39)*	Within-group effect size	High-dose group(n=39)*	Within-group effect size	P value for group by time interaction
Symptom severity					
Baseline	47.60±18.49		42.71±18.49		
2nd treatment	40.53±18.67	0.38	37.48±18.67	0.28	0.88
3rd treatment	38.77±18.86	0.47	35.86±19.05	0.36	0.75
4th treatment	36.39±18.86	0.60	29.11±19.17	0.72	0.71
5th treatment	33.54±18.86	0.75	29.39±19.30	0.70	0.40
End-point	33.30±19.30	0.76	28.99±19.11	0.73	0.96
Health-related quality of life					
Baseline	49.04±10.12		49.04±10.05		
2nd treatment	51.44±10.18	-0.24	49.73±10.12	-0.07	0.44
3rd treatment	52.70±10.30	-0.36	47.64±10.49	0.14	0.83
4th treatment	54.21±10.30	-0.51	52.78±10.55	-0.36	0.33
5th treatment	55.30±10.30	-0.61	52.93±10.68	-0.38	0.70
End-point	55.10±10.62	-0.58	52.74±10.55	-0.36	0.99
Pictorial blood assessment chart					
Baseline	471.49±316.43		397.64±316.43		
2nd treatment	338.69±321.12	0.42	345.39±319.68	0.16	0.31
3rd treatment	337.08±323.55	0.42	313.44±328.30	0.26	0.75
4th treatment	314.55±322.30	0.49	364.93±326.68	0.10	0.85
5th treatment	309.62±322.18	0.51	309.18±330.36	0.27	0.28
End-point	321.43±329.30	0.46	309.09±327.55	0.27	0.82
Pelvic pain					
Baseline	17.00± 10.80		14.49±10.80		
2nd treatment	11.30±10.99	0.52	7.98±10.99	0.60	0.38
3rd treatment	10.15±11.12	0.62	7.33±11.43	0.64	0.24
4th treatment	8.71±11.12	0.76	6.83±11.37	0.69	0.33
5th treatment	7.72±11.18	0.84	7.45±11.55	0.63	0.51
End-point	7.03±11.49	0.89	6.86±11.37	0.69	0.97

* Data are presented as mean ± standard deviation adjusted for last assessment time

Western medicine. TSD does not cause menopause, hot flashes, irritability, insomnia, or other adverse reactions. This study was an interdisciplinary collaboration between clinical researchers and basic science researchers. It demonstrates that it is possible to establish a quality-control programme to monitor the quality of polymedical preparations using botanical and chemical methods.

Conclusions

Both low-dose and high-dose TSD could improve the UF-related symptoms and reduce the fibroid size. There was significant improvement from baseline

TABLE 2. Results of traditional Chinese medicine syndrome, biomarkers, and magnetic resonance imaging (MRI) findings at baseline and end-point

Variables	Low-dose group (n=39)*	Within-group effect size	High-dose group (n=39)*	Within-group effect size	P value for group by time interaction
Traditional Chinese medicine syndrome					
Baseline	20.44±4.06		18.90±4.12		
End-point	12.22±4.12	2.01	12.64±4.18	1.51	0.024
Follicle-stimulating hormone, mIU/mL					
Baseline	9.51±9.06		11.24±9.06		
End-point	8.79±8.93	0.08	11.75±9.18	-0.06	0.61
Oestradiol, pg/mL					
Baseline	76.94±75.00		73.95±76.00		
End-point	78.51±75.00	-0.02	72.28±77.06	0.02	0.89
Haemoglobin, g/dL					
Baseline	10.54±2.25		10.79±2.25		
End-point	10.24±2.31	0.13	10.50±2.31	0.13	0.99
MRI fibroid, cm ³					
Baseline	154.39±273.28		258.83±277.03		
End-point	108.18±273.28	0.17	197.55±277.03	0.22	0.36
MRI uterus, cm ³					
Baseline	863.74±587.34		972.53±595.40		
End-point	735.85±587.34	0.22	875.79±595.40	0.16	0.29

* Data are presented as mean ± standard deviation

TABLE 3. Change from baseline to end-point in the low-dose and high-dose groups

Variable	Low-dose group					High-dose group				
	Baseline*	End-point*	t	df	P value	Baseline*	End-point*	t	df	P value
Symptom severity	44.82±16.59	30.96±16.71	4.42	31	<0.001	40.71±17.16	28.04±20.48	4.15	34	<0.001
Health-related quality of life	46.07±17.08	52.37±16.95	-3.06	31	0.004	53.45±15.82	56.87±22.57	-1.34	34	0.19
Pictorial blood assessment chart	474.91±391.28	322.84±279.62	3.22	31	0.003	336.41±227.07	264.21±227.67	1.67	33	0.11
Pelvic pain	17.69±14.96	7.28±9.33	4.34	31	<0.001	15.29±15.10	7.29±8.72	3.52	33	0.001
Traditional Chinese medicine syndrome	20.30±3.25	12.14±4.62	13.28	36	<0.001	18.44±3.98	12.35±4.40	10.21	33	<0.001
Follicle-stimulating hormone, mIU/mL	9.66±5.91	8.96±8.20	0.49	34	0.63	10.59±9.63	12.08±9.77	-0.74	31	0.47
Oestradiol, pg/mL	77.73±66.83	76.80±86.78	0.06	34	0.95	78.75±73.85	73.73±68.16	0.29	31	0.78
Haemoglobin, g/dL	10.48±2.11	10.19±2.49	1.20	36	0.24	10.81±2.21	10.51±2.31	1.41	34	0.17
MRI fibroid, cm ³	154.39±148.40	108.18±118.88	6.75	36	<0.001	258.83±391.07	197.55±311.88	4.05	35	<0.001
MRI uterus, cm ³	863.74±516.77	735.85±456.61	5.62	36	<0.001	972.53±675.11	875.79±618.72	5.22	35	<0.001

* Data are presented as mean ± standard deviation

2. Tan L, Meng W, Zhang TT. Predisposing factors of hysteromyoma and effect of hualiu recipe on it [in Chinese]. Zhongguo Zhong Xi Yi Jie He Za Zhi 2011;31:635-8.
3. Meng W, Zhao W. Effects of methods of invigorating qi and dissolving stasis on the expression of proliferating and apoptosis of cultured human uterine leiomyoma cells. Chin Arch Tradit Chin Med 2008;2:238-40.
4. Meng W, Li X, Lin WL, Tan L, Dong L. Impact of tumor-shrinking decoction (TSD) and its disassembled prescriptions in blood serum on gene expression in uterine fibroid cells. Cancer Oncol Res 2015;3:21-34.

Danshen Gegen capsule for intermittent claudication in patients with peripheral arterial disease: abridged secondary publication

BPY Yan ^{*}, KP Fung, P Chook, JCM Koon, JYW Chan

KEY MESSAGES

1. We demonstrated in vitro dose-dependent vasodilation and angiogenesis responses to Danshen and Gegen via endothelium-independent mechanism and involvement of inwardly rectifying K⁺ channels and Ca²⁺ channels.
2. We demonstrated an in vivo effect in functional limb recovery and in vitro improvement in blood micro-vessel density and blood perfusion responses to Danshen and Gegen in a limb ischaemic animal model.
3. Danshen and Gegen may be an effective treatment for patients with intermittent claudication, especially for those with severe symptoms

compared with placebo. However, longer-term research in a larger population is needed to determine its safety and efficacy.

Hong Kong Med J 2021;27(Suppl 2):S11-3

HMRF project number: 11120771

¹ BPY Yan, ^{2,3} KP Fung, ⁴ P Chook, ² JCM Koon, ² JYW Chan

The Chinese University of Hong Kong:

¹ Department of Medicine and Therapeutics, Prince of Wales Hospital

² Institute of Chinese Medicine

³ School of Biomedical Sciences

⁴ Centre for Clinical Trials on Chinese Medicine, Institute of Chinese Medicine

* Principal applicant and corresponding author: bryan.yan@cuhk.edu.hk

Introduction

The prevalence of peripheral arterial disease (PAD) secondary to lower limb arterial blockages is increasing.¹ Intermittent claudication is the most common manifestation of PAD and induces dysfunction and muscle pain (claudication pain). Claudication is associated with impairment in walking capacity and physical activity as well as quality of life including social functioning and emotional and mental health.² Effective pharmacotherapy for intermittent claudication is limited. Two traditional Chinese medicines—Danshen and Gegen (DG)—have shown positive therapeutic effect on vascular function and structure in patients with coronary artery disease.³ We hypothesised that a herbal formula consisting DG is an effective treatment for patients with PAD and symptomatic intermittent claudication.

Methods

We evaluated vasodilatory and angiogenic response to DG in an animal chronic limb ischaemic model and assessed efficacy and safety of DG in patients with PAD in a randomised placebo-controlled trial.

For in vitro vasodilation studies, rat femoral artery rings were used. Dose-dependent vasodilatory response to DG was tested with various ion-channel inhibitors. For in vivo studies, the hindlimb ischaemia rat model (right femoral artery ligation) was used to evaluate functional limb recovery and

blood perfusion increase in response to low dose (300 mg/mL) and high dose (600 mg/mL) DG for 28 days. Immunofluorescent and immunohistochemical assessments were performed to evaluate changes in muscle structure and angiogenesis.

A 24-week, prospective, randomised, double-blind, placebo-controlled study was approved by the Clinical Research Ethics Committee of Joint Chinese University of Hong Kong – New Territories East Cluster (reference: 2012.561-T) [ClinicalTrials.org. ID NCT 02380784]. Informed consent was obtained before the study. People aged ≥40 years with stable intermittent claudication (Rutherford class 1–3) secondary to PAD (resting ankle-brachial index <0.90 and a ≥10 mmHg decrease in ankle artery blood pressure after exercise) and without critical limb ischaemia, major lower limb amputation, or surgical or endovascular revascularisation for PAD within 3 months before enrolment were recruited. Patients were allocated at random to the treatment group (n=48) with daily oral DG capsules (1.5 g twice daily) or the control group with placebo (n=47). Primary outcome was the change in maximal walking distance (MWD) in a standardised graded treadmill test (Gardener Protocol), defined as total distance walked from beginning treadmill walking until the subjects can walk no further. Secondary outcomes included changes in pain-free walking distance (PFWD), defined as the distance walked at the onset of claudication. Functional status, quality-of-life, and pro-inflammatory biomarkers including

C-reactive protein, interleukin-6, tumour necrosis factor alpha (TNF- α) were assessed.

Results

In *in vitro* vasodilation studies, endothelium-independent mechanism was shown to involve in the response to DG in a dose-dependent manner. Involvement of both inwardly rectifying K⁺ channel and Ca²⁺ channels in the mechanism of vasodilatory response to DG was confirmed. In the *in vivo* hindlimb ischaemia rat model, significant improvement in functional limb recovery including positive change in maximum contact area, stance phase duration, and print area was observed in DG groups at high and low doses at week 28. Blood perfusion ratio of both DG treatment groups was significantly higher at the end of study. In addition, low dose DG was associated with a significant increase in capillary density, whereas high dose DG achieved a two-fold increase compared with the control group.

Of 95 patients randomly allocated to the treatment group (n=48) or the control group (n=47), 17 (17.9%) dropped out (Fig). Baseline characteristics of patients in both groups were comparable. Overall compliance of patients reached 94.8%. After the 24-week intervention, a significant proportion of participants in the treatment group showed improvement in MWD and PFWD. Considering >50% improvement in walking distance as a clinically meaningful benefit, the proportion of patients who achieved ≥50% improvement in either PFWD or MWD was significantly higher in the treatment group (43.2% vs 22.0%, P=0.044). Significant increase in PFWD was observed in the treatment group after

24-week (P=0.033) and after log transformation, with a 6.8% increase (P=0.075) [Table]. However, the two groups were comparable in terms of the absolute (P=0.287) and the log transformed increases in PFWD (P=0.299).

Subgroup analysis was performed based on patients' baseline walking capacity on an exercise treadmill. Patients with moderate to severe intermittent claudication (baseline MWD <200 m) improved in terms of % change in log-transformed PFWD, compared with placebo (9.9% vs -0.4%, P=0.072), whereas patients with baseline MWD ≥200m did not improve significantly, compared with placebo (P=0.736, Table).

Although ankle-brachial index improved by 23.6% in the treatment group (P=0.029), the two groups were not significantly different in improvement (P=0.213). There were no significant changes in pulse wave velocity within or between groups. There was no significant change in self-perceived quality of life or functional status. The two groups were comparable in terms of results of haematology tests and serum chemistry tests, including lipid profiles. Both plasma interleukin-6 (P=0.011) and plasma TNF- α (P=0.011) levels changed significantly in the treatment group, but the two groups were marginally significantly different in terms of change in plasma TNF- α level (P=0.072).

Discussion

In *in vitro* studies, vasodilation effect of DG was demonstrated in the rat femoral arteries in a dose-dependent manner. Therefore, we speculated that DG could be beneficial to PAD patients to improve the tissue perfusion by dilating the femoral artery and microvasculature. Identifying the involvement of the inwardly rectifying K⁺ channels and Ca²⁺ channels in the vasodilatory response of DG may help subsequent modification on the herbal formula of the capsule for optimising its efficacy. In *in vivo* studies, DG were found to be effective for functional limb recovery in rats with hindlimb femoral artery ligation. The significant improvement was associated with positive changes on blood perfusion and microvessel density after DG treatment.

In patients with PAD, a significant proportion of patients in the treatment group showed a positive response in MWD and PFWD, but the degree of improvement was not significant. The beneficial impact of DG may have been diluted owing to wide variation in baseline walking distances (ie, type II error). Moreover, the study duration of 24 weeks may be insufficient owing to the highly variable onset of clinical responses reported by the patients. Using walking distances as examples, the ranges observed in treatment group (MWD: -55.7% to 276.2%; PFWD: -74.4% to 421.6%) were wider than that in control group (MWD: -56.1% to 197.8%;

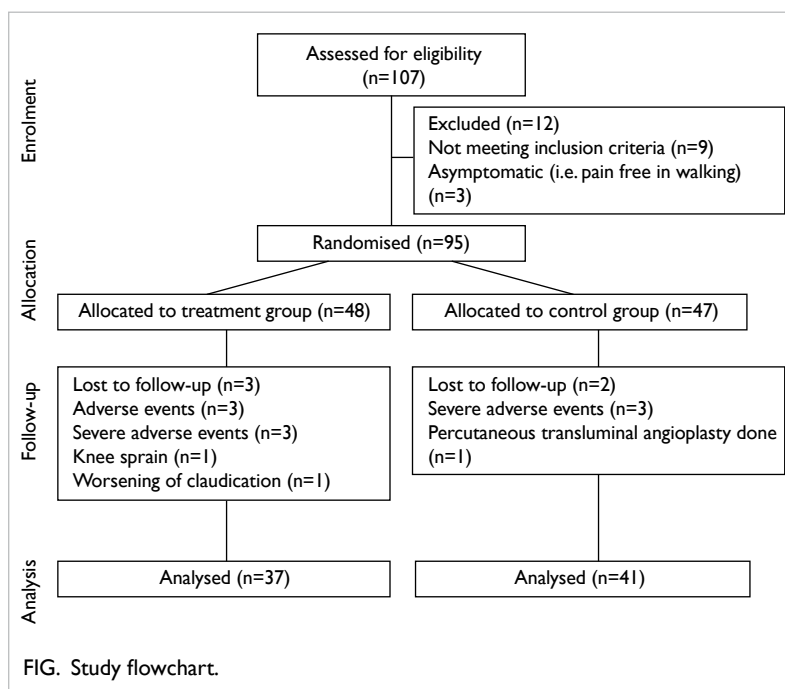


FIG. Study flowchart.

TABLE. Subgroup analysis on maximal walking distance and pain-free walking distance with patients stratified by severity of claudication.

Claudication	Treatment (n=37)							Control (n=41)							Between-group comparison
	Baseline	Week 24	Absolute change	% Change	P value	P value (moderate vs mild)	Baseline	Week 24	Absolute change	% Change	P value	P value (moderate vs mild)	P value		
Maximal walking distance															
Distance, m															
Moderate	119.6±45.2	173.7±111.8	54.1±97.1	43.1±92.8	0.030	0.362	137.0±37.4	162.9±111.6	25.9±99.7	17.0±62.8	0.984	0.514	0.248		
Mild	388.9±180.3	389.9±184.4	1.1±157.1	6.2±44.7	0.977		395.2±147.8	439.0±220.4	43.8±144.2	10.8±40.0	0.217		0.731		
Natural log transformation															
Moderate	4.7±0.4	4.9±0.8	0.2±0.6	3.6±13.0	0.306	0.288	4.9±0.3	4.9±0.6	0.1±0.4	1.0±9.0	0.608	0.549	0.520		
Mild	5.9±0.4	5.9±0.5	0.0±0.4	-0.2±7.0	0.852		5.9±0.3	6.0±0.5	0.0±0.4	0.6±6.6	0.647		0.653		
Pain-free walking distance															
Distance, m															
Moderate	65.4±25.2	110.3±74.4	45.6±72.3	87.2±143.8	0.023	0.249	73.0±36.7	61.1±25.1	-8.0±35.1	7.6±60.3	0.335	0.044	0.064		
Mild	148.3±126.1	154.6±162.2	8.9±88.5	40.6±109.3	0.381		107.9±58.1	154.8±115.8	46.9±98.1	47.7±90.9	0.025		0.758		
Natural log transformation															
Moderate	4.1±0.4	4.5±0.8	0.4±0.7	9.9±18.5	0.051	0.339	4.2±0.6	4.0±0.4	-0.1±0.6	-0.4±14.5	0.569	0.060	0.072		
Mild	4.7±0.8	4.8±0.7	0.1±0.7	3.8±17.8	0.603		4.6±0.5	4.8±0.6	0.3±0.5	6.1±10.1	0.015		0.736		

PFWD: -59.9% to 355.0%). In subgroup analysis, patients with more severe intermittent claudication symptoms at baseline showed significant positive responses to DG, compared with those with mild claudication. Therefore, further longer-term study in patients with severe walking impairment and more restricted distance (eg, <200 m) is warranted.

Conclusion

We demonstrated positive dose-dependent vasodilation and angiogenesis responses to DG via endothelium-independent mechanism. We also demonstrated beneficial effects of DG in functional limb recovery in an in vivo hindlimb ischaemia animal model and significant in vitro improvement in blood microvessel density and blood perfusion rate. DG may be an effective treatment for patients with intermittent claudication, especially for those with severe symptoms. However, longer-term research in a larger population is needed to determine its safety and efficacy.

Acknowledgements

We thank Professor Ping-Chung Leung for design of the preclinical study and preparation of study drugs; Dr Wai-Chun Au for patient evaluation and

assessment; Dr Yuk-Hoi Lam, Dr Ying-Fune Yeung, and Dr Chi-King Micah Chan for subject screening; Dr GuangMing Tan for performing physical examination and providing medical care to patients when necessary.

Funding

This study was supported by the Health and Medical Research Fund, Food and Health Bureau, Hong Kong SAR Government (#11120771). The full report is available from the Health and Medical Research Fund website (<https://rfs1.fhb.gov.hk/index.html>).

References

- Criqui MH, Fronek A, Barrett-Connor E, Klauber MR, Gabriel S, Goodman D. The prevalence of peripheral arterial disease in a defined population. *Circulation* 1985;71:510-15.
- McDermott MM, Liu K, Greenland P, et al. Functional decline in peripheral arterial disease: associations with the ankle brachial index and leg symptoms. *JAMA* 2004;292:453-61.
- Tam WY, Chook P, Qiao M, et al. The efficacy and tolerability of adjunctive alternative herbal medicine (*Salvia miltiorrhiza* and *Pueraria lobata*) on vascular function and structure in coronary patients. *J Altern Complement Med* 2009;15:415-21.

Inflammatory properties of ribosome-inactivating protein momorcharin derived from bitter melon: abridged secondary publication

YJ Chen, ZL Yu, AKW Tse *

KEY MESSAGES

1. The inflammatory responses induced by alpha-momorcharin (α -MMC) derived from *Momordica charantia* (bitter melon) were studied.
2. α -MMC induced cytokines release in human monocytic THP-1 cells.
3. α -MMC-induced inflammatory gene expression were mediated by activation of IKK-NF- κ B and JNK pathways.

4. α -MMC induced inflammatory responses in vivo.

Hong Kong Med J 2021;27(Suppl 2):S14-7

HMRF project number: 11122441

YJ Chen, ZL Yu, AKW Tse

School of Chinese Medicine, Hong Kong Baptist University

* Principal applicant and corresponding author: anfernee@hkbu.edu.hk

Introduction

Ribosome-inactivating proteins (RIPs) are a family of highly potent protein toxins that inhibit protein synthesis by inactivating the ribosomes or by modification of factors involved in translation.¹ The biological activity of RIPs is not completely clarified and, sometimes, independent of the inhibition of protein synthesis. One important biological activity of RIPs is production of cytokines, which may be released by macrophages and inflammatory reactions.² The mechanism of cytokines induction by RIPs is not fully understood. A significant role played by RIPs in inflammation is the activation of kinases (JNK, p38, and MAPK) and key inflammatory regulating transcription factors (NF- κ B, AP-1).

RIPs are almost ubiquitous among plants and are distributed in different plant tissues (seed, leaf, sarcocarp, bark).² RIPs may undergo degradation under high cooking temperature. RIPs can be found in edible plant materials and eaten raw by humans or animals, including plant tissues (such as *Allium coepa*, *Spinacia oleracea*, *Apium graveolens*, *Daucus carota*, *Cucurbita moschata*) and plant organs (such as the seeds of *Lycopersicon esculentum*). The ground powder of the seeds of *Momordica charantia* (bitter melon) contains RIPs such as α - and β -momorcharin (MMC)³ and is commonly used to lower blood pressure, cholesterol level, and blood glucose. Immune-related adverse effects of the seeds of *Momordica charantia* (bitter melon) have been reported,³ but no large-scale studies have been undertaken to establish its safety and potential adverse effects when taken as a nutritional

supplement. We proposed a preclinical study to determine the inflammatory responses induced by recombinant α -MMC using cell culture and animal models. We aimed to define the underlying molecular mechanisms of how α -MMC induces cytokines production.

Methods

This study was conducted from March 2014 to May 2016. Recombinant α -MMC was generated in *Escherichia coli* Rosetta (DE3) pLysS strain and purified by nickel-nitrilotriacetic acid affinity chromatography. Recombinant α -MMC solutions were passed twice through Zeba spin desalting columns and high capacity endotoxin removal spin columns to remove imidazole and endotoxin residues, respectively. Endotoxin contamination was kept below the detection limit of LAL chromogenic endotoxin quantitation kit (Thermo Scientific). The concentration and purity of recombinant α -MMC protein were analysed by SDS-PAGE.

The cytokines concentrations in cell culture supernatants were measured using the human ELISA Kit (eBioscience), and the protein concentrations of corresponding cell extracts were measured using the Bradford method. The cytokines concentrations in mouse serum and duodenum extracts were measured using the mouse ELISA Kit (eBioscience).

Total RNA was extracted using the TRIzol reagent (Invitrogen), and reverse transcription was conducted. cDNA products were analysed using the Human Inflammatory Response & Autoimmunity RT² Profiler PCR Array following the manufacturer's

instruction. Alternatively, real-time PCR on cDNA was carried out in an Applied Biosystems ViiA 7 real-time PCR machine using SYBR Green assays.

Male mice were intragastrically administered with either 6 mg α -MMC/kg/day and saline or saline alone. At the end of treatment, retro-orbital blood samplings under anaesthesia were performed, and sera were collected by centrifugation. Duodenum tissues were dissected and homogenised in ice-cold saline using an ultra-Turrax T-25 homogeniser and then sonicated.

Results

Ribosome-inactivating protein and related proteins can induce activation of IKK-NF- κ B pathway.⁴ After a 60-minute treatment, α -MMC caused a rapid degradation of I κ B α , followed by a slow but dramatic restoration of the I κ B α level at 120 minutes (Fig 1a). Moreover, α -MMC induced p65 levels in the nucleus. Treatment of cells with specific IKK β inhibitors (TPCA-1, SC-514, or BMS-345541) suppressed the α -MMC-induced IL-1 β protein expression (Fig 1b). An IKK β inhibitor TPCA-1 inhibited α -MMC-induced p65 nuclear translocation (Fig 1c), cytokine secretion (Fig 1d), and cytokine mRNA levels (Fig 1e). Taken together, these results suggest that activation of IKK-NF- κ B pathway is indispensable for α -MMC inflammatory action.

A significant role in the inflammatory responses of RIPs is played by the activation of MAPK kinases pathway (including JNK, p38 and ERK).⁵ We detected elevated levels of JNK, but not p38 or ERK, in THP-1 cells treated with α -MMC (Fig 2a). To test whether cytokine expression in response to α -MMC is dependent on JNK activation, we treated THP-1 cells with SP600125 for 30 minutes before the addition of α -MMC. Treatment of JNK inhibitor SP600125 inhibited α -MMC-induced IL-1 β protein expression (Fig 2a), cytokine secretion (Fig 2c), and cytokine mRNA levels (Fig 2d). Overall, these results indicate that activation of JNK pathway is essential for α -MMC-induced inflammatory responses.

To determine whether intragastric administration of α -MMC in mice leads to elevated levels of cytokines in serum and duodenum, four groups of mice treated with vehicle control, TPCA-1 alone, α -MMC alone, or TPCA-1 with α -MMC were exsanguinated at the end of treatment. The serum and duodenum levels of IL-1 β , TNF- α , and MCP-1 protein were up-regulated upon α -MMC treatment, and these effects were inhibited by co-administration of IKK β inhibitor TPCA-1 (Fig 3). These data suggest that the α -MMC induces inflammatory responses *in vivo*.

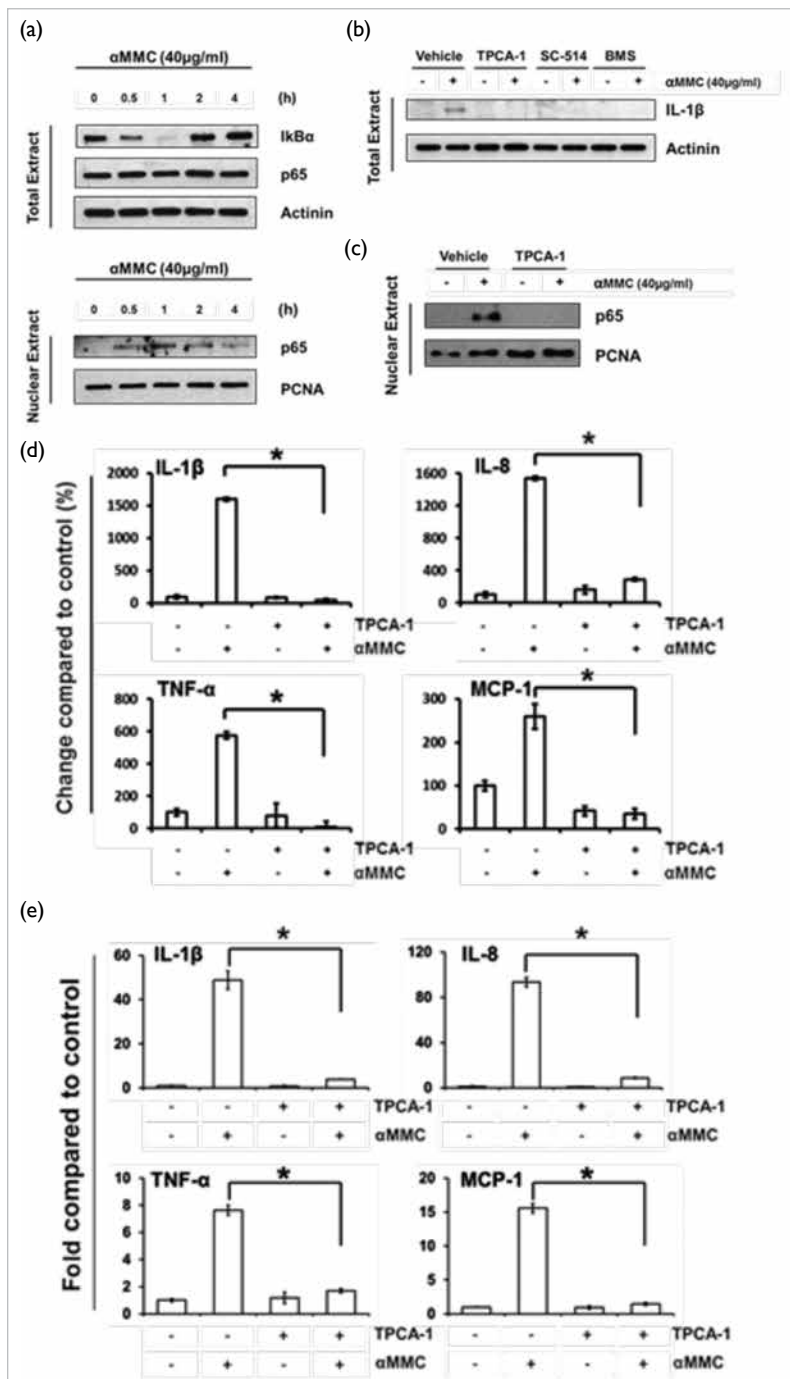


FIG 1. NF- κ B activation is essential for α -MMC-induced inflammatory responses in THP-1 cells. (a) THP-1 cells are treated with α -MMC, and the level of I κ B α and p65 protein in the whole cell, and lysates and p65 protein in the nuclei are assayed by western blotting. (b) THP-1 cells are pretreated with TPCA-1 (5 μ M), SC-514 (50 μ M), BMS-345541 (2.5 μ M) for 30 minutes and then further treated with or without α -MMC (40 μ g/mL) for 24 hours. Whole-cell extracts are analysed for protein expression levels of IL-1 β by western blotting. (c) THP-1 cells are exposed to vehicle or α -MMC (40 μ g/mL) for 24 hours after pretreatments with or without 5 μ MTPCA-1 for 30 minutes. Western blot analysis of nuclei p65 is shown. (d & e) THP-1 cell cultures are pretreated with TPCA-1 (5 μ M) for 30 minutes, followed by the addition of α -MMC (40 μ g/mL) and incubation for 24 hours. (d) The secretion levels of indicated pro-inflammatory cytokines in the cell culture supernatant are examined using corresponding ELISA kits. (e) The mRNA level of the four pro-inflammatory cytokines is analysed by real-time PCR.

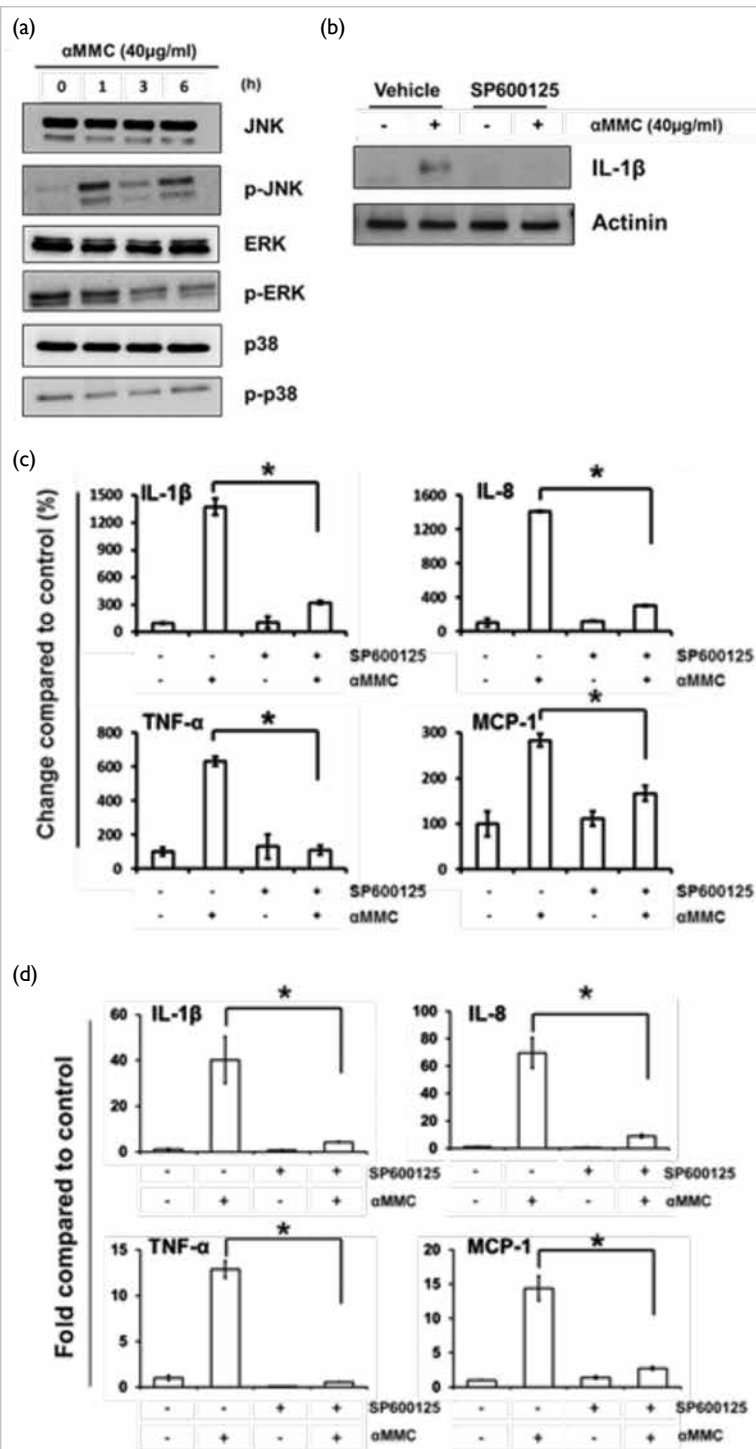


FIG 2. JNK activation is essential for α-MMC induced inflammatory responses in THP-1 cells. (a) THP-1 cells are treated with α-MMC and the whole-cell extracts are subjected to western blot analysis using JNK, ERK, and p38 antibodies and their respective phospho-specific antibodies. (b) THP-1 cells are pretreated with 15 µM SP600125 for 30 minutes, followed by the addition of α-MMC (40 µg/ml) and incubation for 24 hours. Whole-cell extracts are analysed for protein expression levels of IL-1β by western blotting. (c & d) THP-1 cells are exposed to vehicle or α-MMC (40 µg/ml) for 24 hours after pretreatments with or without 15 µM SP600125 for 30 minutes. (c) Levels of IL-1β, IL-8, TNFα, and MCP-1 in the culture medium of THP-1 cells are detected by ELISA. (d) The mRNA level of the indicated cytokines is analysed by real-time PCR.

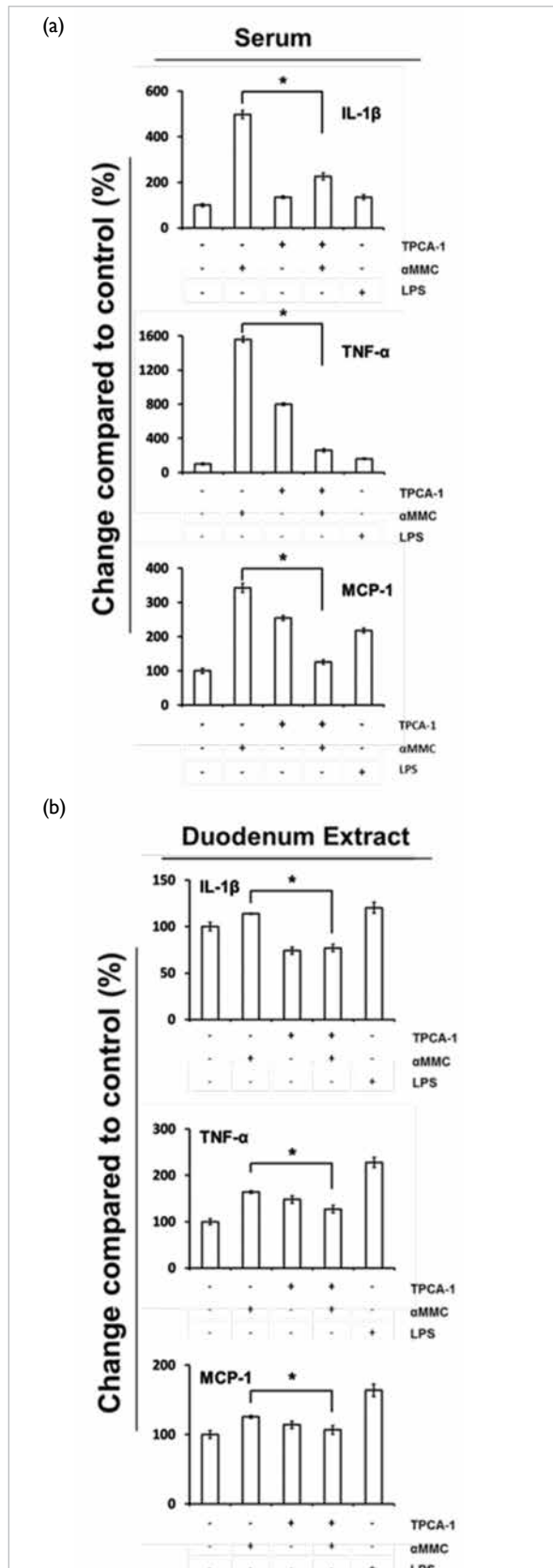


FIG 3. Inflammatory gene expression in mouse after administration of α-MMC and α-MMC plus TPCA-1. Mice are treated with α-MMC (6 mg/kg), TPCA-1 (15 mg/kg), or their combination for 3 consecutive days. LPS (10 mg/kg) is used as positive control. Levels of IL-1β, IL-8, TNFα, and MCP-1 in (a) sera and (b) duodenum extracts are detected by ELISA.

Discussion

Several RIPs have been reported to induce secretion of cytokines. We report that α -MMC, a ribosome-inactivating protein alpha-momorcharin derived from *Momordica charantia* (bitter melon), induces the release of cytokines including IL-1 β , IL-8, TNF- α , MCP-1 in human peripheral-blood mononuclear cells. IL-1 β , TNF- α , and MCP-1 were detected in the plasma and duodenum of α -MMC-treated mice. There are a number of reported immune-related adverse effects of the seeds of *Momordica charantia* (bitter melon).³ Our results suggest that these cytokines produced by α -MMC may contribute to the pathogenesis and other effects after α -MMC poisoning.

The results can enhance our understanding of the function of RIPs and their possible involvement in inflammatory-related diseases. Importantly, these results support the establishment of guidance for the safe use of RIP-containing edible plant materials. Moreover, characterising new RIPs or homogeneous recombinant RIPs may play important roles in cancer treatment, immunotherapy, and treatment of viral diseases.

Taken together, the present study demonstrates that α -MMC induces inflammatory responses via activation of IKK-NF- κ B and JNK MAPK activities in a mouse model and in vitro monocytes.

Acknowledgement

We thank the technical staff in the School of Chinese Medicine, Hong Kong Baptist University for their expertise in all experiments.

Funding

This study was supported by the Health and Medical Research Fund, Food and Health Bureau, Hong Kong SAR Government (#11122441). The full report is available from the Health and Medical Research Fund website (<https://rfs1.fhb.gov.hk/index.html>).

Disclosure

The results of this research have been previously published in:

- Chen YJ, Zhu JQ, Fu XQ, et al. Ribosome-inactivating protein α -momorcharin derived from edible plant *Momordica charantia* induces inflammatory responses by activating the NF- κ B and JNK pathways. *Toxins* 2019;11:694.

References

- Puri M, Kaur I, Perugini MA, Gupta RC. Ribosome-inactivating proteins: current status and biomedical applications. *Drug Discov Today* 2012;17:774-83.
- Barbieri L, Battelli MG, Stirpe F. Ribosome-inactivating proteins from plants. *Biochim Biophys Acta* 1993;1154:237-82.
- Basch E, Gabardi S, Ulbricht C. Bitter melon (*Momordica charantia*): a review of efficacy and safety. *Am J Health Syst Pharm* 2003;60:356-9.
- Korcheva V, Wong J, Corless C, Iordanov M, Magun B. Administration of ricin induces a severe inflammatory response via nonredundant stimulation of ERK, JNK, and P38 MAPK and provides a mouse model of hemolytic uremic syndrome. *Am J Pathol* 2005;166:323-39.
- Li M, Chen F, Liu CP, et al. Dexamethasone enhances trichosanthin-induced apoptosis in the HepG2 hepatoma cell line. *Life Sci* 2010;86:10-6.

Combination of atorvastatin or hydrochlorothiazide/amlodipine with *Salvia miltiorrhiza* (Danshen) and *Pueraria lobata* (Gegen) for atherosclerosis, hyperlipidaemia, and hypertension: a preclinical in vivo study (abridged secondary publication)

DWS Cheung, JCM Koon, PH Wong, KC Yau, ECL Wat, JYW Chan, VKM Lau, ECH Ko, MMY Waye,
KP Fung *

KEY MESSAGES

1. Water extract of Danshen and Gegen (DG) was found to be a potent alternative medicine for atherosclerosis, hyperlipidaemia, and hypertension.
2. Combination of DG and atorvastatin could prevent atherosclerosis and reduce hyperlipidaemia.
3. Combination of DG and hydrochlorothiazide/amlodipine could ameliorate hypertension.
4. DG could help to attenuate adverse effects resulting from atorvastatin or hydrochlorothiazide/amlodipine medication.

Hong Kong Med J 2021;27(Suppl 2):S18-22

HMRF project number: 11120841

¹ DWS Cheung, ^{2,3} JCM Koon, ¹ PH Wong, ¹ KC Yau, ^{2,3} ECL Wat, ^{2,3,4} JYW Chan, ^{2,3} VKM Lau, ^{2,3} ECH Ko, ^{1,4,5} MMY Waye, ^{1,2,6} KP Fung

The Chinese University of Hong Kong:

¹ School of Biomedical Sciences, Faculty of Medicine

² Institute of Chinese Medicine

³ State Key Laboratory of Research on Bioactivities and Clinical Applications of Medicinal Plants

⁴ The Nethersole School of Nursing, Faculty of Medicine

⁵ The Croucher Laboratory for Human Genomics

⁶ School of Chinese Medicine, Faculty of Medicine

* Principal applicant and corresponding author: kpfung@cuhk.edu.hk

Introduction

Most cardiovascular diseases are caused by atherosclerosis secondary to build-up of fatty streaks on the innermost layer. Risk factors include hypertension and hyperlipidaemia. Medications for cardiovascular diseases may have adverse effects. Atorvastatin (AS) is a lipid-lowering drug that has been reported to induce liver problems (indicated by elevated aspartate aminotransferase and alanine transaminase levels) and damage to skeletal muscles (indicated by elevated creatine kinase level). Medications for hypertension are mainly diuretic drugs (ie, hydrochlorothiazide [HCT]) and calcium channel blocker (ie, amlodipine [ADP]). Nonetheless, HCT may cause hypokalaemia, hyperuricaemia, hyperglycaemia, and hyperlipidaemia. ADP may induce peripheral oedema, fatigue, dizziness, nausea, palpitations, and abdominal pain. A herbal formula containing water extract of Danshen and Gegen (DG) [7:3, w/w] has pleiotropic beneficial effects on coronary patients and menopausal women with hypocholesterolaemia.^{1,2} DG is considered safe for clinical use as no adverse effect has been reported in clinical trials. DG in combination with AS or HCT/ADP may yield better treatment effects while reducing adverse effects. This study aimed to verify this hypothesis in animal studies.

Methods

AS, HCT, and ADP were purchased from Pharmasolution (HK). The dried root and rhizome of *Salvia miltiorrhiza* Bunge (Danshen) and the dried root of *Pueraria lobata* (Willd) Ohwi (Gegen) were purchased from a local supplier. The water extract of DG (7:3, w/w) was prepared by boiling with water twice for 1 hour and 0.5 hours, respectively. The water extract was concentrated and lyophilised into powder. Ultra-performance liquid chromatography analysis of DG identified five hydrophilic compounds, including salvianolic acid B (4.367%), puerarin (2.193%), daidzin (0.554%), daidzein (0.159%), and protocatechuic aldehyde (0.047%).³

Male Sprague-Dawley (SD) rats, Wistar-Kyoto (WK) rats, spontaneously hypertensive (SH) rats, and C56BL/6 mice were supplied by the Laboratory Animal Service Centre of The Chinese University of Hong Kong. All protocols of animal research have been approved by the Animal Research Ethics Committee of the university. Animals were kept in a 12-hour circadian cycle and were supplied with food and water *ad libitum*.

For the restenosis study, the carotid artery of SD rats was induced by balloon injury.⁴ Those rats then received drug treatments for 14 days. For the hyperlipidaemia study, C56BL/6 mice were given

a high-fat diet (22% fat and 0.15% cholesterol) for 8 weeks before drug treatments and for another 8 weeks with a high-fat diet feeding concomitantly. For the hypertension study, systolic blood pressure (SBP) of WK and SH rats was measured weekly from 6 weeks old with tail cuffs (CODA system, Kent Scientific, USA). Drug treatments were given to those rats from 9 weeks old for 16 weeks.

Plasma was collected and biochemically assayed for levels of total cholesterol (TC), triglyceride (TG), low-density lipoprotein-cholesterol (LDL-C), high-density lipoprotein-cholesterol (HDL-C), glucose, creatinine, albumin, urea nitrogen, uric acid, aspartate aminotransferase, alanine transaminase, and creatine kinase using commercial kits. Insulin level was determined using ELISA kits.

Carotid arteries of SD rats and livers of C57BL/6 mice were fixed with 4% paraformaldehyde and were sectioned at 5 μ M. Sectioned carotid arteries were immunohistochemically stained with primary antibody against smooth muscle cell α -actin. Sectioned livers were stained with haematoxylin and eosin. Liver fat vacuoles were quantified with ImageJ computer software.

Results

After balloon injury-induced intima/media thickening of carotid arteries, an induced layer known as neointima was clearly shown in the innermost intima layer of the arterial wall (Fig 1). The neointima was mainly composed of massive proliferation of underlying vascular smooth muscle cells as vascular smooth muscle cell α -actin was seen in the neointima (Fig 1). DG 300 mg/kg reduced neointima/media ratio by $10.99\% \pm 1.72\%$, compared with control without medication. AS 40 mg/kg showed no treatment effect on intima/media thickening, whereas AS 80 mg/kg reduced neointima/media ratio by $1.14\% \pm 0.14\%$, compared with control without medication. Combination of AS with DG resulted in stronger treatment effect on reducing neointima/media ratio than did AS alone. AS 40 mg/kg plus DG 300 mg/kg or AS 80 mg/kg plus DG 300 mg/kg reduced neointima/media ratios by $12.81\% \pm 1.73\%$ or $36.14\% \pm 3.86\%$ more than did AS 40 mg/kg or AS 80 mg/kg alone, respectively.

The effects of combined medication of DG and AS on the lipid profile of C57BL/6 mice have been published by us.⁵ Compared with normal diet, high-fat diet caused an increase in plasma TC and TG levels. Single medications of DG 600 mg/kg, AS 8 mg/kg, and AS 16 mg/kg decreased plasma TC and TG levels, compared with controls with fed high-fat diet only. Combined medications (AS 8 mg/kg plus DG 600 mg/kg and AS 16 mg/kg plus DG 600 mg/kg) had stronger effects on decreasing plasma TC and TG levels than did single medications of AS 8 mg/kg and AS 16 mg/kg.

Plasma LDL-C and HDL-C levels were higher in mice fed with high-fat diet than those fed with normal diet. Single medications (DG 600 mg/kg, AS 8 mg/kg, and AS 16 mg/kg) and combined medications (AS 8 mg/kg plus DG 600 mg/kg and AS 16 mg/kg plus DG 600 mg/kg) reduced plasma LDL-C level, compared with controls fed with high-fat diet only. Combined medications reduced plasma LDL-C level more than did single medications of AS 8 mg/kg and AS 16 mg/kg. Plasma HDL-C level slightly increased in groups of AS 8 mg/kg, AS 16 mg/kg, and AS 16 mg/kg plus DG 600 mg/kg, compared with the high-fat diet group, but decreased in groups of DG 600 mg/kg and AS 16 mg/kg plus DG 600 mg/kg.

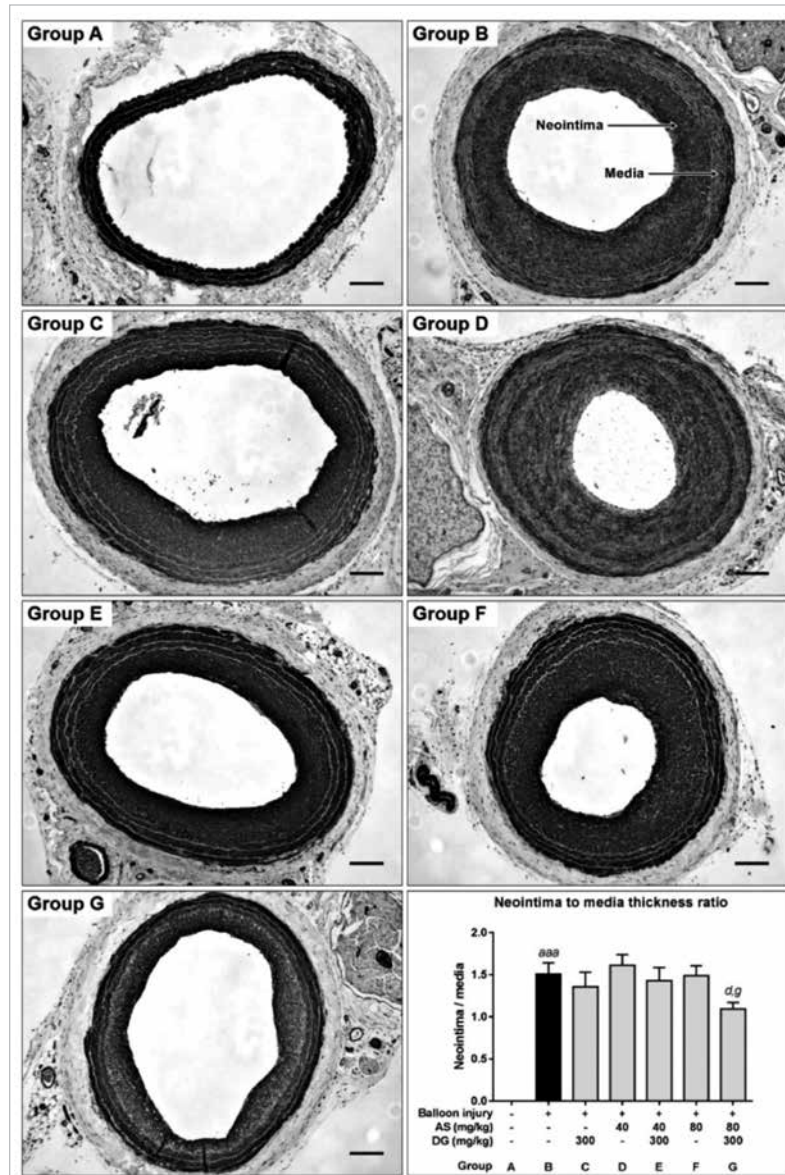


FIG 1. Micrographs showing carotid arteries of Sprague-Dawley rats with/without balloon injury surgery. Sectioned carotid arteries are stained with immunohistochemical staining with antibody against vascular smooth muscle cell α -actin ($\times 50$, scale bar = 100 μ m).

Rats fed pharmacologically high doses of AS 320 mg/kg had approximately three-fold elevation in aspartate aminotransferase and alanine transaminase levels and more than four-fold elevation in creatine kinase level, compared with control without medication (Fig 2). However, rats fed AS 320 mg/kg plus DG 600 mg/kg showed lower aspartate aminotransferase, alanine transaminase, and creatine kinase levels than those fed AS alone.

At baseline, SH rats exhibited generally higher SBP than WK rats (162±2 to 177±7 mmHg vs 137±4 mmHg, Fig 2). Drug treatments were given the next day after SBP measurement in the third week. Medication with HCT 15.6 mg/kg plus ADP 6 mg/kg for 1 week significantly reduced SBP of SH rats (108±9 mmHg). Half doses of HCT and ADP in combination with DG also reduced SBP. Reduction in SBP persisted in a treatment course of 16 weeks with HCT 15.6 mg/kg plus ADP 6 mg/kg (99±5 to 123±8 mmHg), HCT 7.8 mg/kg plus ADP 3 mg/kg plus DG 600 mg/kg (101±10 to 135±13 mmHg), and HCT 7.8 mg/kg plus ADP 3 mg/kg plus DG 1200 mg/kg (101±7 to 128±11 mmHg). SBP of WK rats throughout the treatment course was 133±5 to 145±5 mmHg.

Untreated SH rats had lower TC level than WK rats (28.52±1.45 mg/dL vs 49.15±2.12 mg/dL, Fig 3). TC level was elevated in SH rats receiving HCT 15.6 mg/kg plus ADP 6 mg/kg for 16 weeks (30.97±2.65 mg/dL), compared with control. Half doses of HCT and ADP in combination with DG 600 or 1200 mg/kg resulted in decreased TC

level to 19.51±1.56 mg/dL and 18.8±1.69 mg/dL, respectively. Similarly, TG level was lower in untreated SH rats than in WK rats (8.2±0.48 mg/dL vs 12.88±1.12 mg/dL, Fig. 3). Medication with HCT 15.6 mg/kg plus ADP 6 mg/kg elevated TG level (9.56±1.04 mg/dL) in SH rats, compared with control. Half doses of HCT and ADP in combination with DG 600 or 1200 mg/kg resulted in decreased TG level to 7.21±1.04 mg/dL and 7.11±0.92 mg/dL, respectively.

LDL-C and HDL-C levels in SH rats were lower than in WK rats (31.55±3.24 mg/dL vs 79.16±11.05 mg/dL and 30.74±0.84 mg/dL vs 58.3±3.34 mg/dL, respectively, Fig 3). LDL-C and HDL-C levels were elevated in SH rats receiving HCT 15.6 mg/kg plus ADP 6 mg/kg for 16 weeks (44.65±3.66 mg/dL and 31.04±0.49 mg/dL, respectively). Half doses of HCT and ADP in combination with DG 600 or 1200 mg/kg decreased LDL-C level to 40.48±3.66 mg/dL and 32.01±3.7 mg/dL, respectively, and HDL-C level to 29.9±1.37 mg/dL and 28.4±1 mg/dL, respectively.

Glucose level was lower in untreated SH rats than in WK rats (118.4±4.29 mg/dL vs 135.9±3.74 mg/dL, Fig 3). HCT 15.6 mg/kg plus ADP 6 mg/kg elevated glucose level to 129.3±6.7 mg/dL, compared with control. Half doses of HCT and ADP in combination with DG 600 or 1200 mg/kg elevated glucose level to 132.6±5.78 mg/dL and 133.5±3.49 mg/dL, respectively, which were greater than that in full doses of HCT and ADP.

Insulin level in untreated SH rats and

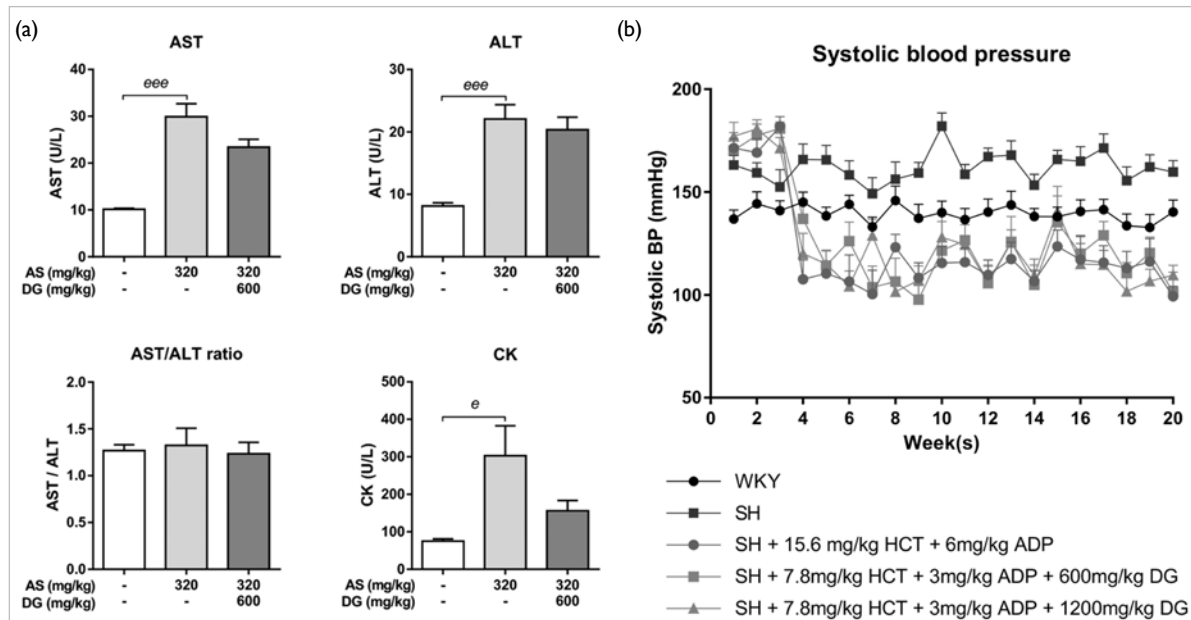


FIG 2. (a) Blood parameters of aspartate aminotransferase (AST), alanine transaminase (ALT), and creatine kinase (CK) levels of Sprague-Dawley rats fed with high doses of atorvastatin (AS), Danshen and Gegen (DG), or both, and (b) blood pressure of spontaneously hypertensive (SH) rats and Wistar-Kyoto (WK) rats.

WK rats was comparable (3.75 ± 0.79 ng/mL vs 3.87 ± 0.79 ng/mL, Fig 3). HCT 15.6 mg/kg plus ADP 6 mg/kg reduced insulin level to 1.9 ± 0.85 ng/mL, compared with control. Half doses of HCT and ADP in combination of DG 600 or 1200 mg/kg resulted in elevated insulin level to 4.06 ± 0.26 ng/mL and 6.09 ± 0.57 ng/mL, respectively.

Creatinine level in untreated SH rats and WK rats was similar (0.59 ± 0.06 mg/dL vs 0.6 ± 0.02 mg/dL, Fig 3). HCT 15.6 mg/kg plus ADP 6 mg/kg increased creatinine level to 0.83 ± 0.15 ng/mL, compared with control. However, half doses of HCT and ADP in combination of DG 1200 mg/kg reduced creatinine level to 0.5 ± 0.04 mg/dL.

Untreated SH rats had higher albumin level than WK rats (8.21 ± 0.32 g/dL vs 7.73 ± 0.25 g/dL, Fig 3). All treatment groups involving HCT plus ADP or HCT plus ADP plus DG reduced albumin level in SH rats to 7.39 ± 0.14 to 7.94 ± 0.28 g/dL. Half dose of HCT plus ADP combining with DG reduced albumin level lower than did full dose of HCT plus ADP.

Untreated SH rats had higher urea nitrogen level than WK rats (15.77 ± 0.84 mg/dL vs 13.83 ± 0.74 mg/dL, Fig 3). HCT 15.6 mg/kg plus ADP 6 mg/kg increased urea nitrogen level to 17.57 ± 0.29 mg/dL, compared with control. Half doses of HCT/ADP with DG reduced levels of urea nitrogen to 17.13 ± 0.28 mg/dL.

Uric acid level in untreated SH rats and WK rats was similar (2.67 ± 0.16 mg/dL vs 2.7 ± 0.14 mg/dL, Fig 3). HCT 15.6 mg/kg plus ADP 6 mg/kg elevated uric acid level to 4 ± 0.05 mg/dL, compared with control. Uric acid level was decreased only in half dose of HCT plus ADP with DG 1200 mg/kg to 3.81 ± 0.03 mg/dL, compared with full dose of HCT and ADP.

Discussion

AS had a potential beneficial effect on vascular thickening, but a high dose was needed for the effect to be manifested. DG 300 mg/kg had an intima media thickness-reducing effect stronger than that of AS 80 mg/kg. AS 80 mg/kg plus DG 300 mg/kg exhibited the most remarkable intima media thickness reduction. AS plus DG (at different doses of AS 10–80 mg/kg) showed generally stronger effect on intima media thickness reduction than single medication alone. Interestingly, the reduction effect of AS 80 mg/kg plus DG 300 mg/kg (27.34%) was higher than the summation effect of AS 80 mg/kg alone (1.12%) and DG 300 mg/kg alone (9.85%), thereby suggesting a synergistic interaction. Lower doses of AS plus DG might achieve a treatment outcome better than higher doses of AS alone in terms of intima media thickness reduction. DG may be used in lieu of AS, because DG 300 mg/kg exerted a stronger effect than AS 80 mg/kg.

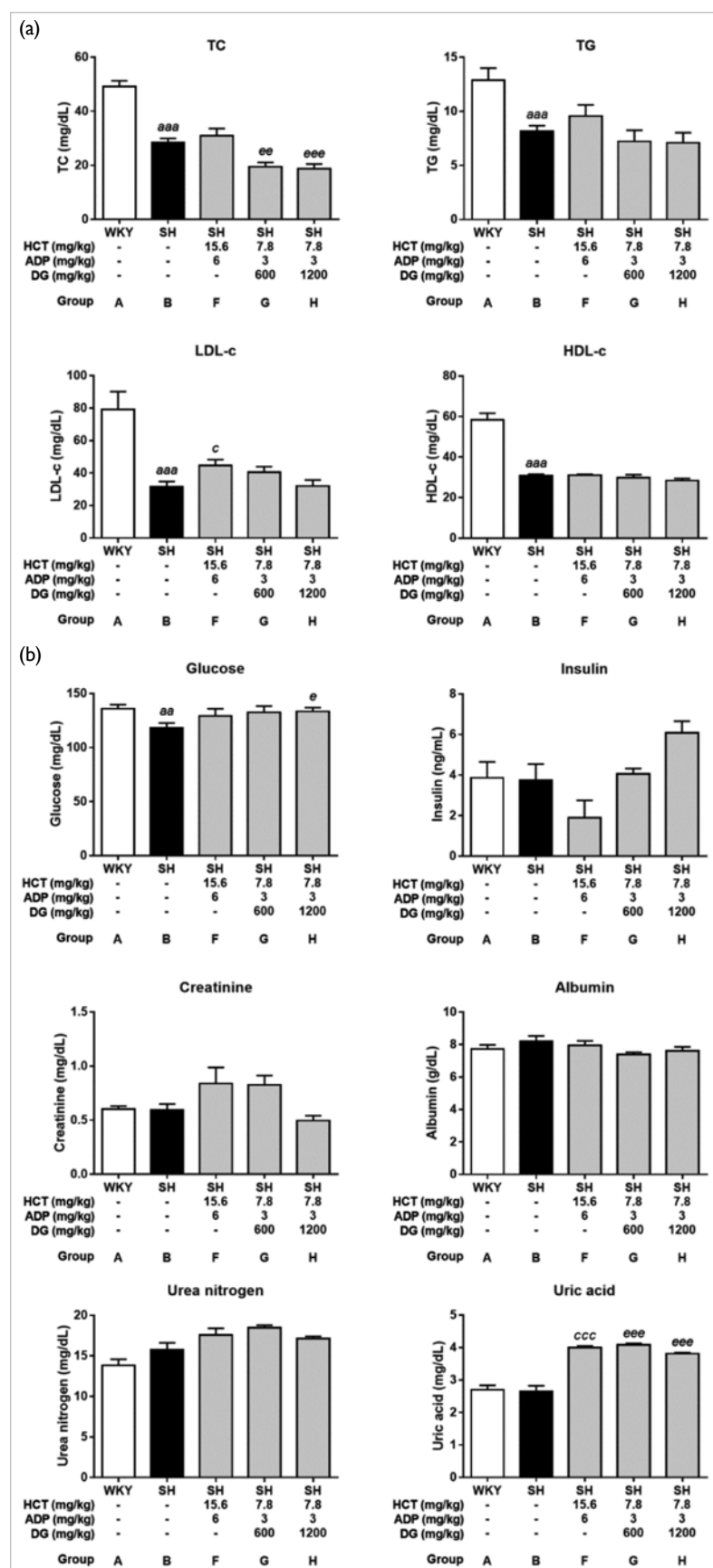


FIG 3. (a) Lipid profile of total cholesterol (TC), triglyceride (TG), low-density lipoprotein-cholesterol (LDL-C), and high-density lipoprotein-cholesterol (HDL-C) as well as (b) blood parameters of glucose, insulin, creatinine, albumin, urea nitrogen, and uric acid of spontaneously hypertensive (SH) rats and Wistar-Kyoto (WK) rats.

AS plus DG resulted in potentiated hypolipidaemic effects. AS plus DG exhibited stronger hypolipidaemic effects than did AS alone. Compared with AS 16 mg/kg, AS 8 mg/kg plus DG 600 mg/kg achieved stronger effects on reducing levels of TC and TG but not LDL-C and HDL-C. This observation suggested that half dose of AS (8 mg/kg) taken together with DG (600 mg/kg) may achieve a comparable hypolipidaemic effect to AS 16 mg/kg alone.

DG might be able to attenuate toxic effects caused by AS. When high doses of AS plus DG were given to SD rats, levels of aspartate aminotransferase, alanine transaminase, and creatine kinase decreased, compared with AS alone. These results suggested that DG acted to attenuate the toxicity caused by AS on the liver and skeletal muscle. Plasma examinations of aspartate aminotransferase, alanine transaminase, and creatine kinase levels showed that combined use of AS and DG was safe and beneficial.

In SH rats, DG appeared to be able to potentiate an anti-hypertensive effect of HCT and ADP, because DG 1200 mg/kg plus half effective doses of HCT and ADP was shown to reduce SBP in a magnitude comparable to full effective doses of HCT and ADP.

Medications with HCT and ADP increased the lipid profile of SH rats as evidenced in the elevation of TG, TC, LDL-C, and HDL-C. This hyperlipidaemia adverse effect significantly decreased in half doses of HCT and ADP in combination with DG in a dose-dependent manner. Reduction of HCT and ADP doses in half may contribute to the lowered lipid profile. DG played a pivotal role in lowering the lipid profile of SH rats receiving medication, as DG possesses hypolipidaemic effect on high-fat diet induced-hyperlipidaemia.

In blood parameters of elevated levels of creatinine, albumin, urea nitrogen, and uric acid, DG plus half doses of HCT and ADP was able to attenuate their elevations shown in full dose of HCT and ADP. Whether this was due to the addition of DG or reduction of doses of HCT and ADP was not known. DG was unable to lower glucose and conversely cause the glucose level to rise. Insulin level was found to increase following the increasing pattern of glucose. Increase in insulin level correlated with DG medication in combination with half dose of HCT and ADP.

Conclusion

DG combined with AS or HCT and ADP resulted in better treatment effects on preventing vascular wall thickening, reducing hyperlipidaemia, and ameliorating hypertension. In addition, DG could also attenuate adverse effects caused by AS or HCT and ADP medication, including elevations in levels of aspartate aminotransferase, alanine transaminase, creatine kinase, as well as TC, TG, LDL-C, HDL-C, creatinine, albumin, urea nitrogen, and uric acid.

Funding

This study was supported by the Health and Medical Research Fund, Food and Health Bureau, Hong Kong SAR Government (#11120841). The full report is available from the Health and Medical Research Fund website (<https://rfs1.fhb.gov.hk/index.html>).

Disclosure

The results of this research have been previously published in:

1. Cheung DW, Koon CM, Wong PH, et al. Evaluating efficacy and safety of combination medication of atorvastatin and a herbal formula containing *Salvia miltiorrhiza* and *Pueraria lobata* on hyperlipidemia. *Phytother Res* 2017;31:1579-89.

References

1. Tam WY, Chook P, Qiao M, et al. The efficacy and tolerability of adjunctive alternative herbal medicine (*Salvia miltiorrhiza* and *Pueraria lobata*) on vascular function and structure in coronary patients. *J Altern Complement Med* 2009;15:415-21.
2. Kwok T, Leung PC, Lam C, et al. A randomized placebo controlled trial of an innovative herbal formula in the prevention of atherosclerosis in postmenopausal women with borderline hypercholesterolemia. *Complement Ther Med* 2014;22:473-80.
3. Koon CM, Woo KS, Leung PC, Fung KP. *Salviae Miltorrhizae Radix* and *Puerariae Lobatae Radix* herbal formula mediates anti-atherosclerosis by modulating key atherogenic events both in vascular smooth muscle cells and endothelial cells. *J Ethnopharmacol* 2011;138:175-83.
4. Tulis DA. Rat carotid artery balloon injury model. *Methods Mol Med* 2007;139:1-30.
5. Cheung DW, Koon CM, Wong PH, et al. Evaluating efficacy and safety of combination medication of atorvastatin and a herbal formula containing *Salvia miltiorrhiza* and *Pueraria lobata* on hyperlipidemia. *Phytother Res* 2017;31:1579-89.

Molecular diversity and evolution of bat group C betacoronaviruses: origin of the novel human group C betacoronavirus (abridged secondary publication)

SKP Lau *, PCY Woo, BJ Zheng

KEY MESSAGES

1. MERS-CoV is closely related to both Pi-BatCoV HKU5 and Ty-BatCoV HKU4. Pi-BatCoV HKU5 may have a better ability to adapt to new host environments along with its host living in diverse habitats.
2. A potentially novel lineage C betaCoV that shares genome similarities to MERS-CoV is identified in two bats in Guangdong province, supporting that *Pipistrellus*-related bats are important host of lineage C betaCoVs.
3. Two other novel betaCoVs—SARSr-Rf-BatCoV strains—were identified from greater horseshoe bats. Genome analysis showed that recombination has occurred around ORF8 between SARSr-Rf-BatCoVs and SARSr-Rs-BatCoVs, leading to the generation of civet SARSr-CoVs with ORF8 likely acquired from SARSr-Rf-BatCoVs.
4. Bats in China are important reservoir for diverse betaCoVs including lineage C viruses. This highlights the importance for conservation of these animals and their habitats. Although there is no evidence of direct transmission of CoVs from bats to humans, humans should avoid contact with wild bats.

Hong Kong Med J 2021;27(Suppl 2):S23-7

HMRF project number: 13121102

SKP Lau, PCY Woo, BJ Zheng

Department of Microbiology, The University of Hong Kong

* Principal applicant and corresponding author: skplau@hkucc.hku.hk

Introduction

In 2012, a novel human coronavirus (CoV) in the Middle East region was found to be associated with severe respiratory illness with high mortality rate. This novel CoV was first isolated from the lung tissue of a 60-year-old Saudi Arabian man with fatal acute pneumonia and renal failure. Subsequently, a resident of Qatar with a recent travel history to Saudi Arabia was diagnosed with similar symptoms and detected with the same virus.¹ This novel lineage C betaCoV was named Middle East respiratory syndrome-related coronavirus (MERS-CoV). As of 27 November 2016, of 1832 laboratory-confirmed cases of MERS-CoV infection reported to World Health Organization, there are 649 deaths, accounting for a crude fatality rate of 35%. The MERS-CoV is most closely related to bat lineage C betaCoVs, including *Tylonycteris* bat coronavirus HKU4 (Ty-BatCoV HKU4) and *Pipistrellus* bat coronavirus HKU5 (Pi-BatCoV HKU5) discovered in bats in 2006.^{2,3} The virus was subsequently found in dromedary camels, which are likely the immediate source of some human cases. However, it remains unknown where and when the camels have acquired the virus, and whether bats are the ultimate reservoir and origin of MERS-CoV-like viruses, as in the

case of SARS-CoV. So far, molecular epidemiology studies on lineage C betaCoVs are scarce, and little is known about how they evolve and diversify. We have reported that CoVs can be transmitted between two bat species of different suborders, implying the natural occurrence of interspecies transmission at any level.⁴ Therefore, more intensive surveillance studies for betaCoVs in bats of different species may help understand the origin of the ancestor of MERS-CoV.

Methods

Prospectively collected samples from different bat species in China over a 10-year period were subject to betaCoV detection by RT-PCR. Positive samples were sequenced for complete RNA-dependent RNA polymerase and spike (S) and nucleocapsid (N) genes and were analysed for molecular diversity and evolution. Potential recombinant strains were selected for complete genome sequencing and analysed for possible recombination events. Evolutionary analysis was performed by molecular clock analysis to estimate time of divergence of different lineage C betaCoVs and emergence of MERS-CoV.

Respiratory and alimentary samples from 9866 bats of 54 different bat species captured from

different locations in Hong Kong and mainland China, including Guangdong, Guangxi, and Yunnan provinces, were collected over a 10-year period (2004 to 2014), in collaboration with Agriculture, Fisheries and Conservation Department of the Hong Kong SAR Government, Yunnan Institute of Endemic Diseases Control and Prevention, and Guangdong Entomological Institute. All specimens were immediately placed in viral transport medium before transportation to the laboratory for RNA extraction. Viral RNA was extracted from the bat samples and subjected to RT-PCR for detection of betaCoVs using a 440-bp fragment of RdRp gene. The PCR product of positive samples were sequenced and compared with known sequences of the RdRp genes of betaCoVs in the GenBank database. A preliminary phylogenetic analysis was then performed using these sequences.

Complete RdRp, S and N genes of 13 Ty-BatCoV HKU4 and 15 Pi-BatCoV HKU5 strains as well as the complete genomes of two SARSr-Rf-BatCoVs and the two strains of a novel lineage C betaCoV detected at different time and/or place were amplified and sequenced. The different complete gene sequences were used to construct the phylogenetic trees afterwards. Complete RdRp and N gene sequences were used to estimate the divergence time of Ty-BatCoV HKU4, Pi-BatCoV HKU5, and MERS-CoV. Moreover, the genome sequences of different SARSr-BatCoVs and SARSr-CoVs were subjected to Bootscan analysis in Simplot to detect possible recombination using sliding window approach with civet SARSr-CoV SZ3 as query.

Results

Molecular epidemiology of lineage C betaCoVs in different bat species in China

Among the 9866 bat samples, 267 (2.7%) were positive for betaCoVs by RT-PCR and sequencing of the partial RdRp gene (Table). Phylogenetic analysis showed the presence of Ty-BatCoV HKU4 in 29 alimentary samples from 241 lesser bamboo bat (*Tylonycteris pachypus*) and Pi-BatCoV HKU5 in 58 alimentary samples from 136 Japanese pipistrelle (*Pipistrellus abramus*), all from bats collected in Hong Kong from 2004 to 2014, whereas 19 alimentary samples from lesser bamboo bat collected in mainland China were also positive for Ty-BatCoV HKU4, and four alimentary samples from four bats collected in mainland China were also found to contain a potentially novel lineage C βCoV and a novel SARSr-Rf-BatCoV (Fig.). In addition, 52 and 105 alimentary samples were found to contain Ro-BatCoV HKU9 and SARSr-Rs-BatCoV HKU3, respectively. None of the respiratory samples were positive for lineage C betaCoVs, suggesting that these viruses may exhibit enteric tropism. Bats positive for Ty-BatCoV HKU4 and Pi-BatCoV

HKU5 were from seven and 13 sampling locations in Hong Kong, respectively, whereas Ty-BatCoV HKU4, the novel lineage C betaCoV and SARSr-Rf-BatCoV were detected in different provinces in mainland China. No obvious disease was observed in bats positive for Ty-BatCoV HKU4 and Pi-BatCoV HKU5. Ty-BatCoV HKU4 was found only in adult bats, whereas Pi-BatCoV HKU5 was found in both adult and juvenile bats.

Molecular diversity, evolution, and potential recombination in lineage C betaCoVs in bats

MERS-CoV was shown to be more closely related to Pi-BatCoV HKU5 than to Ty-BatCoV HKU4 (92.1%-92.3% vs 89.6%-90% identities) in the RdRp gene, but more closely related to Ty-BatCoV HKU4 than to Pi-BatCoV HKU5 in the S gene (66.8%-67.4% vs 63.4%-64.5% identities) and N gene (71.9%-72.3% vs 69.5%-70.5% identities) by comparing the deduced amino acid sequences of the genes. The Ty-BatCoV HKU4 strains and Pi-BatCoV HKU5 strains formed two distinct clusters in the phylogenetic tree of all three genes. Marked sequence polymorphisms were observed in the S gene of Pi-BatCoV HKU5, with up to 12% amino acid differences. Ty-BatCoV HKU4, Pi-BatCoV HKU5, and MERS-CoV probably emerged from a common ancestor about 500 years before the epidemic.

Two samples collected from Chinese pipistrelle bats contained a novel lineage C betaCoV species. This novel lineage C betaCoV shares similar genome organisation with other lineage C betaCoVs and possessed 56.3%-78.3%, 78.4%-90.8%, 89.1%-96.4%, 92.0%-97.0%, 84.7%-97.3%, 76.9%-89.2%, and 84.8%-96.7% amino acid identities to other lineage C betaCoVs in the seven conserved replicase domains: ADRP, nsp5 (3CLpro), nsp12 (RdRp), nsp13 (Hel), nsp14 (ExoN), nsp15 (NendoU), and nsp16 (O-MT), respectively.

In addition, two novel betaCoVs—SARSr-Rf-BatCoV strains—were identified from greater horseshoe bats in mainland China. Their genomes shared 88.2% nucleotide identities to the genomes of SARSr-Rs-BatCoV HKU3 and 93% nucleotide identities to the genomes of human/civet SARSr-CoVs. The sequence identity between the ORF8 of SARSr-Rf-BatCoVs and human/civet SARSr-CoVs (80.4%-81.3% aa identity) was exceptionally high and was much higher than that between human/civet SARSr-CoVs and other SARSr-BatCoVs (23.2%-37.3% aa identity). Phylogenetic and sliding window analyses suggested potential recombination between SARSr-BatCoVs from different bat host species, in which the ORF8 of civet and human SARSr-CoV would have originated from SARSr-Rf-BatCoVs. Several recombination breakpoints were observed, and ORF8 was located between two breakpoints in particular.

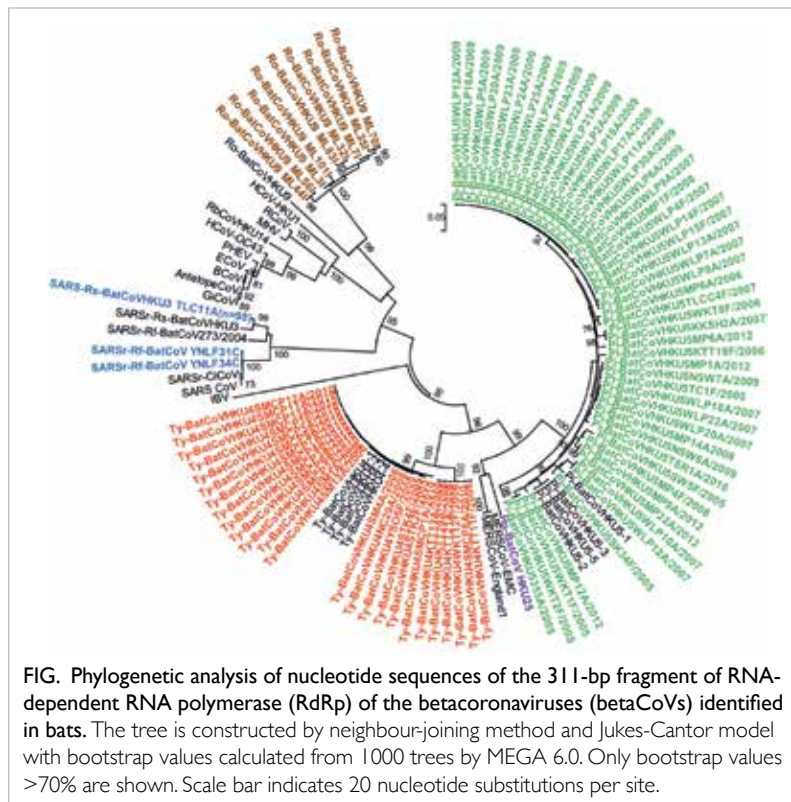
TABLE. Detection of betacoronaviruses (betaCoVs) in bats by RT-PCR

Bat species	Common name	No. of bats tested	No. (%) of bats positive for betaCoVs in alimentary samples	BetaCoV species*
<i>Megachiroptera</i>				
<i>Pteropodidae</i>				
<i>Cynopterus sphinx</i>	Short-nosed fruit bat	130	0 (0)	-
<i>Eonycteris spelaea</i>	Cave nectar bat	6	0 (0)	-
<i>Megaerops ecaudatus</i>	Tailless fruit bat	1	0 (0)	-
<i>Rousettus leschenaulti</i>	Leschenault's rousette	741	52 (7.0)	Ro-BatCoV HKU9 (n ₁ =1; n ₂ =51)
<i>Microchiroptera</i>				
<i>Emballonuridae</i>				
<i>Taphozous melanopogon</i>	Black-bearded tomb bat	25	0 (0)	-
<i>Taphozous sp</i>		19	0 (0)	-
<i>Hipposideridae</i>				
<i>Aselliscus stoliczkanus</i>	Stoliczka's trident bat	48	0 (0)	-
<i>Hipposideros armiger</i>	Himalayan leaf-nosed bat	365	0 (0)	-
<i>Hipposideros larvatus</i>	Intermediate roundleaf bat	142	0 (0)	-
<i>Hipposideros pomona</i>	Pomona leaf-nosed bat	1001	0 (0)	-
<i>Hipposideros pratti</i>	Pratt's roundleaf bat	19	0 (0)	-
<i>Megadermatidae</i>				
<i>Megaderma lyra</i>	Greater false vampire bat	1	0 (0)	-
<i>Rhinolophidae</i>				
<i>Coelops frithi</i>	East Asian tailless leaf-nosed bat	9	0 (0)	-
<i>Rhinolophus affinus</i>	Intermediate horseshoe bat	670	0 (0)	-
<i>Rhinolophus ferrumequinum</i>	Greater horseshoe bat	97	2 (2.1)	SARSr-Rf-BatCoV (n ₁ =0; n ₂ =2)
<i>Rhinolophus luctus</i>	Woolly horseshoe bat	63	0 (0)	-
<i>Rhinolophus macrotis</i>	Big-eared horseshoe bat	18	0 (0)	-
<i>Rhinolophus osgoodi</i>	Osgood's horseshoe bat	1	0 (0)	-
<i>Rhinolophus pearsoni</i>	Pearson's horseshoe bat	24	0 (0)	-
<i>Rhinolophus pusillus</i>	Least horseshoe bat	419	0 (0)	-
<i>Rhinolophus rex</i>	King horseshoe bat	2	0 (0)	-
<i>Rhinolophus siamensis</i>	Thai horseshoe bat	3	0 (0)	-
<i>Rhinolophus sinicus</i>	Chinese horseshoe bat	2430	105 (4.3)	SARSr-Rs-BatCoV HKU3 (n ₁ =99; n ₂ =6)
<i>Rhinolophus stheno</i>	Lesser brown horseshoe bat	34	0 (0)	-
<i>Rhinolophus thomasi</i>	Thomas's horseshoe bat	1	0 (0)	-
<i>Rhinolophus sp.</i>		22	0 (0)	-
<i>Vespertilionidae</i>				
<i>Eptesicus sp.</i>		1	0 (0)	-
<i>Hypsugo pulveratus</i>	Chinese pipistrelle	11	2 (1.8)	novel lineage C betaCoV (n ₁ =0; n ₂ =2)
<i>Ia io</i>	Great evening bat	20	0 (0)	-
<i>Miniopterus fuliginosus</i>	Eastern bent-winged bat	90	0 (0)	-
<i>Miniopterus magnater</i>	Greater bent-winged bat	29	0 (0)	-
<i>Miniopterus pusillus</i>	Lesser bent-winged bat	541	0 (0)	-
<i>Miniopterus schreibersii</i>	Common bent-winged bat	1016	0 (0)	-

* n₁= No. of bats positive for betaCoVs identified in Hong Kong; n₂= No. of bats positive for betaCoVs identified in mainland China.

TABLE. (cont'd)

Bat species	Common name	No. of bats tested	No. (%) of bats positive for betaCoVs in alimentary samples	BetaCoV species*
<i>Myotis aduersus</i>	Large-footed mouse-eared bat	4	0 (0)	-
<i>Myotis altarium</i>	Szechwan myotis	15	0 (0)	-
<i>Myotis chinensis</i>	Chinese myotis	224	0 (0)	-
<i>Myotis daubentonii</i>	Daubenton's bat	98	0 (0)	-
<i>Myotis fimbriatus</i>	Fringed long-footed myotis	6	0 (0)	-
<i>Myotis formosus</i>	Hodgson's bat	1	0 (0)	-
<i>Myotis horsfieldii</i>	Horsfield's bat	7	0 (0)	-
<i>Myotis longipes</i>	Kashmir cave bat	5	0 (0)	-
<i>Myotis muricola</i>	Whiskered myotis	4	0 (0)	-
<i>Myotis pequininius</i>	Beijing mouse-eared bat	29	0 (0)	-
<i>Myotis ricketti</i>	Rickett's big-footed bat	451	0 (0)	-
<i>Myotis sp.</i>		1	0 (0)	-
<i>Nyctalus noctula</i>	Brown noctule	56	0 (0)	-
<i>Nyctalus plancyi</i>	Chinese noctule	1	0 (0)	-
<i>Pipistrellus abramus</i>	Japanese pipistrelle	314	58 (18.5)	Pi-BatCoV HKU5 (n ₁ =58; n ₂ =0)
<i>Pipistrellus minus</i>	Wroughton's pipistrelle	3	0 (0)	-
<i>Pipistrellus pipistrellus</i>	Common pipistrelle	6	0 (0)	-
<i>Pipistrellus tenuis</i>	Least pipistrelle	11	0 (0)	-
<i>Scotophilus kuhlii</i>	Lesser yellow bat	220	0 (0)	-
<i>Tylonycteris pachypus</i>	Lesser bamboo bat	306	48 (15.7)	Ty-BatCoV HKU4 (n ₁ =29; n ₂ =19)
<i>Tylonycteris robustula</i>	Greater bamboo bat	105	0 (0)	-



Discussion

In this extensive epidemiological study, betaCoVs were detected in 267 of 9866 bats, giving a detection rate of 2.7%. At least five different betaCoV species are circulating in specific bat species including Ty-Bat CoV HKU4, Pi-BatCoV HKU5, a novel lineage C betaCoV, SARSr-BatCoVs, and Ro-BatCoV HKU9. This supports bats are important reservoirs for betaCoVs. Ty-BatCoV HKU4 and Pi-BatCoV HKU5 were highly prevalent among lesser bamboo bats and Japanese pipistrelle in Hong Kong, respectively, with detection rates of 21% to 24% in their alimentary samples. Pi-BatCoV HKU5 may have a better ability to adapt to new host/environments, given its high divergence in the S gene sequences. This may be explained by the diverse habitat of its host Japanese pipistrelle, which would favour the evolution of the viral S protein, in particular the receptor binding domain, and allow efficient interspecies transmission to other animals or human. Using molecular clock analysis, we showed that Ty-BatCoV HKU4, Pi-BatCoV HKU5, and MERS-CoV have diverged at least centuries ago from their common ancestor. These two bat lineage C betaCoVs are different from

SARS-CoV, which diverged between civet and bat strains only several years before the SARS epidemic. Therefore, they are not likely the direct ancestor of MERS-CoV. However, another novel lineage C betacov species was detected in two bat samples collected from Chinese pipistrelle. Although the genome of this novel CoV only possessed about 73% nucleotide identities to that of human/camel MERS-CoV, this finding further supports that *Pipistrellus*-related bats are likely important host of lineage C betacovs. To understand how these bat lineage C betacovs may have evolved leading to the emergence of MERS-CoV, more epidemiological studies on bats and other animals are warranted.

In addition to the lineage C betacovs, two novel betacovs—SARS-CoV-Rf-BatCoV strains—were identified from greater horseshoe bats. Their genomes only shared 93% nucleotide identities to that of human/civet SARS-CoVs, but the ORF8 of these two bat CoVs was highly similar to that of civet SARS-CoV among all SARS-CoVs. Based on the results from phylogenetic analysis and the identification of potential recombination sites between SARS-Rs-BatCoVs and SARS-Rf-BatCoVs around the ORF8 region, civet SARS-CoV SZ3 is likely to have originated from genetic recombination between SARS-Rs-BatCoVs and SARS-Rf-BatCoVs from different horseshoe bat species with the ORF8 acquired from SARS-CoV-Rf-BatCoVs. Further studies should be sought to understand how the evolution of ORF8 may have played a role during interspecies transmission of SARS-CoV.

The present results are important for future research on the emergence of CoVs in humans. It has provided clues on the animal origins and the evolutionary pathways of MERS-CoV and SARS-CoV. We have also discovered a potentially novel lineage C betacov closely related to MERS-CoV. Hence, future studies may focus on *Pipistrellus* and *Rhinolophus* or related bats to identify yet closer ancestors of MERS-CoV and SARS-CoV. This will help better understand how CoVs may emerge in humans and predict the next possible epidemic. Our findings support a diversity of betacovs among bats in China. Therefore, it is important to conserve these animals and their habitats. Although there is no evidence of direct transmission of CoVs from bats to humans, humans should avoid contact with wild

bats to prevent transmission of other viruses such as rabies.

Funding

This study was supported by the Health and Medical Research Fund, Food and Health Bureau, Hong Kong SAR Government (#13121102). The full report is available from the Health and Medical Research Fund website (<https://rfs1.fhb.gov.hk/index.html>).

Disclosure

The results of this research have been previously published in:

1. Lau SK, Li KS, Tsang AK, et al. Genetic characterization of Betacoronavirus lineage C viruses in bats reveals marked sequence divergence in the spike protein of pipistrellus bat coronavirus HKU5 in Japanese pipistrelle: implications for the origin of the novel Middle East respiratory syndrome coronavirus. *J Virol* 2013;87:8638-50.
2. Lau SK, Feng Y, Chen H, et al. Severe acute respiratory syndrome (SARS) coronavirus ORF8 protein is acquired from SARS-related coronavirus from greater horseshoe bats through recombination. *J Virol* 2015;89:10532-47.
3. Lau SKP, Zhang L, Luk HKH, et al. Receptor usage of a novel bat lineage C betacoronavirus reveals evolution of Middle East respiratory syndrome-related coronavirus spike proteins for human dipeptidyl peptidase 4 binding. *J Infect Dis* 2018;218:197-207.

References

1. Butler D. SARS veterans tackle coronavirus. *Nature* 2012;490:20.
2. Woo PC, Wang M, Lau SK, et al. Comparative analysis of twelve genomes of three novel group 2c and group 2d coronaviruses reveals unique group and subgroup features. *J Virol* 2007;81:1574-85.
3. Woo PC, Lau SK, Li KS, Tsang AK, Yuen KY. Genetic relatedness of the novel human group C betacoronavirus to *Tylonycteris* bat coronavirus HKU4 and *Pipistrellus* bat coronavirus HKU5. *Emerg Microbes Infect* 2012;11:e35.
4. Lau SK, Li KS, Tsang AK, et al. Recent transmission of a novel alphacoronavirus, bat coronavirus HKU10, from Leschenault's rousettes to pomona leaf-nosed bats: first evidence of interspecies transmission of coronavirus between bats of different suborders. *J Virol* 2012;86:11906-18.

Tropism of the novel human betacoronavirus lineage C virus in human ex vivo and in vitro cultures: potential transmissibility and pathogenesis in humans (abridged secondary publication)

MCW Chan *, RWY Chan, JM Nicholls, JSM Peiris

KEY MESSAGES

1. HCoV-EMC and SARS-CoV infected and productively replicated in human ex vivo lung and bronchus explants.
2. Non-ciliated bronchial epithelial cells, bronchiolar epithelial cells, and type I and type II pneumocytes are major targets for HCoV-EMC infection.
3. HCoV-EMC infection in bronchus and lung failed to induce interferon, with no inhibitory effect in

suppressing HCoV-EMC infection by sialidase.

Hong Kong Med J 2021;27(Suppl 2):S28-32

HMRF project number: 13121132

¹ MCW Chan, ¹ RWY Chan, ² JM Nicholls, ¹ JSM Peiris

LKS Faculty of Medicine, The University of Hong Kong:

¹ School of Public Health

² Department of Pathology

* Principal applicant and corresponding author: mchan@hku.hk

Introduction

Coronavirus infections in humans are generally mild and self-limited. Until the outbreak of SARS in 2003, there was limited research on the tissue tropism and host response on human infection with coronaviruses. Compared with human MERS-CoV (HCoV-EMC), SARS-CoV was deficient at eliciting interferon (IFN)- β innate immune responses, because SARS-CoV encodes several antagonists of IFN sensing and signalling pathways. Tropism of SARS-CoV in the respiratory tract was primarily restricted to differentiated human airway epithelium and alveolar type II pneumocytes. In 2012, the novel HCoV-EMC was detected in two patients from Saudi Arabia and Qatar.¹ Thereafter, more cases were identified prospectively and retrospectively in Saudi Arabia, Qatar, and Jordan. Pneumonia leading to acute respiratory distress syndrome was the primary manifestation of the disease, but renal dysfunction was also observed in some cases. The World Health Organization provided a working case-definition of the disease.² The disease has an incubation period of up to 10 days and is not easily transmitted between humans. The Qatari patient had contact with camels and sheep.³ Investigation (based on clinical disease and RT-PCR testing) of 64 contacts of the patient during his medical stay in the UK has not revealed secondary cases. The European Centre for Disease Prevention and Control reported an outbreak of severe respiratory illness in Jordan in April 2012, but no virological diagnosis was made.

A number of these cases have been retrospectively studied, as has an outbreak of a respiratory illness in an intensive care unit in a hospital in Zarqa, Jordan. Seven nurses and one doctor were among the 11 affected, in which one of the nurses died who had underlying conditions. All cases had high fever and lower respiratory symptoms; only two of them were virologically confirmed to be caused by MERS-CoV.

We have previously used ex vivo cultures of human bronchus and lung explants tissues to investigate tropism of influenza viruses. Productive infection of the upper airways may correlate with the emergence of pandemic potential in swine influenza viruses. In the present study, we used ex vivo organ cultures of the human bronchus and lung to study the tissue tropism, virus replication kinetics, and innate immune response of the acute infection of HCoV-EMC, in comparison with SARS-CoV and (human coronavirus 229E) HCoV-229E. As some coronaviruses use 9O-Sia for virus entry,⁴ HCoV-EMC may also use sialylated glycans as a receptor for binding and entry. We thus evaluated the effect of sialidase to examine if the removal of sialic acids can inhibit the infection with potential as a therapeutic option for patients with HCoV-EMC disease. Inhaled sialidase therapy options are currently in phase 2 clinical trials for influenza A virus.⁵

The aim of the study was to better understand the tissue tropism and pathogenesis of MERS-CoV in the human and to elucidate the possible therapeutic options for human infection of MERS-CoV.

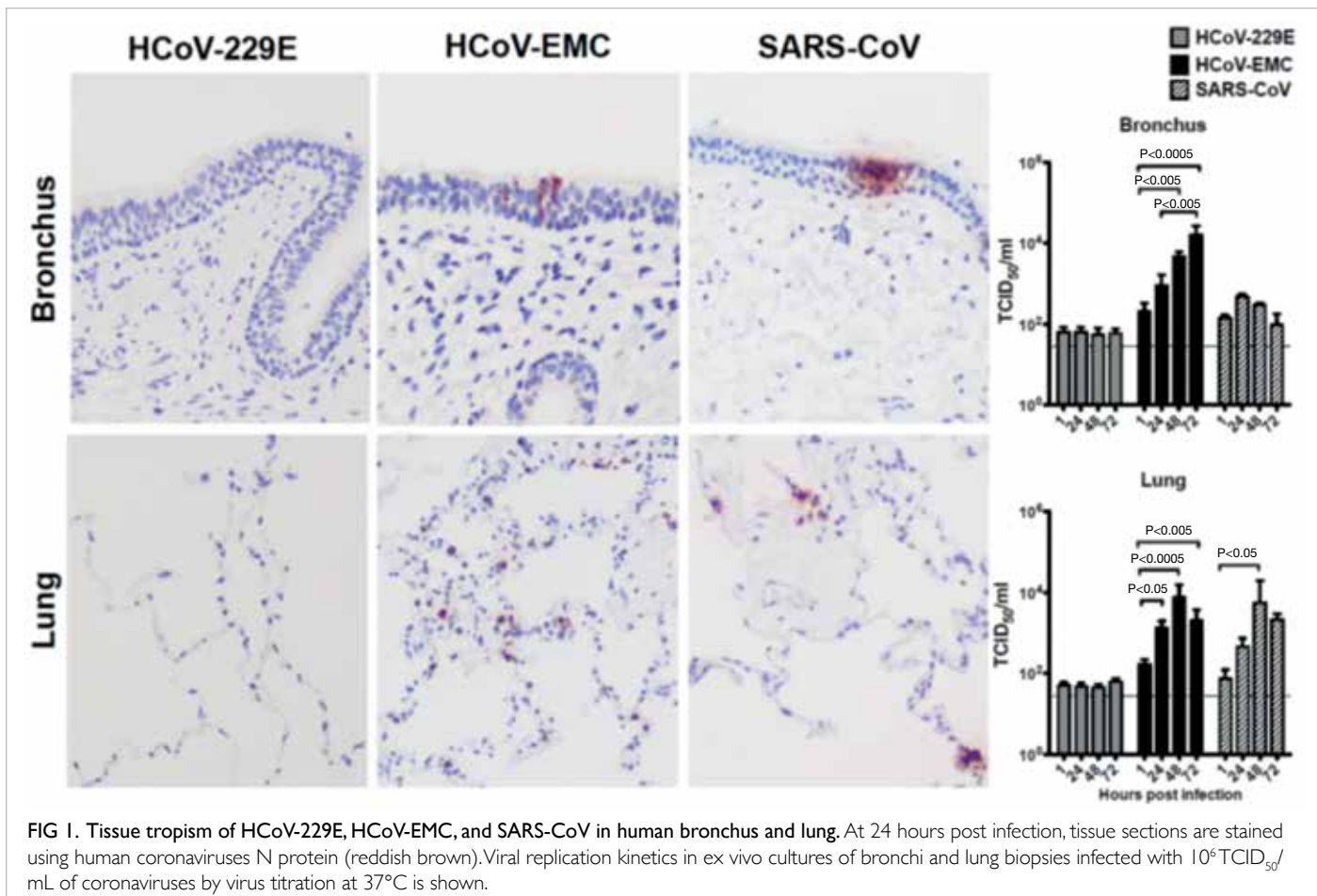


FIG 1. Tissue tropism of HCoV-229E, HCoV-EMC, and SARS-CoV in human bronchus and lung. At 24 hours post infection, tissue sections are stained using human coronaviruses N protein (reddish brown). Viral replication kinetics in ex vivo cultures of bronchi and lung biopsies infected with $10^6 \text{ TCID}_{50}/\text{mL}$ of coronaviruses by virus titration at 37°C is shown.

Methods

We compared HCoV-EMC with SARS-CoV, HCoV-229E, and dromedary camel MERS-CoV in terms of tropism, replication competence, and host innate immune responses, using ex vivo explants cultures of human bronchus and lung, in vitro cell culture of Vero, and human respiratory epithelial cells. We also studied the effect of sialidase treatment of ex vivo human respiratory tissues and Vero cell on HCoV-EMC infection.

Results

HCoV-EMC infected and productively replicated in human ex vivo bronchus explants, whereas SARS-CoV infected bronchus explants and showed limited replication ability (Fig 1). HCoV-229E had no detectable infection or replication in bronchus explants. In ex vivo lung explants, viral antigen was not detected in HCoV-229E inoculated tissues, and no productive replication was observed. HCoV-EMC and SARS-CoV viruses extensively infected and replicated in lung explants.

In bronchus explants, we stained the ciliated

cells and goblet cells using β -tubulin and MUC5AC, respectively (Fig 2). The infected cells (in red) were not co-localised with these two cell types and viral antigen was mainly found in non-ciliated bronchial epithelial cells. In lung, macrophages, epithelial cells, type I pneumocytes were stained with specific markers CD68, AE1/AE3, and podoplanin, respectively. HCoV-EMC did not co-stain with macrophages, but there was overlapping of staining with AE1/AE3 marker, which suggested that the target cells of HCoV-EMC infection were of epithelial origin and focal co-localisation was found in type I pneumocytes. Cellular morphology and immunohistochemistry for viral antigen (nucleoprotein) in the HCoV-EMC-infected lung tissues gave additional information on cell types targeted by HCoV-EMC at 48 hours post infection. Endothelial cells within the medium size interstitial vessels of the lung and bronchiolar epithelial cells were positive. Furthermore, we found extensive expression of cleaved caspase 3, an apoptosis marker, in ex vivo lung explants infected with HCoV-EMC and SARS-CoV but not in mock infected tissue. To investigate if the apoptosis was induced

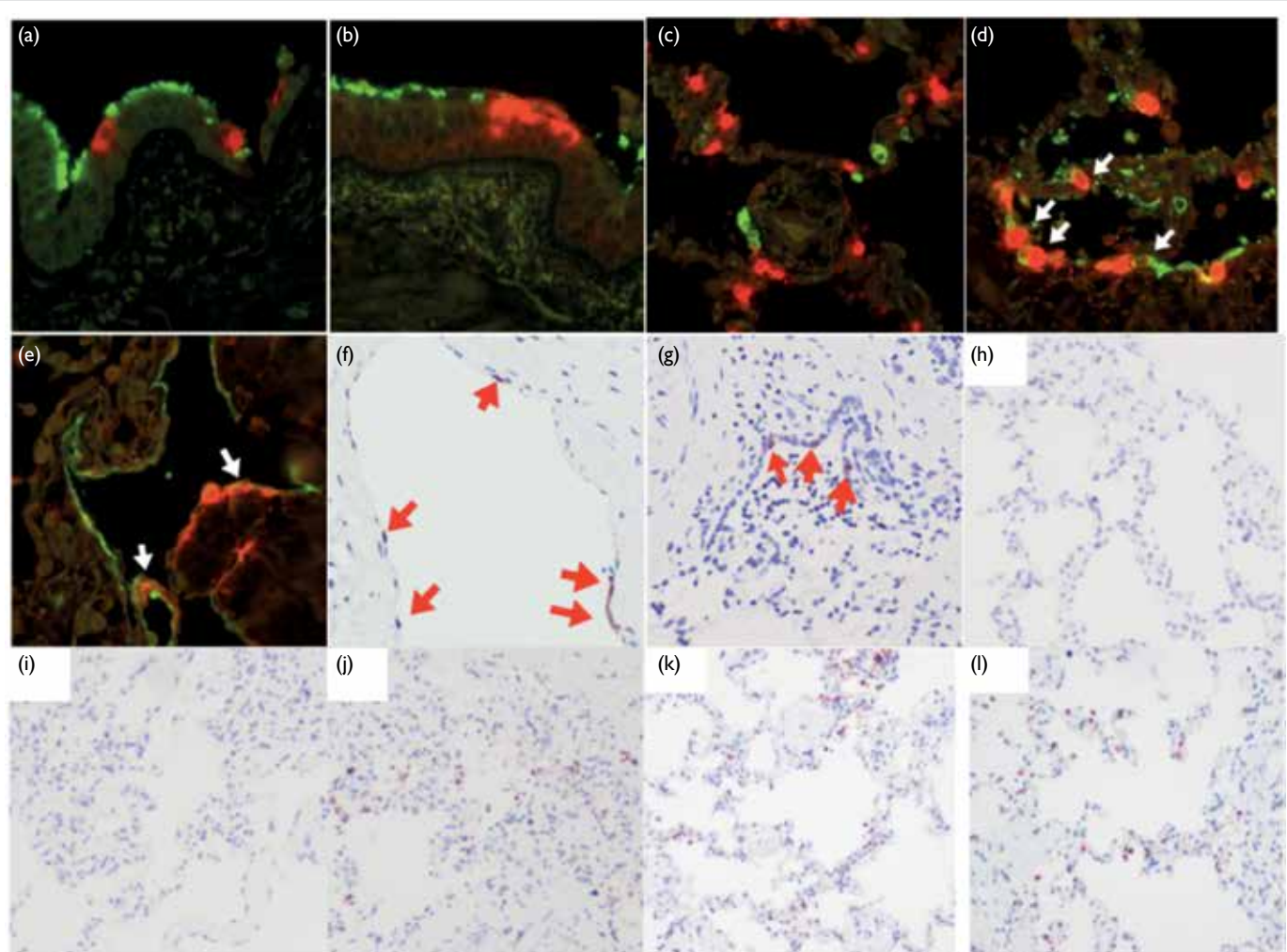


FIG 2. Cellular localisation of HCoV-EMC and induction of apoptosis in lung. HCoV-EMC stained in Vector Red (Red) in bronchus and lung tissue with cell marker conjugated with FITC (green). (a) B-tubulin (ciliated cell marker), (b) MUC5AC (goblet cell marker), (c) CD68 (macrophage marker), (d) AE1/3 (epithelial cell marker), (e) Podoplanin (type I pneumocyte marker) at 24 hours post infection. White arrows indicate cells with co-staining. (f) Cellular tropism of HCoV-EMC in lung with human coronavirus N protein (stained in reddish brown with red arrows) identified in endothelial cells at 24 hours post infection and in (g) bronchiolar epithelial cells at 48 hours post infection. Apoptotic cells are identified in the human lung ex vivo organ culture upon HCoV-EMC and SARS-CoV infection. Ex vivo culture of lung infected with (h) Mock, (i) HCoV-EMC, and (j) SARS-CoV at 48 hours post infection; reddish-brown stain identifies the presence of cleaved-caspase 3. Co-staining of (k) HCoV-EMC and (l) SARS-CoV antigen (pink stain) with cleaved-caspase 3 (reddish-brown stain).

directly by infection, we performed co-staining by immunohistochemistry of HCoV-EMC viral antigen (stained in pink) with cleaved caspase 3 (stained in reddish brown) using HCoV-EMC and SARS-CoV-infected human lung explants. Both HCoV-EMC and SARS-CoV-infected lung tissue revealed that the apoptotic cells were not the viral protein expressing cells suggesting that paracrine mechanisms may contribute to induction of apoptosis.

Ex vivo explants culture of bronchus and lung from three donors were infected with HCoV-EMC. Viral RNA was quantitated by RT-PCR. Host mRNA expression of type I (IFN- β) and type III (IL-29) interferons and cytokines and chemokines

TNF- α and IP-10 was quantitated in HCoV-EMC or mock-infected bronchus and lung tissues. Viral gene expression increased by more than 2000-fold in bronchus and more than 180-fold in lung explants (Fig 3). However, compared to mock, HCoV-EMC infection in bronchus and lung failed to induce both IFN- β and TNF- α . There was marginal induction of IL-29 in virus-infected lung cultures at 48 hours post infection ($P<0.05$) and higher IP-10 mRNA expression at 24 hours post infection ($P<0.05$), compared with mock. IL-1 β , MCP-1, MIP-1 alpha, MIP-1 beta, MIP-2 alpha, IL-6, IL-8, and RANTES mRNA were similarly quantified; no upregulation was detected in bronchus and lung explants.

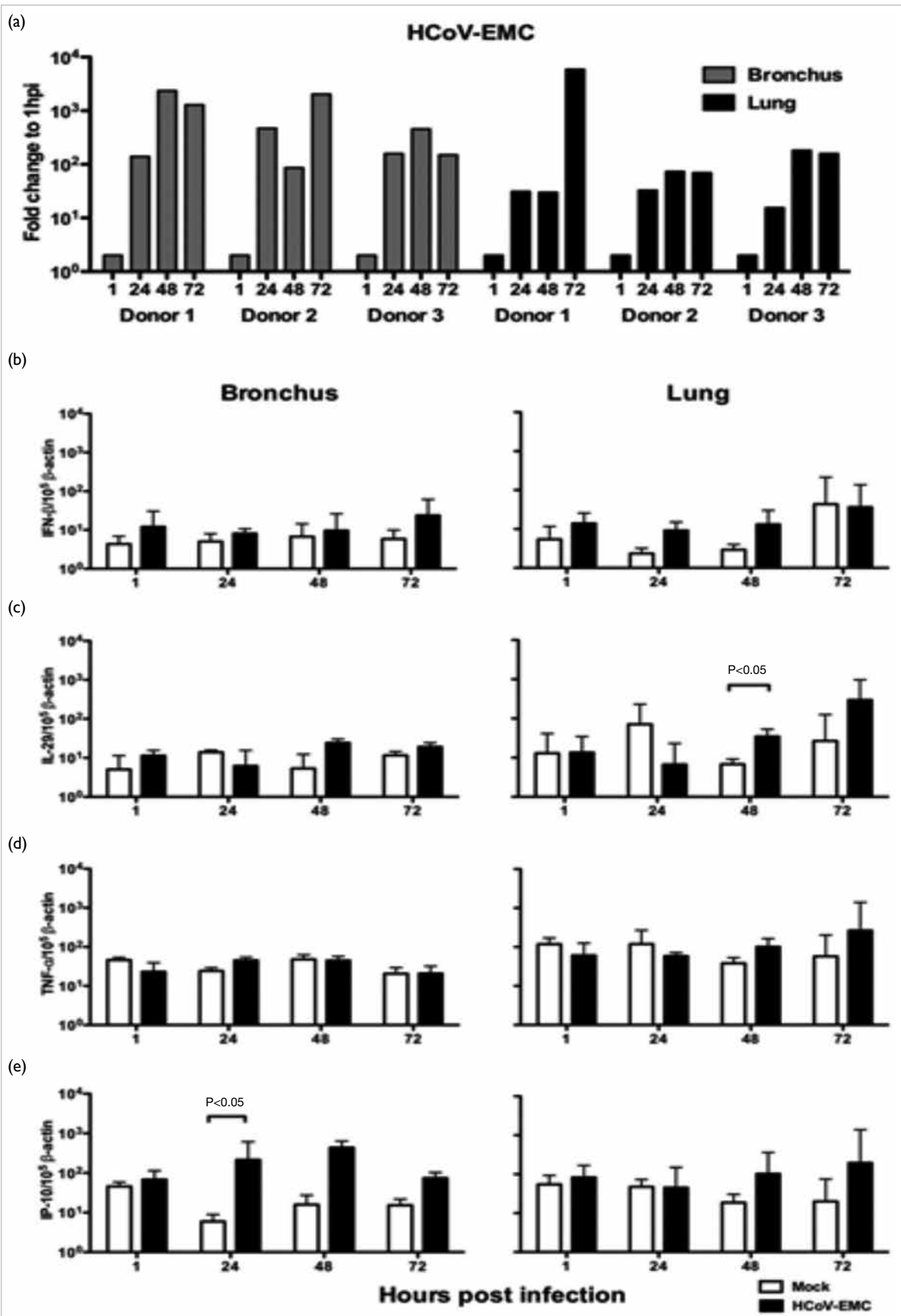


FIG 3. HCoV-EMC and cytokine and chemokine expression in ex vivo human bronchus and lung explants in response to infection. (a) Expression of HCoV-EMC genes at 1, 24, 48, and 72 hours post infection in ex vivo bronchial and lung tissues. (b to e) Expression (numbers of copies of mRNA per 10^5 β -actin copies) of IFN- β , IL-29, TNF- α , and IP-10 in mock-infected and infected ex vivo cultures at 1, 24, 48, and 72 hours post infection.

Discussion

Immunohistochemical analysis of virus-infected ex vivo lung cultures demonstrated that endothelial cells within interstitial blood vessels of the lung were targets for HCoV-EMC infection. This implies that HCoV-EMC may spread systemically to affect distant organs. Thus, renal dysfunction in some patients with HCoV-EMC may be due to virus dissemination to the kidney. Further clinical studies are needed to address whether viral dissemination occurs and whether the renal dysfunction is due to viral invasion of the kidneys.

Immunofluorescence study and transmission electron microscopy of infected ex vivo cultures of lung and bronchus enable further define the cell types targeted by HCoV-EMC. Non-ciliated bronchial epithelial cells, bronchiolar epithelial cells, and type I and type II pneumocytes appear to be the major target for HCoV-EMC infection. We did not observe virus-infected alveolar macrophages in ex vivo lung cultures. Preliminary study on peripheral blood monocyte-derived macrophages did not support the replication of the HCoV-EMC. Human and dromedary MERS-CoV have comparable tropism and replication competence in human respiratory ex vivo cultures. This is the first report of comparative data on living human respiratory tissue *in situ*. Therefore, our study provides novel and crucial information to the understanding of a disease with global public health significance.

Some betacoronaviruses in lineage A (eg, HCoV-OC43) possess an esterase and use 9 O-acetylated Sia as virus entry receptors.⁴ Inhalational therapy with a sialidase may provide some clinical benefit. We had previously shown an antiviral effect of the sialidase DAS181 in ex vivo lung cultures infected with influenza viruses. However, no antiviral effect was observed in suppressing HCoV-EMC infection in lung and bronchus explants and Vero cells. This suggests that HCoV-EMC is not dependent on a sialylated receptor for entry into cells and virus replication. This is in agreement with the genomic information of HCoV-EMC suggesting that the virus does not contain esterase, which is present in HCoV-OC43 and is important in cleaving sialic acids and promoting its progeny virions to spread.

Conclusion

This study illustrates the clinical utility of ex vivo cultures of the human respiratory system to investigate newly emerging respiratory viruses.

There have been no autopsy reports describing the virus-induced pathology in the lung to confirm our findings. Nonetheless, autopsy data often reflect the late-stage disease in patients who may have been on mechanical ventilation for long time. Thus, studies of ex vivo experimental infection of the human respiratory tract are invaluable to understand virus tropism and pathogenesis as well as to provide evaluation of potential therapeutic options.

As current antiviral therapy is not effective and specific against coronaviruses, the potential therapeutic benefit of sialidase (DAS181) treatment, which is in phase II clinical trial, is an important research.

Funding

This study was supported by the Health and Medical Research Fund, Food and Health Bureau, Hong Kong SAR Government (#13121132). The full report is available from the Health and Medical Research Fund website (<https://rfs1.fhb.gov.hk/index.html>).

Disclosure

The results of this research have been previously published in:

1. Chan RW, Chan MC, Agnihothram S, et al. Tropism of and innate immune responses to the novel human betacoronavirus lineage C virus in human ex vivo respiratory organ cultures. *J Virol* 2013;87:6604-14.

References

1. Zaki AM, van Boheemen S, Bestebroer TM, Osterhaus AD, Fouchier RA. Isolation of a novel coronavirus from a man with pneumonia in Saudi Arabia. *N Engl J Med* 2012;367:1814-20.
2. Bermingham A, Chand MA, Brown CS, et al. Severe respiratory illness caused by a novel coronavirus, in a patient transferred to the United Kingdom from the Middle East, September 2012. *Euro Surveill* 2012;17:20290.
3. Centers for Disease Control and Prevention. Severe respiratory illness associated with a novel coronavirus--Saudi Arabia and Qatar, 2012. *MMWR Morb Mortal Wkly Rep* 2012;61:820.
4. Kreml C, Schultze B, Herrler G. Analysis of cellular receptors for human coronavirus OC43. *Adv Exp Med Biol* 1995;380:371-4.
5. Triana-Baltzer GB, Babizki M, Chan MC, et al. DAS181, a sialidase fusion protein, protects human airway epithelium against influenza virus infection: an *in vitro* pharmacodynamic analysis. *J Antimicrob Chemother* 2010;65:275-84.

Mechanism of inflammasome activation by SARS coronavirus 3a protein: abridged secondary publication

DY Jin *, BJ Zheng, HMV Tang

KEY MESSAGES

1. SARS-CoV and its ORF3a protein sufficiently activate pro-IL-1 β transcription and IL-1 β secretion, which are the two signals required for full activation of NLRP3 inflammasomes.
2. Activation of pro-IL-1 β transcription by ORF3a is mediated through NF- κ B, and it requires ubiquitin ligase TRAF3.
3. ORF3a interacts with TRAF3 and an adaptor protein ASC required for NLRP3 inflammasome activation.

4. ORF3a activates NLRP3 inflammasomes by promoting TRAF3-mediated ubiquitination of ASC.

Hong Kong Med J 2021;27(Suppl 2):S33-5

HMRF project number: 13121032

DY Jin, BJ Zheng, HMV Tang

School of Biomedical Sciences and Department of Microbiology, The University of Hong Kong

* Principal applicant and corresponding author: dyjin@hku.hk

Introduction

SARS-CoV and MERS-CoV are more pathogenic than other human coronaviruses, as they are capable of inducing a very potent pro-inflammatory response.¹ Interleukin-1 β (IL-1 β) is a key pro-inflammatory cytokine induced during early infection of SARS-CoV. Its production and secretion require the action of multiprotein complexes called inflammasomes. Inflammasomes can assemble around NLRP3 and AIM2 proteins. When activated, NLRP3 recruits ASC adaptor protein ASC to interact with and activate caspase 1, which catalyses pro-IL-1 β processing. NLRP3 inflammasomes are activated only when two signals that stimulate pro-IL-1 β transcription and promote IL-1 β cleavage are in place.

The first viral activator of NLRP3 inflammasomes identified is influenza M2 ion channel protein.² All currently known viral inflammasome activators including M2 can only induce IL-1 β maturation when signal 1 that stimulates pro-IL-1 β transcription is activated by lipopolysaccharide. Multiple ion channel proteins are also encoded by SARS-CoV. Among them, E protein has been shown to be a virulence factor activating NLRP3 inflammasomes.³ Based on these findings, we extended our analysis to ORF3a ion channel protein, also termed X1. ORF3a coding region is located between S and E. ORF3a is a lineage-specific accessory protein and contains two transmembrane domains. Similar to other SARS-CoV proteins, ORF3a is localised to the Golgi apparatus. In a recombinant ORF3a-deficient virus, ORF3a is non-essential but still contributes to pathogenesis.

ORF3a is multifunctional, particularly it induces the production of chemokines such as IL-8 through NF- κ B. Because the pro-IL1 β promoter is also activated by NF- κ B, it is of great interest to clarify whether ORF3a is a viral modulator of NLRP3 inflammasomes that can simultaneously activate the two signals required for inflammasome activation.

Methods

We performed gain-of-function and loss-of-function experiments to characterise the inflammasome-activating property of SARS-CoV and its ORF3a protein in transfected and infected cells as described.⁴ In addition, we delineated the molecular mechanism, molecular determinants, and biological significance for ORF3a induction of NLRP3 inflammasome activation in the context of SARS-CoV infection.

Results

NLRP3 inflammasome activation by ORF3a and SARS-CoV

Because ORF3a is both an NF- κ B activator and an ion channel protein resembling M2, we hypothesised that ORF3a activates both pro-IL-1 β transcription and IL-1 β secretion. We tested this hypothesis using quantitative RT-PCR analysis of pro-IL-1 β transcript in THP-1 monocytic cells and western blot analysis of IL-1 β in the conditioned media of HEK293 cells reconstituted for NLRP3 inflammasome activation. Indeed, the level of pro-IL-1 β transcript increased eight-fold in ORF3a-expressing THP-1 cells. The amount of mature IL-1 β detected in the conditioned media was also more pronounced. Both pro-IL-1 β

transcription and IL-1 β secretion, which are the two signals required for optimal activation of NLRP3 inflammasomes, were activated by ORF3a.

To validate our finding in the context of SARS-CoV infection, we made use of an infectious clone of SARS-CoV in bacterial artificial chromosome and constructed an ORF3a-deficient SARS-CoV, SARS-CoV Δ 3a. We then compared the mutant virus with wild-type SARS-CoV. Consistent with other study,³ infection of THP-1 monocytic cells with wild-type SARS-CoV boosted the transcription of pro-IL-1 β and the maturation followed by secretion of IL-1 β . Whereas viral replication or infection was not affected by the loss of ORF3a, SARS-CoV Δ 3a could not elevate pro-IL-1 β transcription or the accumulation of mature IL-1 β in the conditioned media. This phenotype was reversed when ORF3a was re-expressed in THP-1 cells. Therefore, ORF3a is absolutely required for SARS-CoV activation of NLRP3 inflammasomes.

ORF3a promotes p50 maturation leading to NF- κ B activation

An I κ B α super-repressor, ie the dominant active S32A S36A mutant of I κ B α , was used to verify the requirement of NF- κ B activation for ORF3a induction of pro-IL-1 β transcription. Indeed, the pro-IL-1 β -inducing activity of ORF3a was lost when the I κ B α super-repressor was expressed. Thus, ORF3a induction of pro-IL-1 β is mediated through NF- κ B. We used the reporter construct driven by the IL-8 promoter as a surrogate marker for our subsequent mechanistic analysis of the activation of NF- κ B by ORF3a.

A systematic analysis of different NF- κ B and I κ B subunit proteins in HEK293 cells overexpressing ORF3a indicated that NF- κ B subunit p50 was abundantly accumulated in the nucleus. Among the different forms of NF- κ B, p65-p50 is most common and also best characterised. p50 is derived from its cytoplasmic precursor p105 through proteolytic processing. Our working model is that ORF3a facilitates p105 cleavage boosting the canonical NF- κ B signalling pathway for NF- κ B activation.

Definition of a TRAF-binding motif in ORF3a

In addition to its previously characterised ion channel and caveolin-binding domains, ORF3a possesses a putative TRAF-binding domain very similar to those found in Epstein-Barr virus LMP1 oncoprotein and other proteins known to bind with TRAF proteins, all of which contain the consensus sequence PxQx(T/S/D), where x could be any residue. Amino acids 36-40 of ORF3a (PLQAS) are compatible with this TRAF-binding motif. To determine which domain of ORF3a is absolutely required for its ability to activate NF- κ B and NLRP3 inflammasomes, we

constructed three point mutants: M-T, M-I, and M-C, in which the TRAF-binding, ion channel, and caveolin-binding domains had been individually inactivated. Whereas M-C and M-I were fully capable of activating NF- κ B and NLRP3 inflammasomes, M-T was unable to activate either IL8-Luc or IL-1 β secretion. To our surprise, caveolin-binding or ion channel activity was dispensable for activation of NF- κ B and NLRP3 inflammasomes by ORF3a. In contrast, TRAF-binding was absolutely essential for both activities of ORF3a.

We next conducted co-immunoprecipitation assays to assess the interaction of ORF3a with three representative TRAF proteins, which are important in NF- κ B activation. The ability of ORF3a to interact with TRAF2/3/6 was validated. In contrast, the M-T mutant of ORF3a had no TRAF-binding activity. In addition, our immunoprecipitation results also indicated the interaction of ORF3a with ASC plausibly through a separate ASC-binding domain. In keeping with these results, substantial co-localisation of ORF3a with TRAF3 and ASC to discrete cytoplasmic punctate structures was found in A549 cells.

ORF3a activation of NF- κ B requires TRAF3

Three deubiquitinases (DUBA, A20, and CYLD), which are able to remove ubiquitin from TRAF proteins specifically, were used to sort out which TRAF protein(s) might mediate ORF3a activation of NF- κ B. Because ORF3a was unable to activate NF- κ B when it was coexpressed with DUBA or A20, but this activity was intact in the presence of CYLD, TRAF2 was not required for ORF3a activation of NF- κ B, whereas TRAF3 was likely required. The results on TRAF6 were inconclusive.

To clarify the role of TRAF3 and TRAF6, CRISPR/Cas9 technology was used to construct TRAF3 $^{-/-}$ and TRAF6 $^{-/-}$ HEK293 cells for additional loss-of-function experiments. Because NF- κ B activation was intact in TRAF6 $^{-/-}$ HEK293 cells but not observed in TRAF3 $^{-/-}$ HEK293 cells, we concluded that only TRAF3 was essential for ORF3a activation of NF- κ B.

ORF3a promotes TRAF3-induced ubiquitination of ASC to facilitate NLRP3 inflammasome activation

ORF3a interacts with TRAF3 ubiquitin ligase and ASC adaptor protein. Because TRAF3 catalyses polyubiquitination of ASC,⁵ we hypothesised that ORF3a might promote TRAF3-mediated ubiquitination of ASC. We performed *in vivo* polyubiquitination assay to test this idea. Because a pronounced polyubiquitination smear of ASC was observed when ORF3a was expressed, and this was less prominent in the case of M-T, ORF3a indeed promoted ASC ubiquitination and TRAF-binding is

indispensable for this activity. K48 and K63 mutants of ubiquitin were then used to demonstrate that ORF3a interacts with TRAF3 and ASC to promote TRAF3-mediated K63-linked ubiquitination of ASC. Finally, *in vivo* polyubiquitination assay was performed in TRAF6^{-/-} and TRAF3^{-/-} HEK293 cells to verify the importance of TRAF3. In keeping with the above results, ASC ubiquitination was only slightly affected in TRAF6^{-/-} cells but completely lost in TRAF3^{-/-} cells. Hence, TRAF3, but not TRAF6, was absolutely required for ORF3a-facilitated ubiquitination of ASC.

Discussion

One critical event in SARS-CoV pathogenesis is the hyperactivation of pro-inflammatory response.¹ Clues for therapeutic intervention might be revealed from the mechanistic details of this process. We provided the first example of a viral activator of NLRP3 inflammasomes, which is fully capable of activating both signals that mediate pro-IL-1 β transcription and IL-1 β proteolytic processing. All previously characterised viral activators of inflammasomes including influenza M2 and PB1-F2 can only activate the second signal, and their operation requires priming by lipopolysaccharide, which activates pro-IL-1 β transcription.

Our study also provides the first example for a viral ion channel protein to promote inflammasome activation through an ion channel-independent mechanism. All previously known viral activators of NLRP3 inflammasomes (except PB1-F2) are ion channel proteins. They are thought to activate NLRP3 inflammasomes in an ion channel-dependent manner. However, the activation of neither NF- κ B nor NLRP3 inflammasomes is affected by the disruption of ion channel domain in ORF3a.

We delineated a new mechanism for viral activation of NLRP3 inflammasomes in which ORF3a stimulates NF- κ B and TRAF3-mediated K63-linked polyubiquitination of ASC, which is a prerequisite

for the assembly of NLRP3 inflammasomes.⁵ A similar strategy might be used by other viruses. Our findings have important implications in disease intervention.

Funding

This study was supported by the Health and Medical Research Fund, Food and Health Bureau, Hong Kong SAR Government (#13121032). The full report is available from the Health and Medical Research Fund website (<https://rfs1.fhb.gov.hk/index.html>).

Disclosure

The results of this research have been previously published in:

1. Siu KL, Yuen KS, Castaño-Rodriguez C, et al. Severe acute respiratory syndrome coronavirus ORF3a protein activates NLRP3 inflammasomes by promoting TRAF3-dependent ubiquitination of ASC. *FASEB J* 2019;33:8865-77.

References

1. Chan JF, Lau SK, To KK, Cheng VC, Woo PC, Yuen KY. Middle East respiratory syndrome coronavirus: another zoonotic betacoronavirus causing SARS-like disease. *Clin Microbiol Rev* 2015;28:465-522.
2. Ichinohe T, Pang IK, Iwasaki A. Influenza virus activates inflammasomes via its intracellular M2 ion channel. *Nat Immunol* 2010;11:404-10.
3. Nieto-Torres JL, Verdiá-Báguena C, Jiménez-Guardeño JM, et al. Severe acute respiratory syndrome coronavirus E protein transports calcium ions and activates the NLRP3 inflammasome. *Virology* 2015;485:330-9.
4. Siu KL, Kok KH, Ng MH, et al. Severe acute respiratory syndrome coronavirus M protein inhibits type I interferon production by impeding the formation of TRAF3.TANK. TBK1/IKKepsilon complex. *J Biol Chem* 2009;284:16202-9.
5. Guan K, Wei C, Zheng Z, et al. MAVS promotes inflammasome activation by targeting ASC for K63-linked ubiquitination via the E3 ligase TRAF3. *J Immunol* 2015;194:4880-90.

Respiratory infectious diseases transmission in high-rise residential environment: abridged secondary publication

JL Niu *, TCW Tung, Y Wu

KEY MESSAGES

- Characteristics of two possible airborne infection transmission routes— intra-building transmission and cross-building transmission— were investigated in high-rise residential environments.
- Infection risks and their factors associated with the two transmission routes were assessed.
- A reliable computational fluid dynamics model was developed for predicting the air movement

and pollutant dispersion in high-rise residential environments.

Hong Kong Med J 2021;27(Suppl 2):S36-9

HMRF project number: 13121442

JL Niu, TCW Tung, Y Wu

Department of Building Services Engineering, The Hong Kong Polytechnic University

* Principal applicant and corresponding author: jian-lei.niu@polyu.edu.hk

Introduction

Airborne transmission may be responsible for the spread of various respiratory infectious diseases.^{1,2} Identifying possible airborne transmission routes and their infection risks are essential for formulating effective control strategies. In a hospital environment, or in an enclosed environment such as an aircraft cabin, relevant guidelines to prevent cross-infection have been provided. However, in densely populated high-rise residential environments, the mechanism of airborne spread routes and the related risk levels are lacking.

In 2003, an outbreak of severe acute respiratory syndrome (SARS) in the Amoy Gardens estate, Hong Kong, infected 321 residents in a period of weeks. Epidemiological examination revealed that both intra-building spread and cross-building spread had occurred. Windows flush with the façade can be a major route for vertical upward spread of pathogen-containing aerosols under the buoyancy effect.³⁻⁵ We aimed to identify possible horizontal transmission mechanisms in high-rise residential buildings under the wind effect.

Methods

From March to May 2015, on-site measurements were carried out to investigate intra-building transmission in three horizontal adjacent units on the same floor of a slab-type 16-story public housing block in Pak Tin Estate, Hong Kong (Fig 1). Four measurement scenarios were carried out: closed window mode, open window mode, corridor dosing mode, and 2-room mode. In closed window mode, all the doors and windows in the three flats were

closed, which is in conformity with the occupant behaviour in cool seasons. In open window mode, the windows on external facades and on the partitions were open at an angle of 45°, which conforms to the occupant behaviour in warm seasons. For corridor dosing mode and 2-room mode, the tracer gas dosing locations were in corridor to investigate the transmission characteristics in the semi-open corridor.

Dual tracers SF₆ and CO₂ were used at low concentrations. SF₆ was used as tracer for pollutant dispersion analysis, whereas monitored CO₂ concentrations were used to calculate the ventilation rates. B&K Multi-gas Monitor 1302 and B&K Multipoint Sampler and Doser 1303 were used for SF₆ dosing and sampling. The CO₂ concentrations were monitored in three units using two sets of TSI Q-Trak and one set of Telaire CO₂ Sensor. The wind conditions on the roof were measured at the same time using Young UVW Anemometers.

Computational fluid dynamics simulation program FLUENT was used to model the cross-building tracer gas dispersion. To accurately reproduce the unsteady vortex shedding flows downstream of building blocks, great efforts were made in evaluating and validating the turbulence models, and the unsteady RANS (URANS) RNG k-ε model and delayed discrete-event simulation turbulence model were compared. In particular, the Strouhal number of the vortex shedding behind the building group predicted by the URANS model is in the range of 0.02 to 0.03, whereas the value predicted by discrete-event simulation model is approximately 0.15, which is more consistent with the value reported in the literature. Thus, the discrete-event

simulation model is more accurate than the URANS model in reproducing the vortex shedding frequency in the wake region of the building group.

A geometry model of a building array with seven cross-type building blocks was built, based on the detailed structures of Amoy Gardens. The computational domain was large enough so that the blockage ratio was <3% as recommended in the Architectural Institute of Japan guidelines. The inflow boundary conditions were determined based on the site wind environment near the Amoy Gardens, available from the *Consultancy Study on Establishment of Simulated Site Wind Availability Data for Air Ventilation Assessments in Hong Kong*.

Results

The daily mean concentrations and concentration profiles of SF₆ in one sampling day for each measurement scenario are presented in Fig 2. All concentrations at the monitored points P-1 to P-6 increased exponentially after the start-up of dosing but reached equilibrium within 1.5 hours. The SF₆ concentrations in the receptor units were about one order lower than that in the index unit in both closed window mode and open window mode.

The simulated cross-building transmission characteristics of tracer gas are presented in Fig 3. The tracer gas was released from the window of a unit on the 16th floor facing the semi-open re-entrance space. The concentration decreased by one order of magnitude at the adjacent floors. On the more upper part of the re-entrance space, the concentration decreased by two orders of magnitude. The tracer gas then dispersed downstream following the prevailing wind. The tracer gas concentrations around blocks A and B, which were situated exactly downstream of the index unit building, were four orders lower than the source room concentration but relatively higher than those around the lateral blocks.

Discussion

The intra-building transmission route of the tracer gas from the index unit to receptor units is across the internal window leakage and the corridor. Along the routes, tracer gas is diluted, especially when passing through the ventilated corridor. Well mixing of air in the measurement units was observed for all four scenarios, when the concentration profiles measured at two different points in each unit were compared.

In cross-building transmission, the tracer gas concentration decreased rapidly when the air moves through the vertical re-entrance space of the index block, and it decreased by three orders of magnitude at the rooftop. However, from the roof of the source block to the downstream blocks, the concentration decreased only by one order of magnitude, so that the cross-infection risk via cross-building airborne



FIG 1. Sampling site and the building plan (unit R1310 and the corridor)

transmission was almost comparable with that of the intra-building transmission. The iso-surface of the normalised concentration level 2 penetrated downstream of the building array to a distance of five times of the array dimension, indicating that the tracer gas dispersion downstream of the buildings arrays was relatively slow (presumably owing to the recirculation effects of the wake flow) and that there were risks of cross-building transmission between closely located high-rise building blocks.

The infection risk of a disease was assessed using the Wells-Riley model in terms of the infection probability P . The mean infection risks in the receptor units were one order lower than that in the index unit, with a maximum infection risk of 9% corresponding to the maximum mass fraction of 0.28 polluted air from the index room. The cross-infection risk was related to the air leakage of the doors and windows facing the corridor. This risk is higher when compared with our previous study^{3,4} on the vertical transmission through the open windows induced by the single-sided natural ventilation, in which the maximum value of infection probability is 6.6% and the maximum mass fraction is <0.09.

Two driven forces of the airflow and dispersion, wind force and thermal buoyant force, were compared by estimating the contribution of thermal flow in total air change rate. The wind force was more dominant than the thermal buoyant force. The characters of tracer gas dispersion and distribution indicate that the wind condition and the geometric feature of the corridor significantly affected the inter-unit transmission. Higher wind speed resulted in more tracer gas inter-unit transmission under the low-wind condition during the measurements. The effect of wind direction on the tracer gas dispersion was more significant than the wind speed. The source in windward side had a higher risk of inter-

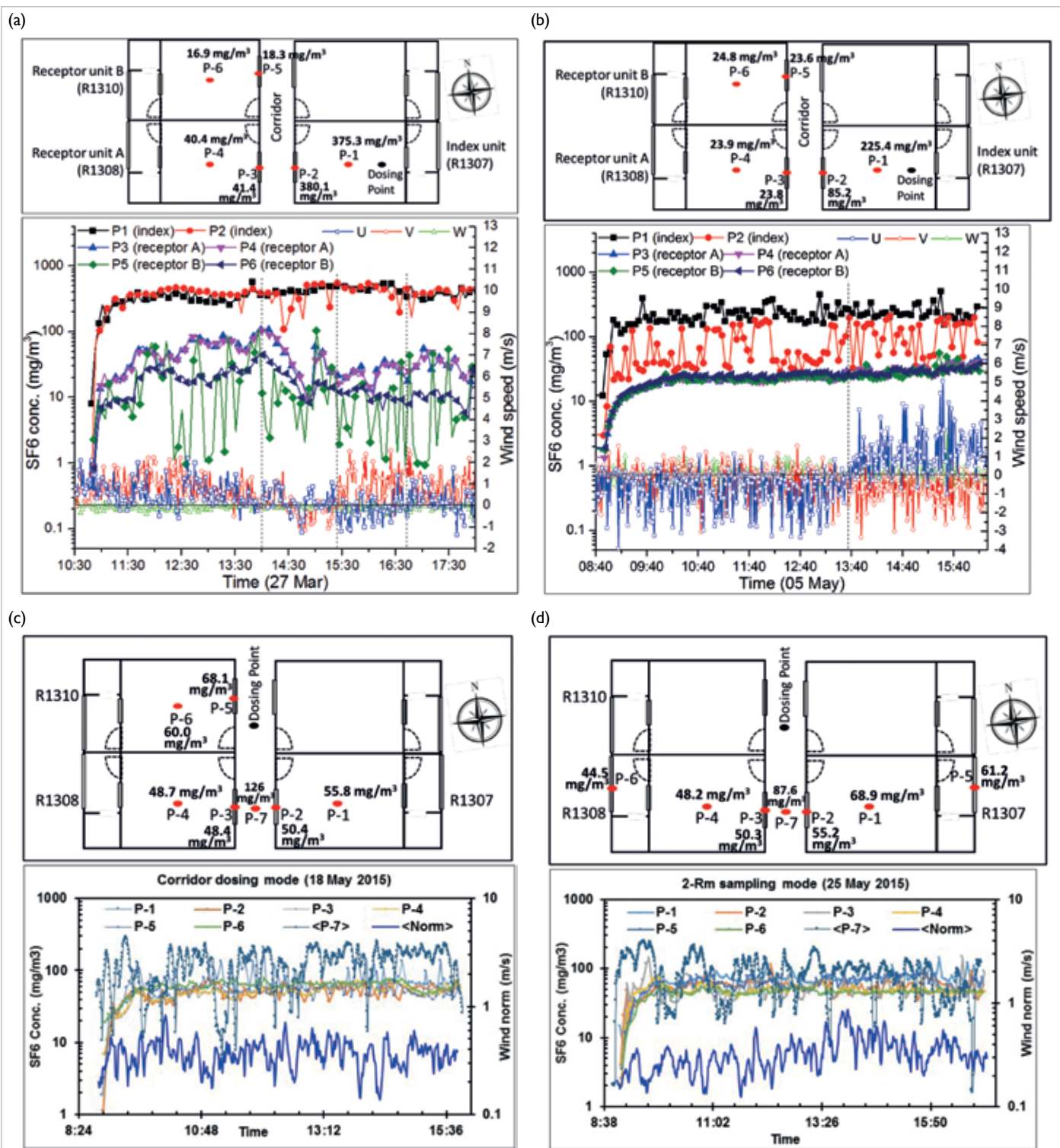


FIG 2. Mean SF₆ concentrations and concentration profiles: (a) closed window mode, (b) open window mode, (c) corridor dosing mode, and (d) 2-room mode

unit dispersion in slab-typed building than the source in leeward side. The rapid dilution of tracer gas in the semi-open corridor indicates that semi-open corridor can prevent the accumulation of contaminants and reduce the inter-unit transmission in slab-typed building.

Conclusion

Tracer gas concentrations in adjacent units are one order lower than that in the source unit, and the infection risks are also one order lower. The intra-building transmission risk through the internal route can be 9%, which is higher than the external spread

through open windows induced by the single-sided natural ventilation airflow. Practically, in residential building design, the internal windows open to closed corridor should be avoided, and the airtightness of individual entrance doors to public spaces should be improved. These strategies also conform to the privacy requirements and fire control in modern constructions.

With regard to the computational fluid dynamics model, the discrete-event simulation model reproduced the unsteady fluctuations of airflow around the building array more accurately than the URANS model. The tracer gas travelled a long distance downstream of the building array with slow concentration decrease. The concentrations near the downstream buildings are only one order of magnitude lower than that at the rooftop of the source building, indicating an infection risk of cross-building in high-density high-rise residential environment.

Acknowledgements

We thank Hong Kong Housing Department and Hong Kong Housing Authority for providing the flats for the on-site measurements.

Funding

This study was supported by the Health and Medical Research Fund, Food and Health Bureau, Hong Kong SAR Government (#13121442). The full report is available from the Health and Medical Research Fund website (<https://rfs1.fhb.gov.hk/index.html>).

Disclosure

The results of this research have been previously published in:

1. Wu Y, Niu JL. Numerical study of inter-building dispersion in residential environments: prediction methods evaluation and infectious risk assessment. *Build Environ* 2017;115:199-214.
2. Wu Y, Niu JL. Assessment of mechanical exhaust in preventing vertical cross-household infections associated with single-sided ventilation. *Build Environ* 2016;105:307-16.
3. Wu Y, Tung TCW, Niu JL. On-site measurement of tracer gas transmission between horizontal adjacent flats in residential building and cross-infection risk assessment. *Build Environ* 2016;99:13-21.

References

1. Yu IT, Li Y, Wong TW, et al. Evidence of airborne

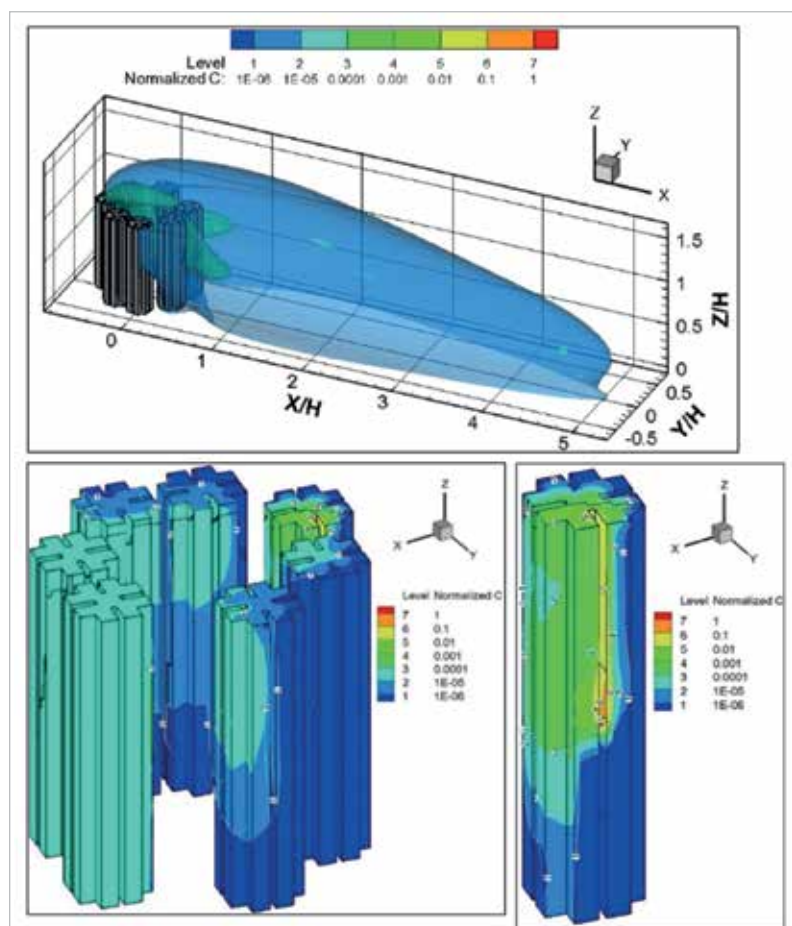


FIG 3. Dispersion and distribution of tracer gas around a group of buildings

transmission of the severe acute respiratory syndrome virus. *N Engl J Med* 2004;350:1731-9.

2. Li Y, Leung G, Tang J, et al. Role of ventilation in airborne transmission of infectious agents in the built environment—a multidisciplinary systematic review. *Indoor air* 2007;17:2-18.
3. Niu J, Tung TC. On-site quantification of re-entry ratio of ventilation exhausts in multi-family residential buildings and implications. *Indoor air* 2008;18:12-26.
4. Gao NP, Niu JL, Perino M, Heiselberg P. The airborne transmission of infection between flats in high-rise residential buildings: tracer gas simulation. *Build Environ* 2008;43:1805-17.
5. Liu XP, Niu JL, Kwok KC, Wang JH, Li BZ. Investigation of indoor air pollutant dispersion and cross-contamination around a typical high-rise residential building: wind tunnel tests. *Build Environ* 2010;45:1769-78.

Prevalence and contextual risk factors of sexually transmitted infections in Hong Kong: abridged secondary publication

WCW Wong *, JD Tucker, HK Man, M Emch, LG Yang, Y Zhao

KEY MESSAGES

1. The prevalence of composite sexually transmitted infections (STIs) was 1.9%, with 1.2% among men and 2.5% among women, and similarly for chlamydia at 1.4% overall, with 1.2% for men and 1.7% for women.
2. However, the prevalence of chlamydial infection was 5.8% in young sexually active women, 4.8% in the sexually active men, and 4.1% in sexually active women aged 40 to 49 years.
3. Three independent risk factors were identified for both composite STIs and chlamydia: younger age, living alone, and males (or females with male

partners) travelled outside Hong Kong in the past 12 months.

4. Mandatory surveillance and reporting of STIs and large population-based screening of chlamydia should be considered.

Hong Kong Med J 2021;27(Suppl 2):S40-3

HMRF project number: 13121242

WCW Wong, JD Tucker, HK Man, M Emch, LG Yang, Y Zhao

Department of Family Medicine and Primary Care, The University of Hong Kong

* Principal investigator and corresponding author: wongwcw@hku.hk

Introduction

Sexually transmitted infections (STIs) are preventable through early identification and effective intervention. Population-based prevalence data can be used to understand the disease burden and distribution as well as effective prevention and control measures. Hong Kong has never conducted any population-based STI prevalence study, and STIs (except hepatitis B) are not notifiable. To provide guidance information for future STI control and prevention, territory-wide STI and sexual health survey (TeSSHS) was conducted to determine the prevalence and associated individual and contextual risk factors of three major STIs (genital chlamydia, gonorrhoea, and syphilis) in a representative sample of adults aged 18 to 49 years in Hong Kong.

Methods

TeSSHS was a population-based household study using geospatial random sampling, computer-assisted personal interview questionnaire. In light of the sensitive nature of the questions, certain portions of the survey were self-completed by the participants to maintain privacy and anonymity. All participants were asked to provide a urine sample to test for *Chlamydia trachomatis* and *Neisseria gonorrhoeae*, with an optional on-site rapid screening test for syphilis.

A stratified geospatial probability sampling of the whole population across Hong Kong's 412 District Council Constituency Areas, each with

approximately 17 000 residents. A proportional sample size was determined, with a total of 79 areas randomly selected in proportion to each of the districts. Random points were dropped using the Geospatial Modelling Environment in accordance with 2011 Census boundary maps. These points were then matched to proximally located residential buildings, and a proportional number of households relative to the buildings were selected. Information was collected for each selected building including number of floors and the living quarters per floor to compile an address list for recruitment. Excel was then used to randomly generate household numbers for the final list of households to be approached by the enumerators. Only one eligible subject was interviewed per household to reduce intra-class correlation of family members with similar risk factors. Next birthday method was used when more than one member would like to join the study. The sample size for TeSSHS was based on the chlamydia prevalence estimate (2.3%) from the Chinese Health and Family Life Survey.¹ To detect prevalence with a precision of $\pm 1\%$ with 95% confidence, a total of 863 participants were estimated.

The questionnaire was based on a review on the risk factors of STIs/HIV among the Chinese population² and a previously validated questionnaire used in mainland China,¹ with additional questions on travel, condom self-efficacy, and mental health (PHQ-9). Invitation letters were sent to the selected households 1-2 weeks before the visits. Three attempts were made at each address at different

time and days of the week before it was considered 'no contact'. The survey was conducted either at the participants' homes or through appointments at one of the four centres across the city. The participants could select if and how they would like to be informed of the test results.

The overall prevalence of composite and individual STIs was weighted for age, sex ratio, and birthplace according to the 2011 Census. Prevalence estimates for all, sexually experienced, and sexually active (reported sexual intercourse in the past 12 months) were calculated. Multivariable analysis was performed to identify risk factors after univariate analysis, with chlamydia and composite STI rates as outcome variables. Further analysis involving environmental factors, spatial analysis (Global Moran's I), and multilevel modelling using svy module using Stata 14.1 (Stata Corp, College Station [TX], US) was performed to identify contextual factors.

Results

Between November 2014 and March 2016, 893 participants were successfully recruited in TeSSHS, with a response rate of 24.5%. After weighting, 47.2% were males and 52.8% were females, with similar proportions in three age-groups, although those aged 40–49 years were slightly over-represented at 36.1% (Table 1).

All the 16 positive cases for *C trachomatis* were identified from heterosexual participants. Among the three gonorrhoea cases, two were heterosexual and one was homosexual. The overall prevalence of the composite STIs was 1.9%, with 1.2% for men and 2.5% for women, and similarly for chlamydia at 1.4% overall, with 1.2% for men and 1.7% for women (Table 2). However, the prevalence of composite STIs was high among sexually active young participants: 4.8% among males and 8.7% among females. The prevalence of chlamydia was 5.8% in young sexually active women, 4.8% in sexually active men, and 4.1% in sexually active women aged 40 to 49 years. There was a U-shape distribution curve among female participants.

In univariate analysis, residency status, birthplace, living status, living with the only sexual partner, and males (or females with male partners) had travelled outside Hong Kong within past 12 months were identified as significant factors in contracting either composite STIs or chlamydia. Relevant negative factors included multiple sexual partners, partner change, no condom use, lower education level, and ethnicity. Three independent risk factors ie, younger age, living alone, and male (or female with male partner) travelled outside Hong Kong in the past 12 months were identified in the multivariate model (Table 3). Compared with participants aged 27 to 39 years, those aged 18 to

TABLE 1. Demographic and socio-economic information of participants (n=881)

	Unweighted observations, No. (%)			Weighted distributions, %		
	Male (n=346)	Female (n=535)	All (n=881)	Male (47.2)	Female (52.8)	All (100)
Age, y						
18-29	146 (42.2)	152 (28.4)	298 (33.8)	35.4	31.4	33.3
30-39	91 (26.3)	158 (29.5)	249 (28.3)	29.6	31.3	30.6
40-49	109 (31.5)	225 (42.1)	334 (37.9)	35.0	37.3	36.1
Education						
≤Junior high school	69 (19.9)	181 (33.8)	250 (28.4)	20.7	28.0	24.5
Senior high school	115 (33.2)	183 (34.2)	298 (33.8)	34.0	36.0	35.1
>Senior high school	162 (46.8)	171 (32.0)	333 (37.8)	45.3	36.0	40.4
Birthplace						
Hong Kong	249 (72.0)	269 (50.3)	518 (58.8)	77.1	67.8	72.2
Mainland China/ Macau/Taiwan	93 (26.9)	263 (49.2)	356 (40.4)	21.7	31.4	26.8
Other	4 (1.2)	3 (0.6)	7 (0.8)	1.2	0.8	1.0
Residency						
Permanent	335 (96.8)	472 (88.2)	807 (91.6)	97.3	91.6	94.3
Non-permanent	11 (3.2)	63 (11.8)	74 (8.4)	2.7	8.4	5.7
Reasons moved to Hong Kong (n=343)						
Work	7 (7.4)	13 (5.2)	20 (5.8)	7.9	4.8	6.1
Family reunion	79 (84.0)	227 (91.2)	306 (89.2)	83.4	91.6	88.3
Study or others	8 (8.5)	9 (3.6)	17 (5.0)	8.7	3.7	5.7
Profession (n=585)						
Manual labour	44 (17.0)	14 (4.3)	58 (9.9)	16.4	2.7	9.9
Sales/service	79 (30.5)	136 (41.7)	215 (36.8)	30.4	37.6	33.8
Self-employed	31 (11.9)	26 (8.0)	57 (9.7)	11.8	6.8	9.5
Clerical worker	44 (17.0)	112 (34.4)	156 (26.7)	17.5	38.9	27.6
Technical worker	42 (16.2)	28 (8.6)	70 (12.0)	16.2	10.6	13.5
Civil servant	19 (7.3)	10 (3.1)	29 (5.0)	7.7	3.5	5.7
Household income, HK\$ (n=751)						
0-12 499	47 (15.5)	102 (22.8)	149 (19.8)	14.7	20.9	17.8
12 500-\$39 999	190 (62.7)	281 (62.7)	471 (62.7)	62.8	62.5	62.6
40 000-≥100 000	66 (21.8)	65 (14.5)	131 (17.4)	22.6	16.7	19.6
Housing type (n=866)						
Public housing	217 (63.8)	334 (63.5)	551 (63.6)	63.1	59.9	61.4
Home ownership scheme	43 (12.6)	86 (16.3)	129 (14.9)	13.0	18.7	16.0
Private	80 (23.5)	106 (20.2)	186 (21.5)	23.9	21.4	22.6
No. of people living with						
0	20 (5.8)	15 (2.8)	35 (4.0)	6.4	3.4	4.8
1-2	131 (37.9)	182 (34.0)	313 (35.5)	37.5	33.3	35.3
>2	195 (56.4)	338 (63.2)	533 (60.5)	56.1	63.3	59.9

26 years were 6 to 9 times more likely to contract composite STIs and 7 to 10 times more likely to contract *C trachomatis*. Compared with participants

TABLE 2. Prevalence of composite sexually transmitted infections (STIs) and chlamydia

	% (95% confidence interval)		
	All (n=881)	Sexually experienced (n=733)	Sexually active (n=566)
Prevalence of the composite STIs	1.9 (1.2-2.9)	2.3 (1.4-3.6)	2.7 (1.7-4.3)
Male (n=346)	1.2 (0.5-2.8)	1.5 (0.6-3.6)	1.9 (0.8-4.4)
Age, y			
18-26	1.7 (0.4-6.7)	3.3 (0.8-12.0)	4.8 (1.2-17.6)
27-39	1.3 (0.3-5.1)	1.6 (0.4-6.2)	1.8 (0.4-7.0)
40-49	0.6 (0.1-4.6)	0.7 (0.1-4.8)	0.9 (0.1-6.1)
Female (n=535)	2.5 (1.5-4.1)	2.9 (1.7-4.8)	3.5 (2.0-5.9)
Age, y			
18-26	3.3 (1.2-8.6)	5.3 (2.0-13.5)	8.7 (3.2-21.4)
27-39	0.7 (0.2-2.9)	0.8 (0.2-3.3)	1.0 (0.2-3.9)
40-49	3.8 (1.9-7.5)	4.0 (2.0-7.9)	4.5 (2.1-9.2)
Prevalence of chlamydia	1.4 (0.8-2.5)	1.8 (1.0-3.0)	2.3 (1.3-3.9)
Male (n=346)	1.2 (0.5-2.8)	1.5 (0.6-3.6)	1.9 (0.8-4.4)
Age, y			
18-26	1.7 (0.4-6.7)	3.3 (0.8-12.0)	4.8 (1.2-17.6)
27-39	1.3 (0.3-5.1)	1.6 (0.4-6.2)	1.8 (0.4-7.0)
40-49	0.6 (0.1-4.6)	0.7 (0.1-4.8)	0.9 (0.1-6.1)
Female (n=535)	1.7 (0.9-3.1)	2.0 (1.1-3.7)	2.6 (1.4-4.9)
Age, y			
18-26	2.2 (0.7-6.9)	3.5 (1.1-11.0)	5.8 (1.7-18.2)
27-39	0.3 (0-2.3)	0.4 (0.1-2.6)	0.4 (0.1-3.1)
40-49	2.8 (1.2-6.2)	2.9 (1.3-6.5)	4.1 (1.8-9.0)

living with more than two people, those living alone were 12 times more likely to contract composite STIs. Compared with males or females whose male partners did not travel out of Hong Kong in the past 12 months, those who had travelled were 6 to 8 times more likely to contract composite STIs and 5 to 11 times more likely to contract chlamydia. Compared with those preferred testing in private clinics, those who preferred testing in public facilities were 3 times more likely to contract STIs.

The spatial analysis showed total randomness. The finding in the multilevel modelling was no different from univariate analysis. Key environmental factors were used as univariate variables to test their association with the STI outcomes. The presence of dermatological clinic within 1 km was associated with *C trachomatis* infection (OR=3.47, 95% CI=1.18-10.19).

Discussion

This study identifies high STI prevalence in sexually active young people and middle-aged women. Younger age, living alone, and males (females with male partners) travelled outside Hong Kong in the

past 12 months were three independent risk factors for STI. STIs could be silently infecting anyone with a normal sexual life.

The strengths of this study include the use of comprehensive theoretical framework of social epidemiology; systematic review for risk factors of HIV/STIs; geospatial modelling environment for sampling; and objective outcome measures including polymerase chain reaction and syphilis rapid tests. However, owing to the sensitive nature of TeSSHS, participants might have underreported the number of sexual partners. In addition, the sample size calculation was based on the prevalence of composite STI, which might lead to insufficient cases for further spatial and multilevel analyses. The relatively low response rate is understandable and is comparable to those reported in the UK³ and to the Hong Kong Family Planning Association Report of Youth Sexuality Study, which does not require samples for STI testing, with an overall response rate of 25.9%.

The overall chlamydia prevalence in Hong Kong is similar to that in the UK (1.5% among females and 1.1% among males)³ and in the US⁴ (2.0% among females and 1.4% among males) but lower than that in mainland China¹ (2.6% among females and 2.1% among males). In the UK, the highest prevalence group was females aged 18 to 19 years, with prevalence of 4.7%, compared with 0.3% among females aged 35 to 44 years.³ However, TeSSHS finds a higher prevalence of chlamydia in sexually active females aged 40 to 49 years, with prevalence of 4.1%. Interestingly, such a U-shape pattern was found in HPV infection in Hong Kong, with the first peak in females aged 26 to 30 years (12.4%) and the second peak in females aged 46 to 50 years (5.8%).⁵ It is hypothesised that changes in sexual behaviours or hormones may be the reason.⁵ Further research is necessary to assess the mechanism of the U-shape pattern of infection in Hong Kong.

Based on the theoretical framework of an epidemic, the basic reproductive rate (R_0) is calculated as $R_0 = \beta cD$, where β indicates the pathogen's infectiveness, c the number of contacts, and D the duration of infectivity. To control chlamydia, D could be reduced through earlier detection and treatment; therefore, mandatory surveillance of STIs should be considered. As up to 85% of the males and 90% females infected with chlamydia are asymptomatic, large population-based screening such as those in the US, the UK, and Australia could be considered. More effective sexual health education targeted at the risk factors and specific age-groups is needed. About 70% of TeSSHS participants would seek testing and treatment in the private sector if STIs are suspected. This suggests that 80% of STI cases in Hong Kong are managed in the private sector. Optimal ways in partner notification and linkage-to-care deserve further exploration.

TABLE 3. Logistic regression of factors associated with composite sexually transmitted infections (STIs) and chlamydial infection

Factors	Adjusted odds ratio (95% confidence interval)					
	Composite STIs			Chlamydial infection		
	All (881)	Sexually experienced (733)	Sexually active (566)	All (881)	Sexually experienced (733)	Sexually active (566)
Male (n=346)						
Female (n=535)	3.46 (1.13-10.6)*	2.78 (0.97-7.94)†	2.56 (0.88-7.41)†	2.27 (0.74-6.96)	1.87 (0.65-5.35)	1.78 (0.62-5.16)
Age-group, y						
27-39 (n=322)						
18-26 (n=225)	5.81 (1.39-24.4)*	7.08 (1.72-29.1)*	9.48 (2.33-38.6)*	6.82 (1.36-34.2)*	8.04 (1.67-38.6)*	9.96 (2.09-47.5)*
40-49 (n=334)	3.08 (0.78-12.2)	2.98 (0.76-11.6)	2.96 (0.71-12.3)	3.32 (0.72-15.2)	3.24 (0.72-14.7)	3.67 (0.80-16.8)†
Born in Hong Kong						
Yes (n=518)						
No (n=363)	2.46 (0.72-8.40)	2.19 (0.67-7.19)	2.8 (0.83-9.48)†	3.79 (0.96-15.0)†	3.32 (0.89-12.4)†	3.21 (0.82-12.6)†
Living with others						
>2 (n=533)						
0 (n=35)	12.1 (2.07-70.2)*	12.2 (2.13-70.2)*	12.1 (2.03-72.1)*	12.1 (1.85-79.1)*	12.3 (1.93-78.8)*	11.9 (1.89-75.1)*
1 or 2 (n=313)	3.87 (1.36-11.1)*	3.87 (1.37-11.0)*	3.27 (1.12-9.53)*	2.12 (0.74-6.09)	2.15 (0.74-6.24)	2.21 (0.71-6.90)
Male (or female with male partner) travelled out of Hong Kong						
No (n=425)						
Yes (n=456)	8.21 (2.38-28.3)*	6.37 (1.99-20.4)*	7.01 (1.73-28.4)*	11.1 (2.65-46.6)*	8.4 (2.10-33.5)*	5.35 (1.25-22.8)*
STI testing facilities						
Private (n=569)						
Public (n=312)	2.97 (1.04-8.45)*	3.18 (1.12-8.99)*	2.74 (1.02-7.36)*	2.5 (0.78-8.04)	2.67 (0.84-8.46)†	2.77 (0.97-7.91)†

* P<0.05

† P>0.05 to <0.1

Acknowledgements

We thank all the participants and interviewers. Special thanks to Prof William L Parish who contributed greatly to this project.

of HIV and other sexually transmitted infections in China: a systematic review of reviews. PLoS One 2015;10:e0140426.

Funding

This study was supported by the Health and Medical Research Fund, Food and Health Bureau, Hong Kong SAR Government (#13121242). The full report is available from the Health and Medical Research Fund website (<https://rfs1.fhb.gov.hk/index.html>).

References

- Parish WL, Laumann EO, Cohen MS, et al. Population-based study of chlamydial infection in China: a hidden epidemic. JAMA 2003;289:1265-73.
- Zhao Y, Luo T, Tucker JD, Wong WC. Risk factors of HIV and other sexually transmitted infections in China: a systematic review of reviews. PLoS One 2015;10:e0140426.
- Sonnenberg P, Clifton S, Beddows S, et al. Prevalence, risk factors, and uptake of interventions for sexually transmitted infections in Britain: findings from the National Surveys of Sexual Attitudes and Lifestyles (Natsal). Lancet 2013;382:1795-806.
- Torrone E, Papp J, Weinstock H; Centers for Disease Control and Prevention. Prevalence of Chlamydia trachomatis genital infection among persons aged 14-39 years--United States, 2007-2012. MMWR Morb Mortal Wkly Rep 2014;63:834-8.
- Chan PK, Chang AR, Yu MY, et al. Age distribution of human papillomavirus infection and cervical neoplasia reflects caveats of cervical screening policies. Int J Cancer 2010;126:297-301.

Disclosure

The results of this research have been previously published in:

- Wong WC, Zhao Y, Wong NS, et al. Prevalence and risk factors of chlamydia infection in Hong Kong: a population-based geospatial household survey and testing. PLoS One 2017;12:e0172561.
- Zhao Y, Wong CK, Miu HY, et al. Translation and validation of a Condom Self-Efficacy Scale (CSES) Chinese version. AIDS Educ Prev 2016;28:499-510.
- Zhao Y, Luo T, Tucker JD, Wong WC. Risk factors

Symptom-specific health-seeking behaviour for common infectious diseases and implications in disease control and surveillance: abridged secondary publication

EHY Lau *, IOL Wong, DKM Ip, KO Kwok, BJ Cowling

KEY MESSAGES

1. Health-seeking behaviour varies considerably across patients with different symptoms.
2. Characterising and understanding factors associated with symptom-specific health-seeking behaviour facilitate planning of healthcare resources and development.
3. Worry of disease transmission is the most important factor associated with reduction in contacts. It is associated with sick leave taking

for symptoms such as fever, dizziness, cough, myalgia, and headache only.

Hong Kong Med J 2021;27(Suppl 2):S44-7

HMRF project number: 13121262

EHY Lau, IOL Wong, DKM Ip, KO Kwok, BJ Cowling

School of Public Health, Li Ka Shing Faculty of Medicine, The University of Hong Kong

* Principal applicant and corresponding author: ehylau@hku.hk

Introduction

From the patient's perspective, health-seeking behaviour tends to be responsive to discomfort or symptoms rather than diagnosis or type of diseases, which is unknown before medical consultation. Therefore, symptom-specific behaviour may more realistically reflect responses to risk communication during epidemics of emerging diseases and to facilitate planning of health care resources.

We carried out longitudinal telephone surveys to gather information on public health-seeking behaviour associated with common symptoms. How health-seeking behaviour relates to interpretation of the surveillance data and disease control was explored. Health-seeking behaviour was linked to symptoms explicitly to provide additional symptom-specific information. This will fill the gap of how the general population response to different symptoms under different level of anxiety. Employment-based medical benefits are associated with higher access or intensity of medical consultation.¹ Surveillance data can be better utilised if associations of consultation are identified. We also derived subgroup incidence based on surveillance data with the knowledge of symptom-specific health-seeking behaviour.

Methods

Longitudinal telephone surveys with respondents aged ≥16 years recruited from randomly selected households were conducted from February 2014 to May 2015. One adult was invited for an interview in each selected household. Information about

children (aged <16 years) was taken from caregivers. Three subsequent calls were carried out to capture changes in health-seeking behaviour at periods with different patterns of disease burden or anxiety level. To avoid potential selection bias owing to illness during a particular season, respondents received all subsequent calls, even if they reported no illness episode in the first interview.

Weekly sentinel surveillance data for influenza and acute diarrhoeal diseases provided by general practitioners (GP), general outpatient clinics (GOPC), and traditional Chinese medicine practitioners (TCMP) were retrieved from the website of Centre for Health Protection.²

Descriptive analyses were carried out for the healthcare-seeking pattern, preventive measures, and change in contact pattern by each symptom. Multivariable analyses were carried out to identify factors associated with healthcare seeking, contact pattern, or other preventive measures, adjusted for confounders such as age, sex, chronic conditions, medication, medical benefits, and household income. Relative importance of specific symptoms was estimated. Because subjects were followed up for several rounds of interview, general estimating equations were used to account for correlation within subjects. An exchangeable correlation structure was used by assuming constant correlations between interview rounds.

Results

In all four rounds of the survey, there were 4370

illness episodes, accounting for 50.1% of all person-round interviewed. Among 4370 individuals with any symptoms, 44.6% sought for healthcare service and 55.4% did not. Of those who sought healthcare

service, 31.5% consulted a GP, whereas only 6.6% and 7.4% went to GOPC and TCMP, respectively (Table 1). Multivariable analysis showed that younger age-group (0-15 years), women, chronic conditions

TABLE I. Symptom-specific health-seeking behaviour for the top 10 symptoms

Symptom	No. of episodes	% (95% confidence interval)					
		30-day incidence	General practitioner	General outpatient clinic	Traditional Chinese medicine practitioner	Accident & emergency department	No health-seeking behaviour
Fatigue	1189	10.4 (6.8-14.0)	11.7 (8.1-15.3)	0.8 (0.0-4.4)	9.7 (6.1-13.3)	0.0 (0.0-3.6)	81.1 (77.5-84.7)
Headache	980	7.0 (4.4-9.6)	56.0 (53.4-58.6)	1.3 (0.0-3.9)	7.5 (4.9-10.1)	0.7 (0.0-3.3)	33.4 (30.8-36)
Runny nose	957	8.4 (7.4-9.4)	26.2 (25.2-27.2)	3.5 (2.5-4.5)	5.3 (4.3-6.3)	0.5 (0.0-1.5)	31.4 (30.4-32.4)
Low back pain	722	7.1 (3.6-10.6)	4.6 (1.1-8.1)	9.7 (6.2-13.2)	13.5 (10.0-17.0)	0.9 (0.0-4.4)	63.2 (59.7-66.7)
Cough	707	10.5 (6.9-14.1)	52.8 (49.2-56.4)	6.4 (2.8-10.0)	4.0 (0.4-7.6)	1.0 (0.0-4.6)	38.9 (35.3-42.5)
Myalgia (aches or pain in muscles)	597	4.6 (2.0-7.2)	4.1 (1.5-6.7)	0.7 (0.0-3.3)	3.2 (0.6-5.8)	0.0 (0.0-2.6)	84.1 (81.5-86.7)
Sore throat	584	5.5 (2.9-8.1)	60.5 (57.9-63.1)	4.1 (1.5-6.7)	9.6 (7.0-12.2)	0.0 (0.0-2.6)	30.5 (27.9-33.1)
Dizziness	466	5.0 (1.9-8.1)	34.4 (31.3-37.5)	1.1 (0.0-4.2)	3.0 (0.0-6.1)	0.0 (0.0-3.1)	57.3 (54.2-60.4)
Fever	282	4.3 (2.4-6.2)	86.5 (84.6-88.4)	3.4 (1.5-5.3)	8.1 (6.2-10.0)	2.4 (0.5-4.3)	8.8 (6.9-10.7)
Loss of appetite	253	4.7 (2.1-7.3)	18.5 (15.9-21.1)	1.2 (0.0-3.8)	11.7 (9.1-14.3)	0.3 (0.0-2.9)	70.0 (67.4-72.6)
Any symptom	4370	42.0 (36.1-47.8)	31.5 (22.9-40.1)	6.6 (0.9-12.3)	7.4 (3.0-11.8)	0.8 (0.2-1.4)	55.4 (46.4-64.4)

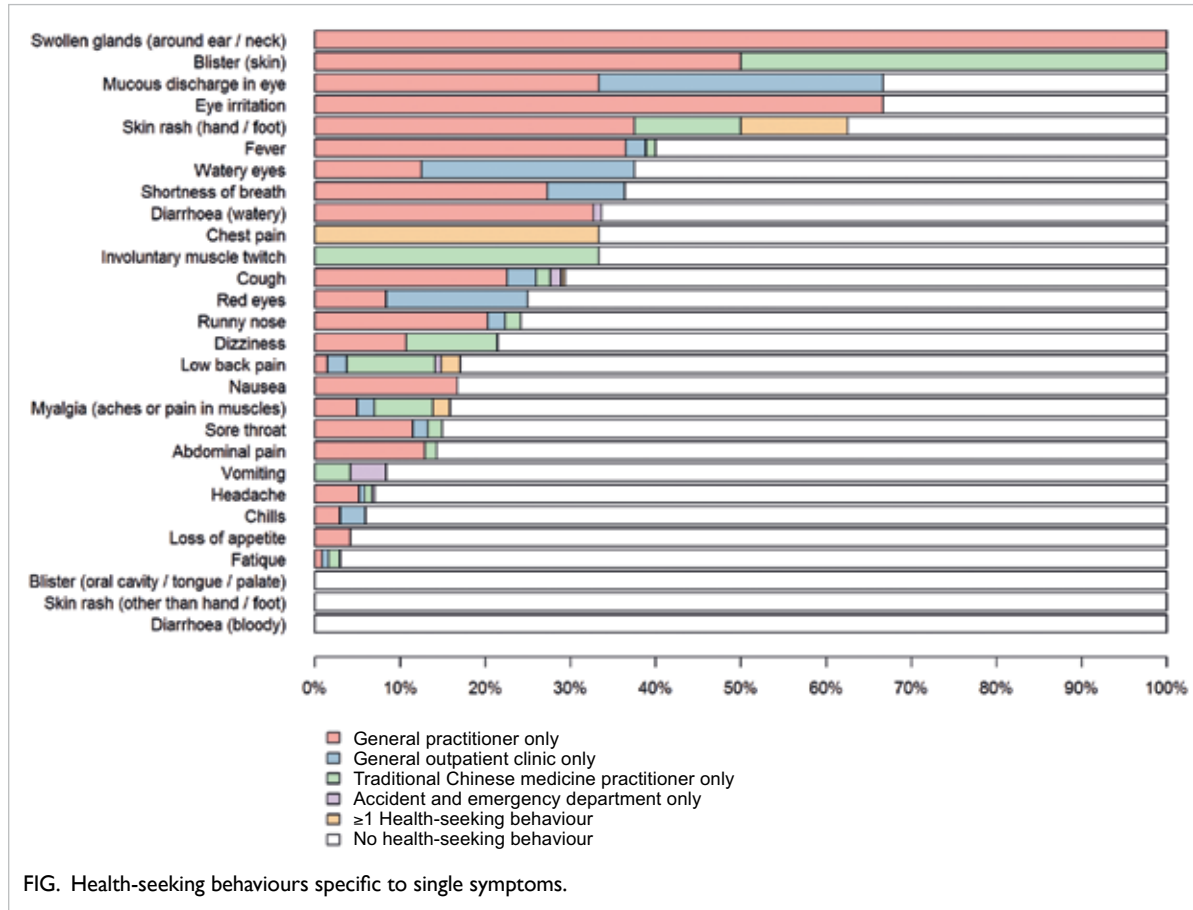


FIG. Health-seeking behaviours specific to single symptoms.

TABLE 2. Factors associated with general practitioner consultation by general estimating equation model

Factors	Odds ratio (95% confidence interval)	P value
Sex		
Female	1	
Male	0.68 (0.60-0.80)	<0.01
Age-group, y		
0-15	2.11 (1.40-3.20)	<0.01
16-54	1	
≥55	1.06 (0.80-1.50)	0.73
Household income, HK\$		
<20 000	0.83 (0.50-1.40)	0.49
20 000-29 999	1	
≥30 000	1.21 (0.90-1.60)	0.14
Refuse to answer	1.12 (0.90-1.40)	0.37
Chronic disease		
No	1	
Yes	2.64 (1.10-6.10)	0.02
Medication status		
No	1	
Yes	1.55 (0.70-3.20)	0.24
Having symptoms		
Fever	10.00 (7.30-13.70)	<0.01
Chills	0.99 (0.70-1.40)	0.96
Headache	1.18 (0.90-1.50)	0.2
Cough	2.95 (2.30-3.70)	<0.01
Shortness of breath	1.16 (0.60-2.20)	0.65
Dizziness	1.23 (0.90-1.70)	0.24
Runny nose	2.81 (2.30-3.50)	<0.01
Sore throat	2.00 (1.60-2.60)	<0.01
Diarrhoea (watery)	7.03 (4.90-10.20)	<0.01
Nausea	1.25 (0.70-2.20)	0.45
Vomiting	3.66 (2.20-6.00)	<0.01
Loss of appetite	1.01 (0.70-1.60)	0.96
Abdominal pain	1.55 (1.00-2.40)	0.05
Myalgia (aches or pain in muscles)	0.78 (0.50-1.30)	0.36
Low back pain	0.56 (0.40-0.90)	0.02
Fatigue	0.46 (0.30-0.70)	<0.01
Other	3.29 (2.00-5.40)	<0.01
Round		
1	1.00 (0.80-1.30)	0.99
2	1	
3	2.35 (1.80-3.10)	<0.01
4	2.12 (1.50-3.10)	<0.01
Medical insurance		
None	1	
Employer-provided medical benefits	1.03 (0.70-1.50)	0.88
Private medical insurance	0.89 (0.60-1.30)	0.53
Both	1.13 (0.80-1.60)	0.48

were significantly associated with GP consultation (Table 2). Fever, diarrhoea, and vomiting were associated with higher GP consultation, whereas low back pain and fatigue were associated with lower GP consultations.

Patients with chronic symptoms such as low back pain, myalgia, and fatigue were less likely to perform preventive measures, compared with those with influenza-related symptoms such as fever, cough, and sore throat. Patients with influenza-like illness were more likely to have preventive measures compared with patients with acute respiratory infections and acute diarrhoeal disease. For those who reported change in contacts with colleagues or classmates, >70% of those with fever, chills, nausea, and diarrhoea took sick leave. 87.1% and 78.6% of those with influenza-like illness and acute diarrhoeal disease, respectively, took sick leave. <20% of subjects with fatigue, headache or abdominal pain alone would seek for healthcare service (Fig). Allopathic medicine remained the main form of healthcare service sought (82.6%).

Multivariable analysis showed that worry of disease transmission was the most significant factor in changing contact with their colleagues for all symptoms (all odds ratios [OR] >4), including low back pain which was less likely to be infectious. Male patients with fatigue (OR=0.39, P<0.001), cough (OR=0.58, P<0.01) or sore throat (OR=0.46, P<0.001) were less likely to change contacts with colleagues. Worry of serious complication was associated with change in contacts with colleagues for low back pain (OR=3.56, P<0.01), myalgia (OR=3.20, P<0.05), dizziness (OR=9.22, P<0.001), and loss of appetite (OR=26.8, P<0.001).

Worried of transmission was associated with taking sick leave for fever (OR=43.1, P<0.001), dizziness (OR=42.5, P<0.01), cough (OR=10.3, P<0.001), myalgia (OR=9.1, P<0.05), and headache (OR=5.9, P<0.001). Consistent with the change in contact with colleagues, men (OR=0.15, P<0.05) were less likely to take sick leave owing to fatigue, whereas older adults were less likely to take sick leave owing to fever (OR=0.05, P<0.01) or sore throat (OR=0.38, P<0.05).

Conclusions

Men with illness were less likely to seek healthcare service from GP, but there was no significant sex difference for GOPC and TCMP, consistent with previous studies.³ Older patients were more likely to visit TCMP, consistent with previous studies.^{4,5} Young patients were more likely to visit GP, probably because of parents' worry and asking for more immediate healthcare although the situation may not be urgent.⁶

Worry of disease transmission was the most important factors associated with reduction in

contacts with colleagues for all symptoms. However, it was associated with taking sick leave only for symptoms of fever, dizziness, cough, myalgia, and headache. Simulation analysis has estimated that 72% of influenza cases in the workplace are due to presenteeism.⁷ The study assumed a presenteeism rate of 48%, which is higher than that reported in Hong Kong, suggesting a potentially higher impact of workplace transmission of influenza. This may have implications in the healthcare setting.⁸ Data generated from this study are useful for healthcare utilisation, control of infectious diseases, and interpretation and design of surveillance systems.

Funding

This study was supported by the Health and Medical Research Fund, Food and Health Bureau, Hong Kong SAR Government (#13121262). The full report is available from the Health and Medical Research Fund website (<https://rfs1.fhb.gov.hk/index.html>).

Disclosure

The results of this research have been previously published in:

1. Zhang Q, Feng S, Wong IOL, Ip DKM, Cowling BJ, Lau EHY. A population-based study on healthcare-seeking behaviour of persons with symptoms of respiratory and gastrointestinal-related infections in

Hong Kong. *BMC Public Health* 2020;20:402.

References

1. Wong IO, Lindner MJ, Cowling BJ, Lau EH, Lo SV, Leung GM. Measuring moral hazard and adverse selection by propensity scoring in the mixed health care economy of Hong Kong. *Health Policy* 2010;95:24-35.
2. Centre for Health Protection. Statistics on Communicable Diseases - Sentinel Surveillance. http://www.chp.gov.hk/en/dns_submenu/10/26/44.html
3. Hunt K, Adamson J, Hewitt C, Nazareth I. Do women consult more than men? A review of gender and consultation for back pain and headache. *J Health Serv Res Policy* 2011;16:108-17.
4. Chung V, Lau CH, Yeoh EK, Griffiths SM. Age, chronic non-communicable disease and choice of traditional Chinese and western medicine outpatient services in a Chinese population. *BMC Health Serv Res* 2009;9:207.
5. Shao S, Zhao F, Wang J, et al. The ecology of medical care in Beijing. *PLoS One* 2013;8:e82446.
6. Hugenholtz M, Bröer C, van Daalen R. Apprehensive parents: a qualitative study of parents seeking immediate primary care for their children. *Br J Gen Pract* 2009;59:173-9.
7. Kumar S, Grefenstette JJ, Galloway D, Albert SM, Burke DS. Policies to reduce influenza in the workplace: impact assessments using an agent-based model. *Am J Public Health* 2013;103:1406-11.
8. Jena AB, Baldwin DC Jr, Daugherty SR, Meltzer DO, Arora VM. Presenteeism among resident physicians. *JAMA* 2010;304:1166-8.

AUTHOR INDEX

Chan JYW	11, 18	Ng HYE	8
Chan MCW	28	Nicholls JM	28
Chan RWY	28	Niu JL	36
Chan SKC	4	Peiris JSM	28
Chen JP	8	Rong JH	8
Chen YJ	14	Su J	8
Cheung DWS	18	Tang HMV	33
Chong CCN	4	Teoh AYB	4
Chook P	11	Tse AKW	14
Cowling BJ	44	Tse YK	4
Emch M	40	Tucker JD	40
Fung KP	11, 18	Tung TCW	36
Ip DKM	44	Wat ECL	18
Jin DY	33	Waye MMY	18
Ko ECH	18	Wong IOL	44
Koon JCM	11, 18	Wong PH	18
Kwok KO	44	Wong WCW	40
Lai PBS	4	Woo PCY	23
Lam PYF	8	Wu JCY	4
Lao L	8	Wu Y	36
Lau EHY	44	Yan BPY	11
Lau JYW	4	Yang LG	40
Lau SKP	23	Yau KC	18
Lau VKM	18	Yeung WF	8
Lee E	8	Yu YMB	8
Leung WW	4	Yu ZL	14
Lin WL	8	Zhang YB	8
Man HK	40	Zhang ZJ	8
Meng W	8	Zhao Y	40
Ng EKW	4	Zheng BJ	23, 33

Disclaimer

The reports contained in this publication are for reference only and should not be regarded as a substitute for professional advice. The Government shall not be liable for any loss or damage, howsoever caused, arising from any information contained in these reports. The Government shall not be liable for any inaccuracies, incompleteness, omissions, mistakes or errors in these reports, or for any loss or damage arising from information presented herein. The opinions, findings, conclusions and recommendations expressed in this publication are those of the authors of the reports, and do not necessarily reflect the views of the Government. Nothing herein shall affect the copyright and other intellectual property rights in the information and material contained in these reports. All intellectual property rights and any other rights, if any, in relation to the contents of these reports are hereby reserved. The material herein may be reproduced for personal use but may not be reproduced or distributed for commercial purposes or any other exploitation without the prior written consent of the Government. Nothing contained in these reports shall constitute any of the authors of these reports an employer, employee, servant, agent or partner of the Government.

Published by the Hong Kong Academy of Medicine Press for the Government of the Hong Kong Special Administrative Region. The opinions expressed in the *Hong Kong Medical Journal* and its supplements are those of the authors and do not reflect the official policies of the Hong Kong Academy of Medicine, the Hong Kong Medical Association, the institutions to which the authors are affiliated, or those of the publisher.